INVESTIGATION OF AIR CONCENTRATION AND PRESSURES OF A STEPPED SPILLWAY EQUIPPED WITH A CREST PIER

by
JAN ALBERTUS CALITZ

Thesis presented in fulfilment of the requirements for the degree of Master of Engineering in the Faculty of Civil Engineering at Stellenbosch University

Supervisor: Prof. GR BASSON

December 2015

DECLARATION

By submitting this thesis electronically, I declare that the entirety of the work contained therein is my own, original work, that I am the sole author thereof (save to the extent explicitly otherwise stated), that reproduction and publication thereof by Stellenbosch University will not infringe any third party rights and that I have not previously in its entirety or in part submitted it for obtaining any qualification.

Name .....

Signed .....

Std no. .....

ABSTRACT

The evolution of roller compacting concrete has led to stepped spillways becoming increasingly popular over recent decades, mainly credited to the fact that the stepped profile of the downstream dam wall can be incorporated into a spillway chute. However, the discharge over stepped chutes in current use has been limited, due to the risk of local cavitation damage to the concrete of stepped chute structures.

A general accepted practice to combat cavitation is to aerate the flow. Would it be possible, when adding a pier to the spillway crest, to introduce air into the flow upstream of the inception point in order to reduce the cavitation potential on the chute, and subsequently allow discharges greater than the current recommended values to be safely passed?

A physical hydraulic model was constructed at a scale of 1:15 to investigate the air concentration along the pseudo-bottom and minimum pressures at the upper vertical step face for areas on the spillway chute where cavitation could be imminent for large discharges. The tests were conducted using a conventional stepped spillway with no pier as the control, to which the test results of two different pier configurations fixed on the spillway crest were compared.

The recorded results showed an increase in air concentration and minimum pressures downstream of the pier for both tested crest pier designs. The Type 1 pier is recommended over the Type 2 pier due to the increased ability of the former pier to aerate the flow that consequently alleviates minimum pressures found on the spillway chute.

In summary, the literature recommends a maximum discharge of 18 m^2/s, but the experimental study has shown through a cavitation evaluation of the air concentration and minimum pressures that, for a no-pier stepped spillway with a chute angled at 51.3° and a prototype step height of 1.5 m, a maximum discharge of up to 25 m^2/s can be allowed. For a spillway equipped with a Type 1 pier, Method A suggested that a unit discharge of at least 30 m^2/s could be safely passed.

OPSOMMING

Die ontwikkeling van rollergekompakteerde beton het daartoe gelei dat damwal-konstruksie met die kenmerkende trap-profiel ’n gewilde konstruksie-opsie oor die afgelope paar dekades geword het. Dit is grotendeels te danke aan die feit dat die trap-profiel aan die stroomafkant van die dam terselfdertyd as ’n oorloopgeut gebruik kan word. Nietemin word die eenheidsdeurstroming oor trap-oorlope beperk weens die kavitasierisiko vir lokale skade aan die beton van damoorloopstrukture.

Om kavitasieskade te voorkom is dit algemeen aanvaarde praktyk om die watervloei te belug. Sou dit moontlik wees om ’n pyler aan die oorloopkruin te heg wat die vloei stroomop van die beluggingspunt belug om kavitasiepotensiaal op die oorloop te verminder en sodoende die toelaatbare eenheidsdeurstroming te verhoog?

’n Fisiese hidrouliese model op ’n skaal van 1:15 is gebou om die lugkonsentrasie op die pseudo-bodem, asook minimum drukke op die boonste vertikale trap te ondersoek vir gebiede op die oorloop waar kavitasie gewisse gevaar inhou vir groot deurstromings. Die toetse is gedoen met behulp van ’n konvensionele trapoorloop sonder ’n pyler wat as kontrolegeval gedien het, en is vergelyk met die toetsresultate van twee oorlope, elk met ’n unieke pylerontwerp.

Die waargenome toetsresultate toon 'n toename in die lugkonsentrasie en minimum drukke stroomaf van die pyler vir albei pylerontwerpe. Die Tipe 1 pyler word bo die Tipe 2 pyler aanbeveel weens die verhoogde vermoë van eersgenoemde pyler om die vloei te belug, wat tot verhoogde minimum drukke op die oorloop lei.

Ter opsomming beveel die literatuur ’n maksimum eenheiddeurstroming van 18 m²/s aan, maar die eksperimentele studie het deur middel van die kavitasie-evaluering van lugkonsentrasiedata en minimum drukke bewys dat maksimum deurstromings van tot 25 m²/s toegelaat kan word vir ’n trapoorloop sonder ’n pyler, maar met ’n oorloopgeut teen ’n hoek van 51.3° en ’n prototipe traphoogte van 1.5 m. Vir ’n trapoorloop toegerus met ’n Tipe 1-pyler het Metode A bewys dat ’n eenheidsdeurstroming van ten minste 30 m²/s veilig toelaatbaar is.

ACKNOWLEDGEMENTS

The author would like to acknowledge the contributions of the following individuals and funding institution:

- Prof GR Basson, for the support and guidance he provided as study leader.

- The laboratory personnel of Stellenbosch University, for arranging the construction of the physical model, assisting with modifications during the test phase and assisting with the testing.

- University of Stellenbosch, for funding the construction of the physical hydraulic model and the instrumentation.

- My colleague, Stephan Kleynhans, for encouraging me to enrol for a Master's degree and providing me with exceptional guidance and support during my study period.

- My wife, Elrika, for her selfless support and encouragement. Without her continuous support, this thesis would have not been possible.

TABLE OF CONTENTS

LIST OF FIGURES

LIST OF TABLES

LIST OF ABBREVIATIONS

ASCE	American Society of Civil Engineers
C	air concentration (%)
C_b	air concentration at pseudo-bottom (%)
C_m	mean air concentration (%)
C_e	spillway crest discharge coefficient
C_o	spillway ogee crest discharge coefficient
CEDEX	Rangel Centro de Estudios de Carreteras
CFD	computational fluid dynamics
D_{wi}	hydraulic diameter at inception point
F_r	Froude roughness number
Fr_b	Froude roughness number $\left(q_w/\sqrt{g \times \sin\theta \times h^3}\right)$
Fr_*	Froude roughness number $\left(q_w/\sqrt{g \times \sin\theta \times (h \times \cos\theta)^3}\right)$
f_{bi}	friction factor at pseudo-bottom $\left(0.5 - 0.42 \times \sin 2\theta \times \left(\frac{k}{D_{wi}}\right)^{0.2}\right)$
f_i	friction factor $\left(1/\left(2.16 + 1.24 \times \log\frac{y}{k}\right)\right)^2$
g	gravitational acceleration
h	step height
h_a	velocity head $\left(v^2/\sqrt{2g}\right)$
H_d	design head of spillway crest
H_e	actual considered head on spillway crest
Hz	hertz
kHz	kilohertz
k	step roughness height $(h \times \cos\theta)$
K_a	spillway abutment contraction coefficient
K_p	spillway pier contraction coefficient
L	length along pseudo-bottom
L_i	length to inception point along pseudo-bottom
L_{cr}	length to critical point along pseudo-bottom

l	litre
l_s	step tread length
m	metre
m²	metre square
m³	metre cube
mm	millimetre
mA	milliampere
min	minute
No	number
p	pressure
p_m	mean pressure
P	height of upstream spillway face
q_w	discharge per unit width
R	electrical resistance
RCC	roller compacting concrete
Re	Reynolds number
s	second
s_i	dimensionless distance $\left((L_i - L) / H_e\right)$
TNP	Thermal Needle Probe
USBR	United States Bureau of Reclamation
V	volt
U_w	clear water velocity
VAW	Versuchsanstalt für Wasserbau, Hydrologie und Glaziologie (Laboratory of Hydraulics, Hydrology and Glaciology)
We	Weber number
x	coordinate across spillway along step tread
y	coordinate perpendicular to the pseudo-bottom
y_i	flow depth at inception point

y_c	critical depth for rectangular channel $\left(\sqrt[3]{\frac{q_w^2}{g}}\right)$
z	coordinate vertical to the step riser originating from the spillway crest
%	percentage
θ	spillway angle from horizontal
γ	specific weight of water
ρ	density of water
σ_{cr}	critical cavitation index
⌀	diameter
Ω	ohm
δ	thickness of boundary layer

1. INTRODUCTION

1.1 BACKGROUND

Stepped spillways have become increasingly popular over recent decades, due to the evolution of roller compacting concrete (RCC) as a dam construction method. For RCC dam construction, concrete is placed in successive horizontal layers at a downstream slope that results in a stepped dam face. The time and financial savings of RCC construction has directed the attention of engineers to incorporate the stepped profile of the downstream dam wall as a spillway chute.

Advantages of a stepped spillway not only include the economic integration of the spillway as part of the dam wall, but such a spillway also offers significant energy dissipation along the chute, which reduces the potential for cavitation when compared to a smooth overflow spillway. However, research has shown that the discharge over stepped chutes should be limited due to the risk of cavitation occurring.

Cavitation is initiated within low-pressure zones. Low-pressure zones for a stepped chute can be found at the upper vertical step face, with such zones being caused by flow separation over the step edge. Specific discharge over a stepped spillway is limited by the fact that increased velocity over the step edges tends to decrease the pressure at the vertical step face to a point of cavitation inception.

One measure that can be used to protect a spillway from cavitation is to aerate the flow. Peterka (1953) proved that an air concentration of approximately 5 to 8% at a spillway surface is sufficient to avoid cavitation damage, which can be attributed to the compressibility of the air-water mixture that absorbs the impact of the imploding vapour-filled bubbles.

Self-aeration of a flow down a spillway is achieved once the growth of the turbulent boundary layer has reached the free surface flow. At this specific point, which is known as the inception point, air is entrained into the flow. A certain distance downstream of the inception point, the pseudo-bottom air concentration reaches the required 5 to 8% that is sufficient to prevent cavitation. This specific air concentration is reached at a point known as the critical point. Downstream of the critical point, the air concentration increases to a uniform value (Boes & Hager, 2003b).

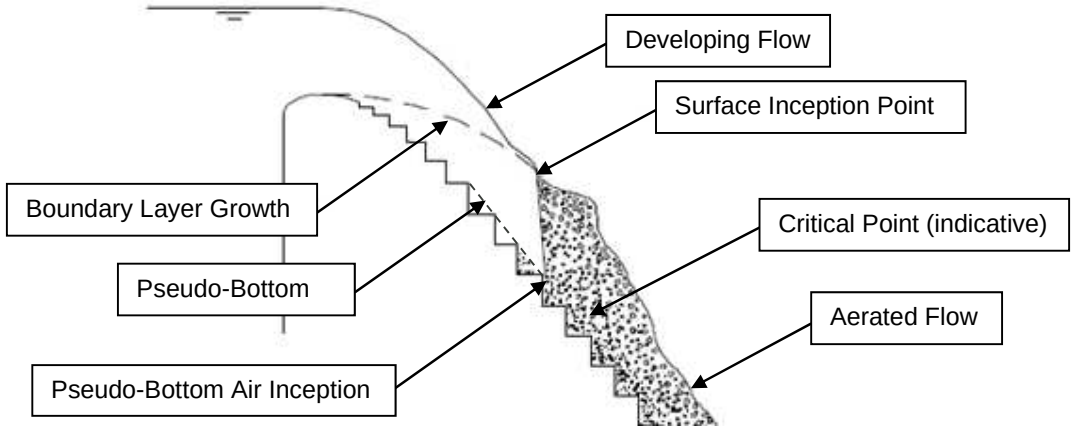

Figure 1-1: Self-aeration of stepped spillway (Amador, et al., 2004)

Its stands to reason that, if a stepped spillway needs to discharge a flow that is higher than the current recommended values, the designer would need to give considerable attention to areas prone to cavitation, which are located upstream of the critical point, below the pseudo-bottom, and within the non-aerated developing flow region. (Refer to **Figure 1-1**.) The pseudo-bottom is defined as the imaginary line that connects the outer step edges.

One of the options for combating cavitation for high discharges would be to aerate the upstream flow by either artificially introducing air into the flow, or by creating an earlier onset of air entrainment than would otherwise be the case. Whether it would be possible to aerate the flow by altering the spillway structure upstream of the inception point is debatable. *This is the question that the current researcher would like to explore in this study*.

The aim of this thesis is to investigate whether the introduction of a pier at the spillway crest can entrain air directly downstream of the pier, or whether it can accelerate the growth of the turbulent boundary layer to the point of initiating premature self-aeration.

1.2 OBJECTIVE OF STUDY

The objective of this study is to investigate, by means of a physical model study, whether an earlier onset of air entrainment at the pseudo-bottom can be achieved by introducing piers at the crest of a stepped spillway. The end result would be to ascertain whether, by creating an earlier inception of air, discharges greater than the recommended values can safely be passed through a stepped spillway without the spillway being at risk of cavitation damage.

The following two central model criteria were used in the experimental research:

i. A standard stepped spillway model (control test).
ii. The stepped spillway model, as used in (i), with two different pier configurations at the spillway crest.

The control test was conducted to obtain comparable results in relation to a spillway with no crest piers. The test data from model setups with different crest pier arrangements were compared to the data from the control test to conclude whether the inception of air at the spillway pseudo-bottom could be accomplished at an earlier stage.

With respect to cavitation being the largest deterrent to large discharges, the majority of the experiments were focused at, and upstream of, the critical point. The following variables were investigated within the specific study region for all model setups:

- Location of the inception point.
- Air concentration at the pseudo-bottom.
- Pressure measurements at the upper vertical step face, to support the hypothesis that the successful introduction of air can alleviate negative pressures.

It should be noted that all parameters and experimental results recorded in the model study and presented for this document have been transformed to reflect the values, as would have been observed in the prototype, unless otherwise stated.

1.3 BRIEF OVERVIEW OF THESIS

The report is structured as follows:

- A short summary defining the methodology used for achieving the stated objective, employing a physical model study is described in **Chapter 2**.
- The literature review is discussed in **Chapter 3**. At first, the reader is introduced to the history of stepped spillways, and to the different flow conditions that are associated with a stepped spillway. The chapter then evolves to explore the research conducted by others for a stepped spillway on: a) the location of the inception point; b) the air concentration; c) the different pressures involved; and d) cavitation on the chute. The flow effects of the pier and the possible scaling effects associated with physical hydraulic models are also discussed. At the end of the chapter, a short summary of the reviewed literature and of how the findings of the literature will apply for this specific model study is provided.
- **Chapter 4** describes the experimental setup, the instrumentation, and the different test procedures. The section also presents the results and findings of the preliminary tests conducted that were used to modify the final pier design and testing procedures.
- The experimental test results are presented in **Chapter 5**.
- The experimental test results are discussed and compared for the different model setups in **Chapter 6**.
- **Chapter 7** contains the conclusion of the study.
- A recommendation for future research to be conducted is presented in **Chapter 8**.

2. METHODOLOGY

2.1 PHYSICAL MODEL STUDY

A scale model of a stepped spillway was required to achieve the objective stated. The design of the model was based on two basic criteria, namely:

- The model scale should be large enough to mitigate hydraulic scale effects effectively. The aeration properties measured within a model will not reflect the true behaviour of the prototype, due to the fact that the size of an air bubble is not influenced by the model scale. It is, therefore, of paramount importance to use a sufficiently large scaled model to avoid distortion of the aeration characteristics for the two-phase flow.
- The flow down the spillway model must be able to reach the stage of air inception for all model discharges. The height of the model is influenced by this criterion. The flow downstream of the critical point was not considered for this study, but additional model height was provided to ensure that the inception and critical point were not affected by the hydraulic jump that formed at the toe of the model.

A 1:15 scale model at a height of 3.9 m from crest to toe and a channel width of 1.0 m was constructed at Stellenbosch University's Hydraulic Laboratory. The spillway consisted of a sloped chute at 1:0.8 (V:H) with a 100 mm step height, and a standard ogee crest.

2.2 MODELLING METHODOLOGY

The objective of the study was to determine whether crest piers can induce an earlier onset of air entrainment at the pseudo-bottom. The following plan which was formulated in order to achieve the objective is shown in **Figure 2-1**. Note that the plan is illustrated as a hierarchical process.

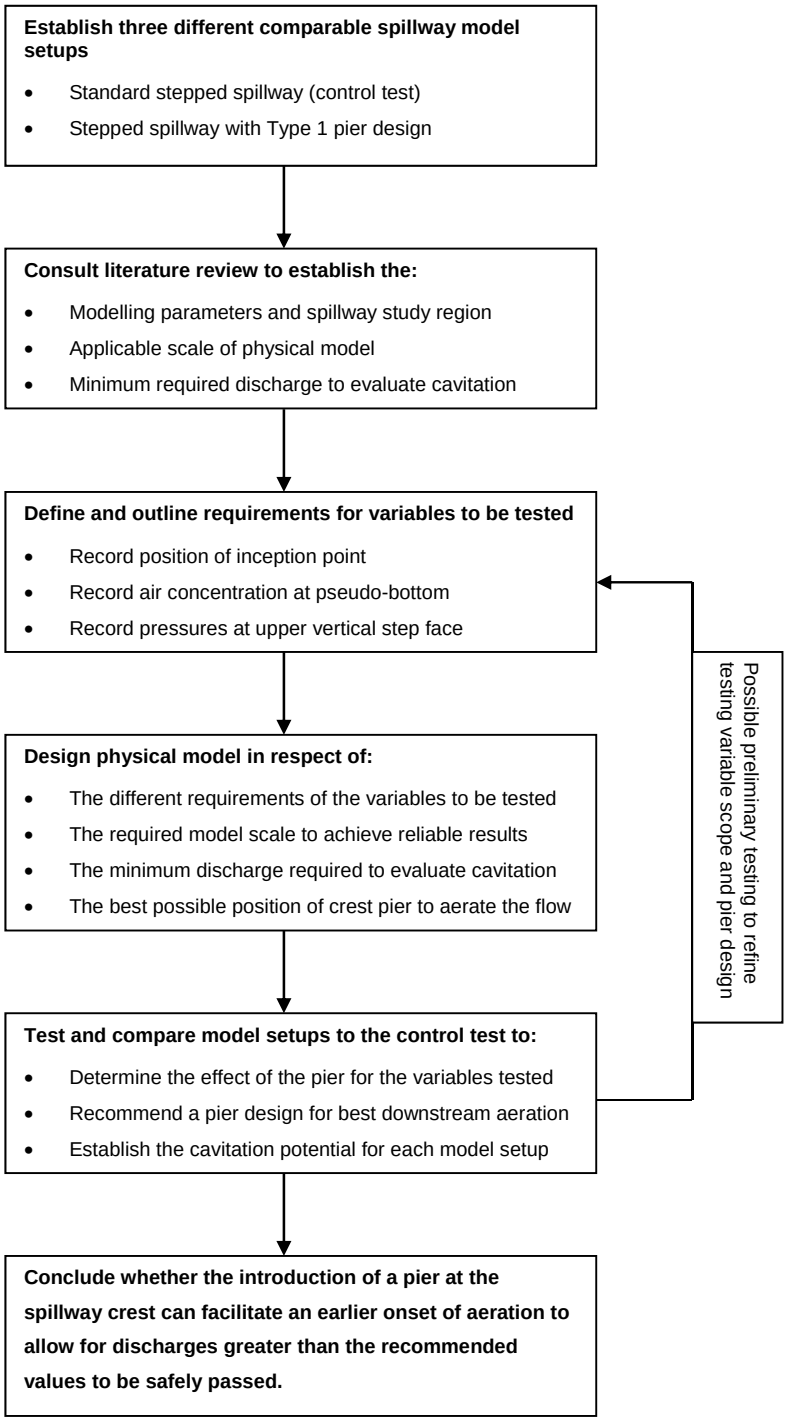

Figure 2-1: Modelling methodology

3. LITERATURE REVIEW

A detailed account of the literature reviewed for the stated study objective is provided in this chapter. The chapter begins by introducing the reader to the history and typical flow characteristics of a stepped spillway, and it later moves on to explore research more inclined to the subject matter, consisting of air concentration, pressures and cavitation on a stepped spillway. A short summary of the reviewed literature and how the findings of the literature will apply for this specific model study is provided at the end of this chapter.

3.1 KEY FEATURES OF STEPPED SPILLWAYS

3.1.1 General Overview and Brief History of Stepped Spillways

“A spillway is the overflow device for an impounded body of water” (Webber, 1979). The function of a spillway is to release surplus water or floodwater that cannot be contained within the water storage body. The spillway needs to be designed to discharge water in a safe and controlled manner without harming the impounding structure or creating excessive downstream scour. The design of a spillway is subject to a range of factors, such as:

- The dam type and height considered.
- The dam volume, including the frequency and duration of water discharge via the spillway.
- Whether the crest is controlled or uncontrolled.
- Economic factors, such as construction time, available materials, and others.

As water passes over the spillway crest and down the chute, potential energy is converted into an increasing amount of kinetic energy. In general, measures are taken to dissipate the kinetic energy, preventing damage to the structure, so as to avoid undesirable scour effects downstream of the spillway. The amount of kinetic energy to be dissipated is a function of the dam height and the volume of discharge to be released.

Methods for energy dissipation at the toe of the spillway include a stilling basin to induce hydraulic jump, or a ski jump structure to aerate the flow before it plunges into a downstream pool. The use of a stepped spillway provides the option of dissipating a portion of the total kinetic energy along the chute. The rough surface of the stepped profile increases the flow resistance significantly, thereby reducing the total amount of energy to be controlled at the end of the spillway.

The reduction of the total energy leads to a smaller energy-dissipating structure being required at the spillway toe. Subsequently, this increases financial savings and reduces construction time.

The use of stepped spillways, weirs and channels has been around for over 3 500 years, originating in the early ancient Greece and Romans era (during the classical antiquity period). The design of these early stepped structures were based on the construction materials and method of that time, which involved the use of cut-stone masonry and timber cribs on the sloped section of the structure.

Following the classical antiquity period, the eastern Mediterranean Muslims continued to make use of stepped structure architecture in the Middle East. The technology travelled with the Muslim conquerors as they invaded the Hispanic peninsula. The Muslim civil engineers employed the stepped design for various irrigation schemes and overflow spillway dams during the seventh to fourteenth centuries, leaving a strong hydraulic influence in Iraq, Saudi Arabia and Spain.

Following the reconquest of Spain after the fourteenth century, the Catholic Spanish adopted the stepped profile design from the Muslims. The Spanish stepped form of architecture influenced some European countries as the Spanish Empire grew, but the civil engineering approach was found to be more widespread on the American continent, as a result of the Spanish conquest of the New World (the Americas).

The Spanish built the largest overflow stepped spillway dam in 1791, namely the Puentes Dam, but in 1802 it washed out, due to foundation failure (Refer to **Figure 3-1**). The structural failure of the dam unleashed a 12 m high wave that destroyed everything in its path, and which claimed over 600 lives. Various dams and historical ruins, constructed with a stepped overflow spillway, can still be found in Central America (i.e. Mexico) to this date.

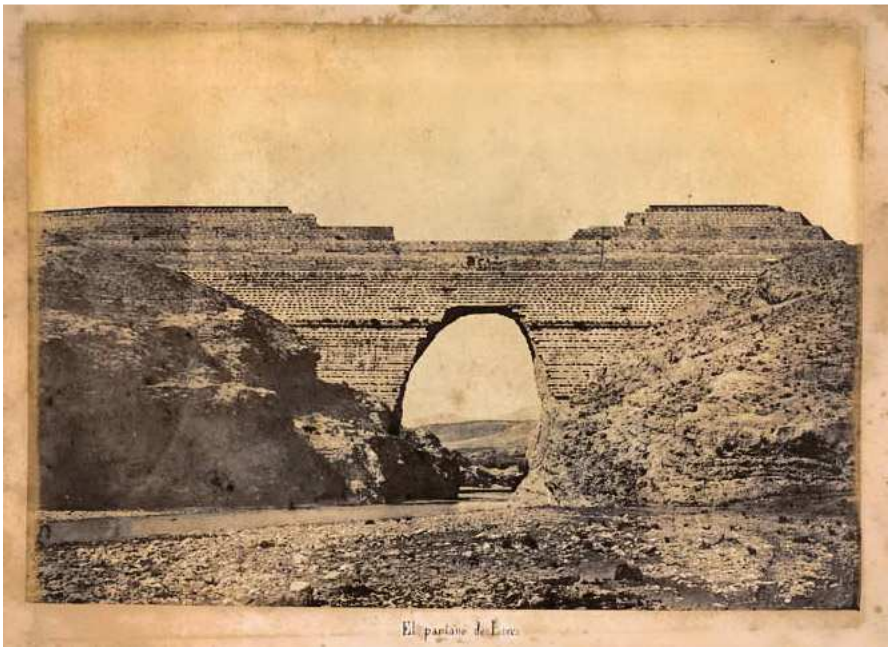

Figure 3-1: Puentes Dam after catastrophic failure (Farooq, 2013)

According to Chanson (1994), the early stepped spillway design was selected by civil engineers due to the simplicity of the shape and to contribute to the stability of the dam. Since the nineteenth century, civil engineers have started to realise the energy dissipation characteristics of the stepped profile, which has led them to start employing the stepped blueprint more frequently. The New Croton Dam was the first dam to be designed to make use of the energy dissipation function of a stepped spillway. However, the stepped spillway lost favour in the early twentieth century as more progress was made in coming to

an understanding of the principle of energy dissipation within hydraulic jumps. Stilling basins offered larger energy dissipation possibilities than were available before, as well as requiring smaller structures, when compared to stepped chutes.

Since 1970, design engineers have regained interest in the stepped spillway, largely due to the advances that have been made in the use of construction materials, and to the introduction of a new construction method, namely RCC.

3.1.2 Introduction to Roller Compacted Concrete (RCC)

RCC is defined as a special blend of concrete that is compacted by means of roller compaction that, in its unhardened state, is capable of supporting a vibratory roller while compaction is taking place. RCC differs from conventional concrete principally in terms of the ratio of materials mixed, the no-slump consistency obtained thereby, and the increasing use of special add mixtures such as natural pozzolan, slag and fly ash (Mehta & Monteiro, 2007).

RCC construction has been employed extensively for new dam construction, as well as for existing dam rehabilitation, over the last five decades. The construction method of RCC is very similar to that of paving, whereas concrete is delivered by trucks or conveyors, spread by bulldozing equipment, and finally compacted by vibratory rollers.

RCC is typically placed and compacted in 300 mm thick horizontal layers. Subsequent layers are placed until the required step height is reached. A step height can vary between 0.6 and 3.0 m. Each step is classified as a ‘vertical lift’, and the associated formwork is suited to a single lift. Once the RCC lift has attained the initial set, the formwork is removed and reused for the next step face (Mehta & Monteiro, 2007).

Advances in earthmoving technology, and the introduction of self-propelled concrete conveyors and vibratory rollers, has considerably decreased the time of RCC dam construction. The project time and financial savings of RCC construction have focused the attention of engineers on incorporating the stepped profile of the dam as an overflow spillway chute. Using the stepped contour of the dam wall eliminates the need for a separate spillway structure.

3.1.3 Flow Regimes

The flow over stepped spillways is characterised into two distinct flow regimes, namely nappe and skimming flow. The nappe flow regime, which is found for low spillway discharges, transforms into skimming flow with increasing flow discharge. A third, less significant, flow condition, which is characterised as the transitional flow regime, is observed between the nappe and skimming flow regimes (Boes & Minor, 2000). The different flow regimes are discussed in the following subsections.

i. Nappe flow.
ii. Skimming flow.
iii. Transition flow.

3.1.3.1 Nappe Flow

Nappe flow is defined as a succession of free-falling nappes down a stepped chute. Water plunges from the upper step to the lower step tread, and it then cascades down the remainder of steps in a series of free nappes. The flow condition normally occurs for low discharges down stepped chutes. **Figure 3-2** indicates the nappe flow regime.

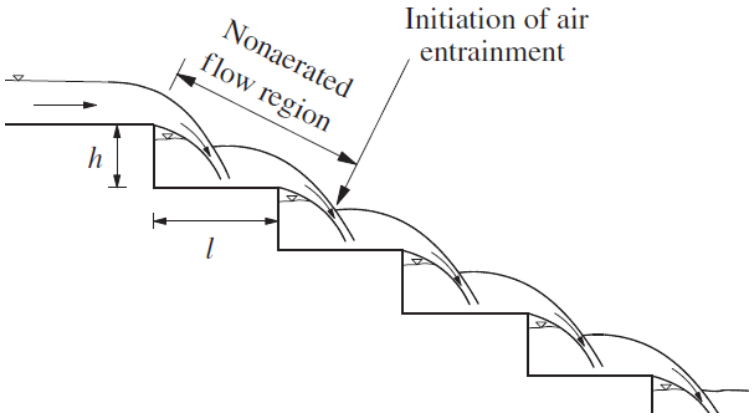

Figure 3-2: Nappe flow (Baylar, et al., 2006)

3.1.3.2 Skimming Flow

For skimming flow, the water flows as a coherent stream over the pseudo-bottom. The outer step edges form the pseudo-bottom, over which the flow passes. Below the pseudo-bottom, recirculating vortices develop within the triangular cavities of the step faces, and is maintained through the transmission of shear stress from the fluid flowing past the step edges. Generally, skimming flow takes place for large unit discharges. **Figure 3-3** shows a general schematic of the skimming flow regime.

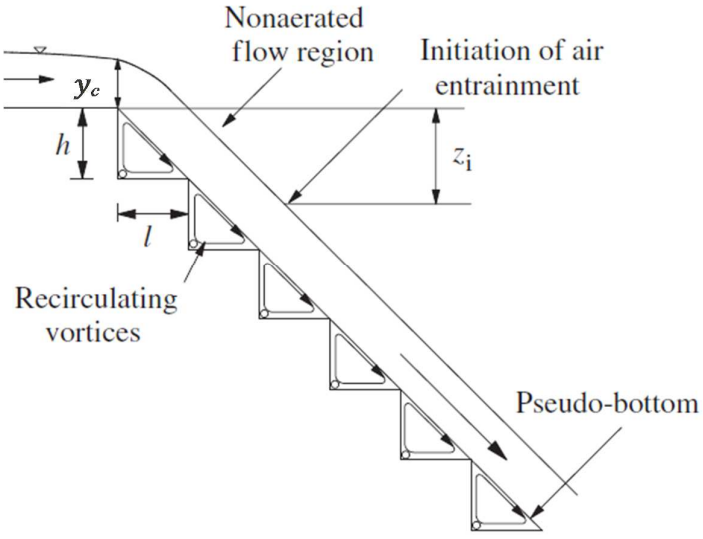

Figure 3-3: Skimming flow (Baylar, et al., 2006)

3.1.3.3 Transition Flow

The transition flow regime (**Figure 3-4**) cannot be labelled exactly as a distinct flow regime, because, for this flow condition, both the nappe and skimming flows occur simultaneously on different parts of the stepped spillway (Ohtsu & Yasuda, 1997). The difficulties encountered in identifying the regime are problematic, but it can be viewed as the zone of the upper limit of nappe flow and the lower limit for skimming flow (Boes & Hager, 2003a).

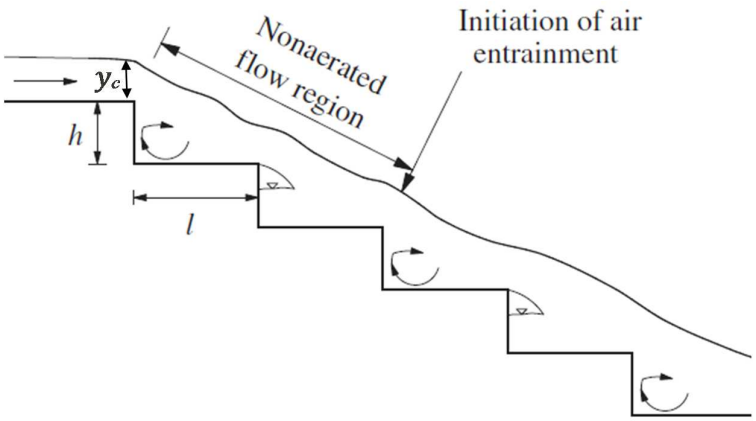

Figure 3-4: Transitional flow (Baylar, et al., 2006)

3.1.3.4 Onset of Skimming Flow

Extensive research has been done to determine the onset of the skimming flow regime. Chanson (1994) showed that the full onset of skimming flow is characterised by a value of critical depth given by the equation (refer to **Figure 3-4** for declaration of tread length symbol '*l*'):

$$\frac{y_c}{h} = 1.057 - 0.465 \times \frac{h}{l} \qquad \textbf{(3-1)}$$

Chamani and Rajaratnam (1999) suggest that the following equation should be used to determine the upper boundary of nappe flow:

$$\frac{h}{l} = 0.405 \left(\frac{y_c}{h}\right)^{-0.62} \qquad \textbf{(3-2)}$$

and

$$\frac{h}{l} = \sqrt{0.89 \left[\left(\frac{y_c}{h}\right)^{-1} - \left(\frac{y_c}{h}\right)^{-0.62} + 1.5\right] - 1} \qquad \textbf{(3-3)}$$

for the lower boundary of skimming flow.

However, **Equation (3-3)** is likely to underestimate the onset of skimming flow. The reason for the result concerned differing from that of other authors may be attributed to a different definition being used for the transition of nappe to skimming flow (Boes & Hager, 2003a). Boes and Hager (2003a), on performing various related experiments, found that the start of skimming flow can be formulated as:

$$\frac{y_c}{h} = 0.91 - 0.14\tan(\theta) \quad \textbf{(3-4)}$$

During the transitional flow regime, undesirable wave action is observed that might be caused by hydrodynamic instabilities, due to the change of nappes from a state of being aerated to a state of being unaerated, and vice versa (Boes & Hager, 2003a). Experimental results within the transitional flow regime are likely to be unreliable and inconclusive in relation to the research objective. It is of importance to note that either the nappe, or the skimming flow condition, applies for the experimental study.

As the aim of this research is to examine the different air and pressure qualities for high unit discharges along a steep sloped stepped spillway, the skimming flow regime is the required flow condition. The onset of skimming flow must be determined to ensure that the skimming flow is applicable to all experimental observations and measurements. **Figure 3-5** shows a comparison of dimensionless critical depth over step height versus a range of unit discharges of previous experimental studies to determine the onset of skimming flow.

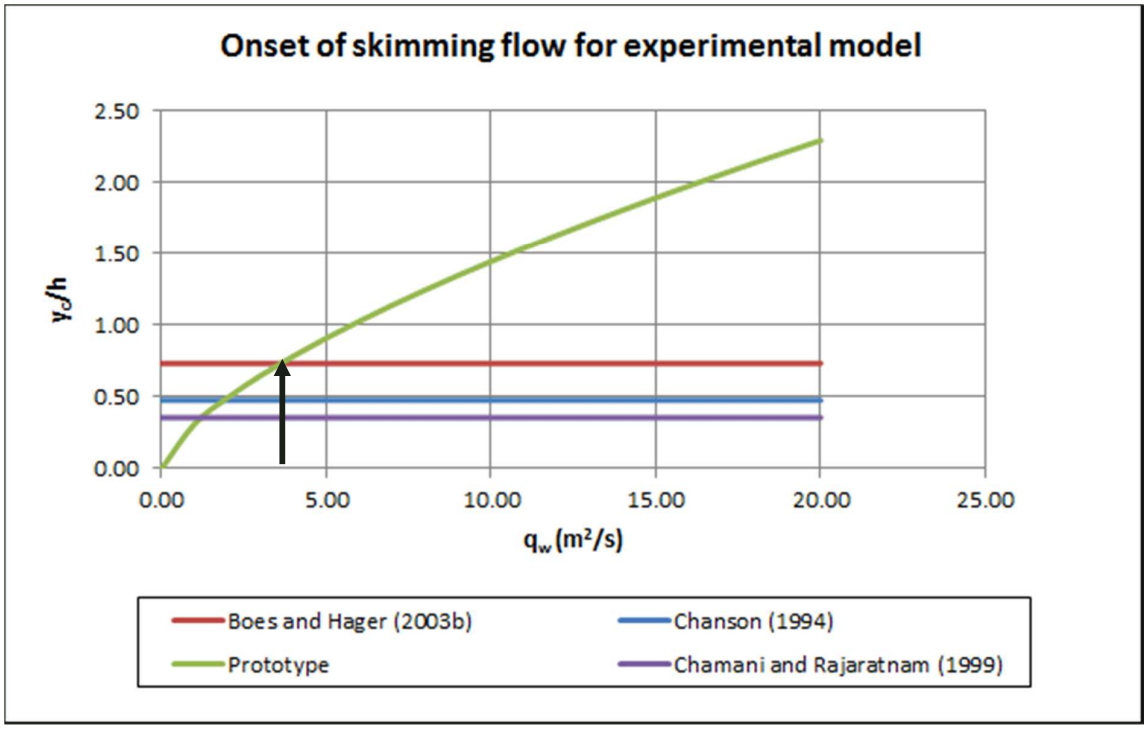

Figure 3-5: Onset of skimming flow, according to different authors, as basis for determining experimental model unit discharge in this thesis

It is evident from **Figure 3-5** that the minimum prototype unit discharge should not be less than 4 m^2/s, if the criteria of Boes and Hager (2003a) are considered.

3.1.4 Flow Regions

Skimming flow along a stepped chute can be divided into four distinct regions (Amador, et al., 2004), namely:

1. Developing flow (black water).
2. Rapidly varied flow (surface and pseudo-bottom inception point).
3. Gradually varied flow (white water).
4. Uniform flow (white water).

Figure 3-6 graphically illustrates the four distinct regions, as listed in numeric order.

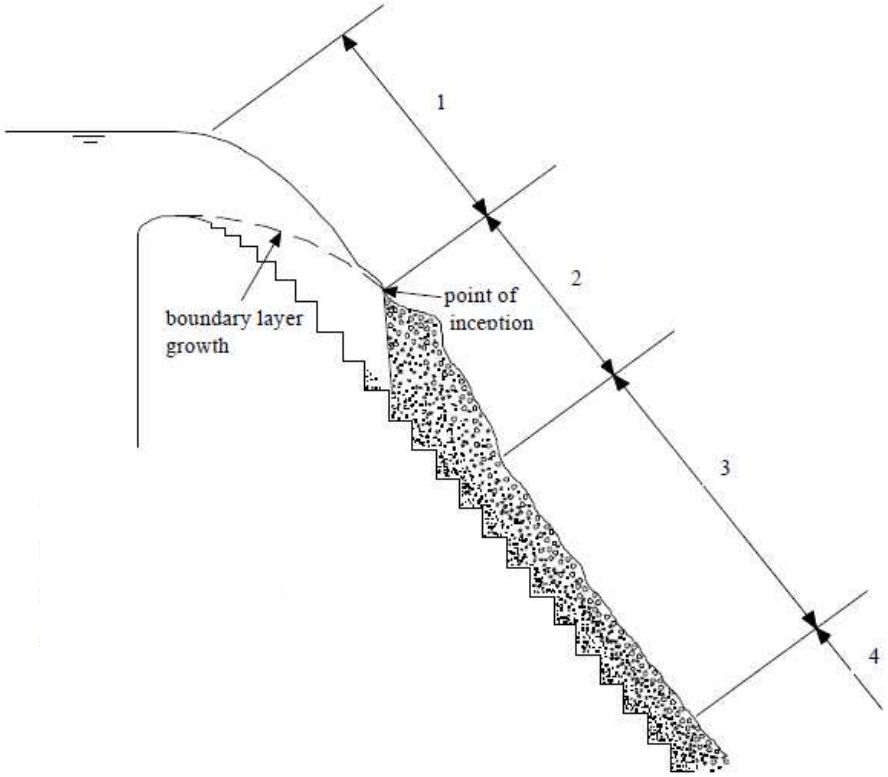

Figure 3-6: Flow regions along stepped spillway (Amador, et al., 2004)

3.1.4.1 Developing Flow Region (Region 1)

Flow is accelerated as it passes over the spillway crest, and down the spillway chute. Immediately downstream of the crest, the free surface is smooth and glassy, and no air entrainment occurs (Amador, et al., 2006). A turbulent boundary develops as the flow passes over the steps, which initiates the growth of the boundary layer. The amount of flow resistance caused by water flowing over the steps is a function of the step height, which is termed the 'roughness height'. The boundary layer growth rate along the spillway is essentially a factor of the flow direction and the roughness height.

When the thickness of the boundary layer reaches the free surface, and flow turbulence overcomes the surface tension, air is entrained, at the air-water interface, into the flow (Pfister & Hager, 2010). The point of entrainment is known as the 'surface inception point', and it marks the border of the developing flow region.

3.1.4.2 Rapidly Varied Flow Region (Region 2)

The specific zone of flow development is generally regarded as the region that forms the border between the surface inception and pseudo-bottom inception point. **Figure 3-7** illustrates the separate inception points.

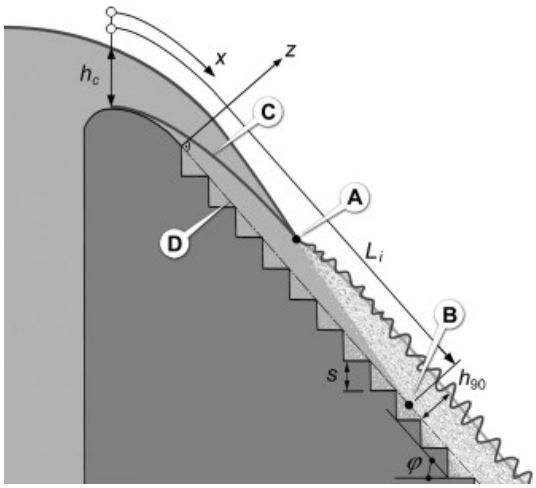

Figure 3-7: Schematic sketch of: (A) surface inception point; (B) pseudo-bottom inception point; (C) growth of boundary layer; and (D) pseudo-bottom (Pfister & Hager, 2010)

The start of free surface aeration into the flow is classified as the surface inception point, and the process is briefly described in **Subsection 3.1.4.1**. The pseudo-bottom inception point is mathematically defined as the location where the air concentration at the pseudo-bottom is equal to 1% (Boes & Hager, 2003b). Downstream of the pseudo-bottom inception point, air is entrained within the full flow depth.

The concept of the pseudo-bottom inception point is an important stepped spillway fundamental that is essential to this thesis, as sufficient air concentration along the spillway pseudo-bottom can absorb the impact of collapsing vaporised bubbles, thereby effectively eliminating or reducing cavitation (Pfister & Hager, 2010).

3.1.4.3 The Gradually Varied Flow Region and the Uniform Flow Region (Regions 3 and 4)

Fully developed two-phase flow is found for both the gradually varied flow region and the uniform flow region. Downstream of the rapid varied flow region, the flow gradually changes form and flow characteristics towards those of a uniform flow envelope. Finally, a downstream equilibrium is reached in the uniform flow region, where the flow depth, velocity and mean air concentration values would not vary further down the stepped spillway (Amador, et al., 2004).

3.2 AIR ENTRAINMENT

3.2.1 The Boundary Layer

When a real fluid flows past a solid surface, the fluid is severely retarded in the vicinity of the surface boundary, due to viscous shearing action. The velocity at the surface is equal to zero (**Figure 3-8**). The layer of fluid adjacent to a surface where the viscous effects are evident is called the boundary layer (Webber, 1979).

Initially, the flow is laminar, with a parabolic velocity distribution where a laminar boundary layer is developed along the surface. At the transition point, the laminar flow becomes unstable and eddying starts. After a short transitional zone, full turbulence flow is developed.

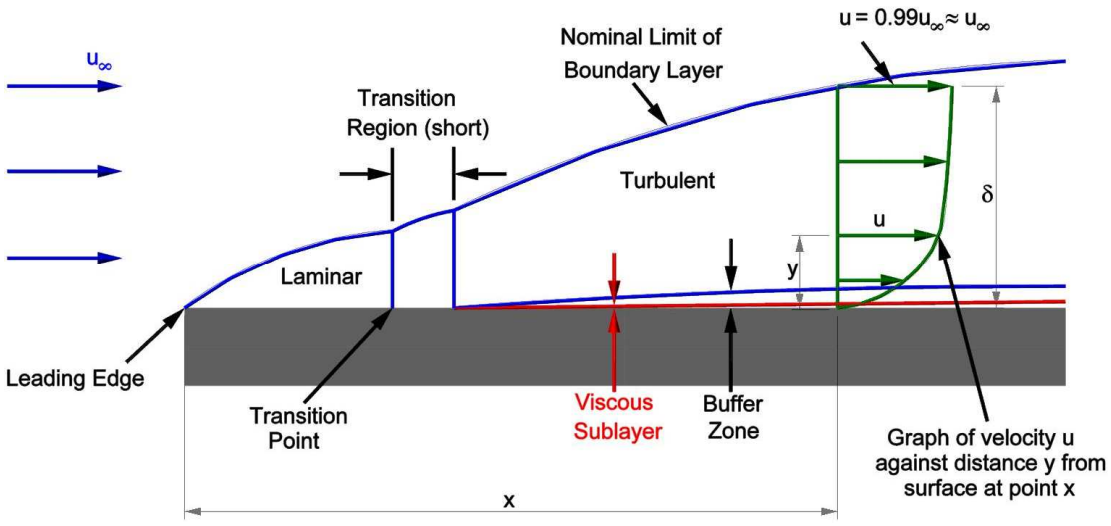

Figure 3-8: Development of boundary layer on a solid surface (Atencio, 2011)

The boundary layer thickness (δ) for a stepped spillway is defined as the perpendicular distance from the pseudo-bottom to where the velocity is equal to 99% of the maximum velocity (**Figure 3-8**). Chanson (1994) expressed the boundary layer development as follows:

$$\frac{\delta}{x} = a\left(\frac{x}{k_s}\right)^{-b} \quad \textbf{(3-5)}$$

where

δ = boundary layer thickness (m)

x = streamwise distance from the start of the boundary layer growth (which is the starting point accepted as the spillway crest in the case of a dam spillway) (m)

k_s = roughness height (m)

a, b = constants

When the boundary layer thickness reaches the free surface, air is entrained into the flow, as is described in **Subsection 3.1.4.1**. This point is known as the 'surface inception point'.

The rate of the boundary layer development is of relevance to this study, as an accelerated growth rate ensures an early onset of air entrainment into the flow. The growth rate of the boundary layer is a function of the roughness height (k_s) and of the flow discharge.

3.2.2 Surface Roughness

When the surface profile of any flow boundary is enlarged to a sufficient scale, it can be seen that the surface is comprised of irregular peaks, valleys and rough protrusions. The effective height of all the surface irregularities is known as the roughness height (k_s). The roughness height for a conventional 'smooth' surface boundary is represented in **Figure 3-9**.

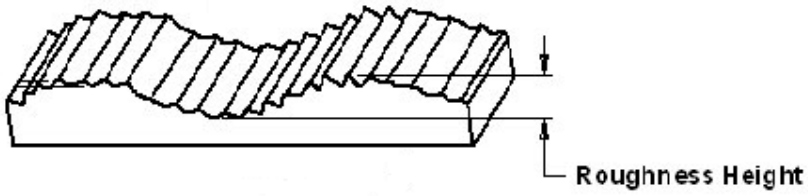

Figure 3-9: Roughness height for surface boundary

The roughness height for a stepped spillway is defined as $k = h\cos\theta$. As observed, a change in step height (h) and spillway angle (θ) influences the thickness and rate of development of the boundary layer.

3.2.3 Inception Point

The point of surface inception is defined in **Subsection 3.1.4**, with reference to **Figure 3-7**. The location of the inception point is important for the designer of a stepped spillway, as it provides a reasonable estimate of the developing flow region (unaerated spillway zone) that is prone to cavitation due to large, fluctuating subatmospheric pressures.

The following authors, who have done considerable research into the field of air entrainment, have, subsequently, published various formulas to help determine the point of inception along the stepped spillway. The different formulas are discussed in this section under subheadings naming various authors who have contributed to the related literature in this field, and an overall review is presented in **Subsection 3.8.1**. Note that, if it is not specifically stated, the inception point that is referred to in this section can generally be defined as the surface inception point.

3.2.3.1 Wood, et al. (1983)

The author concluded that air is entrained into the flow due to the energy of the turbulent eddies once the boundary layer has reached the surface. Wood, et al. (1983) used laboratory studies with dimensional analysis to establish the point of inception from the crest for a smooth concrete spillway. The nondimensional power formula is shown below:

$$\frac{L_i}{k_s} = 13.6 \ \sin\theta^{0.0796} \ \mathrm{Fr}_*^{0.713} \qquad \textbf{(3-6)}$$

where

k_s = roughness height (m)

with k_s being defined as:

$$k_s = h \times \cos\theta \qquad \textbf{(3-7)}$$

3.2.3.2 Chanson (1994)

The author expanded on the work done by Wood, et al. (1983) to develop an equation representing the distance to inception for stepped spillways. The validity of the research was confirmed by means of the use of observations from model studies on stepped spillways and gabions with spillway slopes ranging from 27° to 52°. The statistical analysis of the observation data showed that the inception point is best correlated by means of applying the following formula:

$$\frac{L_i}{k} = 9.719 \ \sin\theta^{0.0796} \ \mathrm{Fr}_*^{0.713} \qquad \textbf{(3-8)}$$

3.2.3.3 Matos (2000)

Matos (2000) showed, with experimental investigations based on air concentration and velocity measurements, that the inception point for a stepped spillway is located upstream of the location predicted by visual observation. With slopes approximately equal to 53.1°, the point of inception can be determined by use of the following equation:

$$\frac{L_i}{k} = 6.289\ \mathrm{Fr}_*^{0.734} \tag{3-9}$$

3.2.3.4 Boes and Minor (2000)

Hydraulic model experiments on skimming flow were conducted at the Laboratory of Hydraulics, Hydrology and Glaciology (VAW) of ETH Zurich, Switzerland on a 30° and 50° spillway. The authors` argue that the unaerated spillway length (L_i) from the spillway crest to the inception point is described by means of the following equation:

$$\frac{L_i}{k} = 9.72\ \mathrm{Fr_b}^{0.86} \tag{3-10}$$

with Fr_b denoted as the Froude number, which is slightly different to Fr_*:

$$Fr_b = q_w / \sqrt{g\ \sin\theta\ \mathrm{h}^3} \tag{3-11}$$

3.2.3.5 Chamani (2000)

A model was built, adjusted for two different slopes at 51° and 59°, respectively, to investigate the air inception characteristics for skimming flow on a stepped spillway. A high-speed video camera was used to analyse flow properties during air entrainment. Measurements of distance (L_i) to the inception point were used in conjunction with the image data to derive an empirical equation for estimating the location of the inception point, as follows:

$$\frac{L_i}{k} = 8.29\ \mathrm{Fr_i}^{0.85} \tag{3-12}$$

with F_i derived as:

$$Fr_i = q_w / \sqrt{g\ \frac{h}{l}\mathrm{k}^3} \tag{3-13}$$

and

l = step tread length (m)

3.2.3.6 Boes and Hager (2003b)

The point of inception for this particular study was defined as the location where the pseudo-bottom air concentration is equal to 1%. The air concentration was measured using fibre-optic instrumentation. The model was configured at three different slopes, namely at 30°, 40° and 50°, and all measurements were conducted during the skimming flow regime. The equation presented by Boes and Hager (2003b) is given below:

$$\frac{z_i}{h} = 5.90\ \mathrm{Fr_b}^{0.80} \quad \textbf{(3-14)}$$

where

z_i = vertical distance from crest to inception point (m)

3.3 AIR CONCENTRATION

3.3.1 Streamwise Development of Air Concentration

The local air concentration for a spillway chute is defined as the volume of air per unit volume over an averaged time period (Matos, 2000). The air concentration in the water flow varies along the spillway, until a steady mean air concentration is reached in the uniform flow region. The mean air concentration figure is a broad term that can be classified as the depth-averaged local air concentration at a certain point along the spillway chute, or as the homogenous air concentration within the uniform flow region.

The development of the mean depth-averaged air concentration at any point along the spillway chute can be expressed as (Matos, 2000):

$$C_m = \frac{1}{Y_{90}} \int_0^{Y90} C\ (y)\ dy \quad \textbf{(3-15)}$$

where

C_m = depth-averaged mean air concentration

Y_{90} = depth at which local air concentration is equal to 90% (m)

C = local air concentration

3.3.1.1 Air Concentration along a Stepped Spillway

Air concentration along the length of the spillway can also be categorised into three distinct regions that are best described by **Figure 3-10**, as taken from Meireles, et al. (2007).

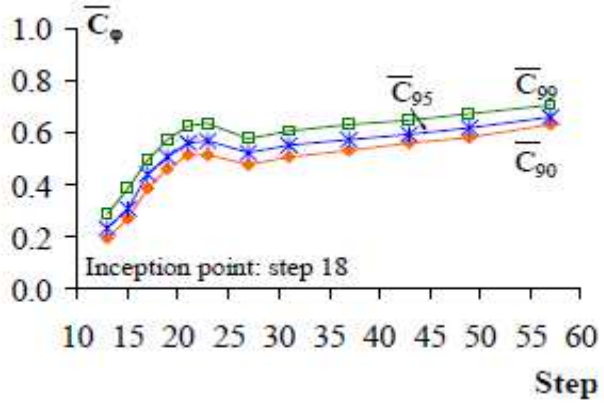

Figure 3-10: Mean air concentration (C_{90}, C_{95}, C_{99}) along stepped spillway (53.1°) for h = 4 cm; q_w = 0.08 m³/s (Meireles, et al., 2007)

i. The first region is centralised about the inception point (step 18), where the mean air concentration increases rapidly and attains a maximum local value (step 23) for a short distance. The increase of air concentration can be attributed to air being entrained into the flow at the surface inception point.

ii. For the subsequent downstream region, the air concentration decreases from the maximum value that was reached (step 23) towards a minimum local value (step 27) along the chute. The reason for decreased air concentration is believed to be the curvature of flow that is found in this region, which tends to promote the release of air bubbles (Matos, 2000).

iii. Within the third and final region, a steady increase of air concentration is observed. The mean air concentration approaches the equilibrium value of self-aerated flows at the downstream end of the chute. This flow region is commonly known as the uniform flow region. **Figure 3-10** does not indicate the self-attained equilibrium state of air concentration within the flow, with only the stable increase being shown prior to uniform flow.

3.3.1.2 Air Concentration over Flow Depth

Figure 3-11 illustrates the depth-averaged air concentration across the flow depth at various x/L_i positions, where x is the streamwise coordinate originating from the spillway crest, s is defined as the step height, and h_c as the critical flow depth. The symbol z represents the flow depth measured normal to the pseudo-bottom, with z = 0 being at the pseudo-bottom. The flow depth (z) is normalised with the depth at which air concentration is 90% (h_{90}).

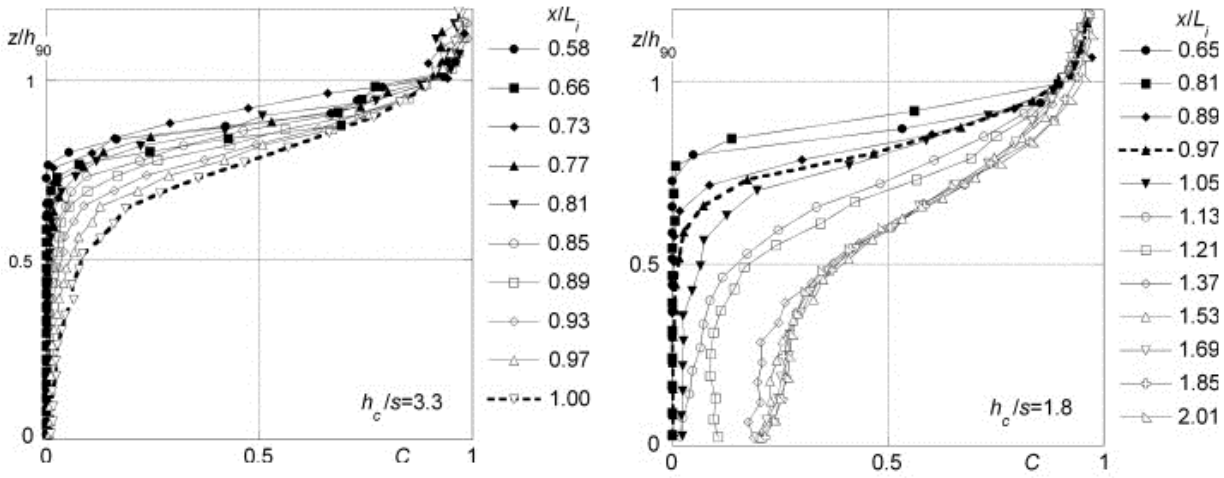

Figure 3-11: Normalised air concentration profiles across the flow depth for a 50° chute (Pfister & Hager, 2010)

The air concentration over the flow depth for a conventional stepped chute follows an S-shaped pattern, with a limited increase in air concentration for points located upstream of the inception point (x/L_i = 1.0), and a substantial air increase downstream of the inception point.

As shown in **Figure 3-11**, the air distributed upstream of the inception point (in the developing flow region) along the pseudo-bottom exists in very small quantities, whereas, downstream of the inception point, the air concentration increases to an equilibrium value of approximately 25%.

3.3.1.3 Pseudo-bottom Air Concentration

Air concentration at the pseudo-bottom is an important consideration for this study. A bottom air concentration of about 5-8% is regarded as sufficient to avoid cavitation damage to a containment surface, due to the compressibility of the air-water mixture that can absorb the impact of imploding vapour-filled bubbles (Peterka, 1953).

The pseudo-bottom air concentration down a stepped chute is normally characterised as follows:

i. Generally speaking, no air concentration is found upstream of the inception point (in the developing flow region) but very small concentrations do prevail close to the pseudo-bottom. These air concentration levels are not, however, sufficient to prevent cavitation.

ii. At the pseudo-bottom inception point, the time-averaged air concentration is approximately 1%.

iii. The air concentration increases beyond 5% downstream of the pseudo-bottom inception point, until an equilibrium flow condition is reached, where the time-averaged bottom air concentration does not vary.

The percentage of air concentration downstream of the pseudo-bottom inception point for a conventional stepped spillway is considered adequate to prevent or reduce downstream cavitation damage, but it is not adequate upstream to prevent or reduce large discharges. Therefore, it is evident that the designer should either aim to initiate an earlier onset of air entrainment, or to artificially introduce air into the flow, when considering cavitation prevention for large discharges.

3.3.2 Pseudo-Bottom Inception Point

The pseudo-bottom interception point is defined as the time-averaged point where the air concentration (C_b) at the pseudo-bottom is equal to 1% (Boes & Hager, 2003b). Pfister and Hager (2010) visually observed flow behaviour in a range of experiments that were conducted using a high-speed camera in the vicinity of the bottom inception point. The visual findings of Pfister and Hager (2010), whereby they explained the entrainment mechanism of air to the pseudo-bottom, is pictorially summarised in **Figure 3-12**.

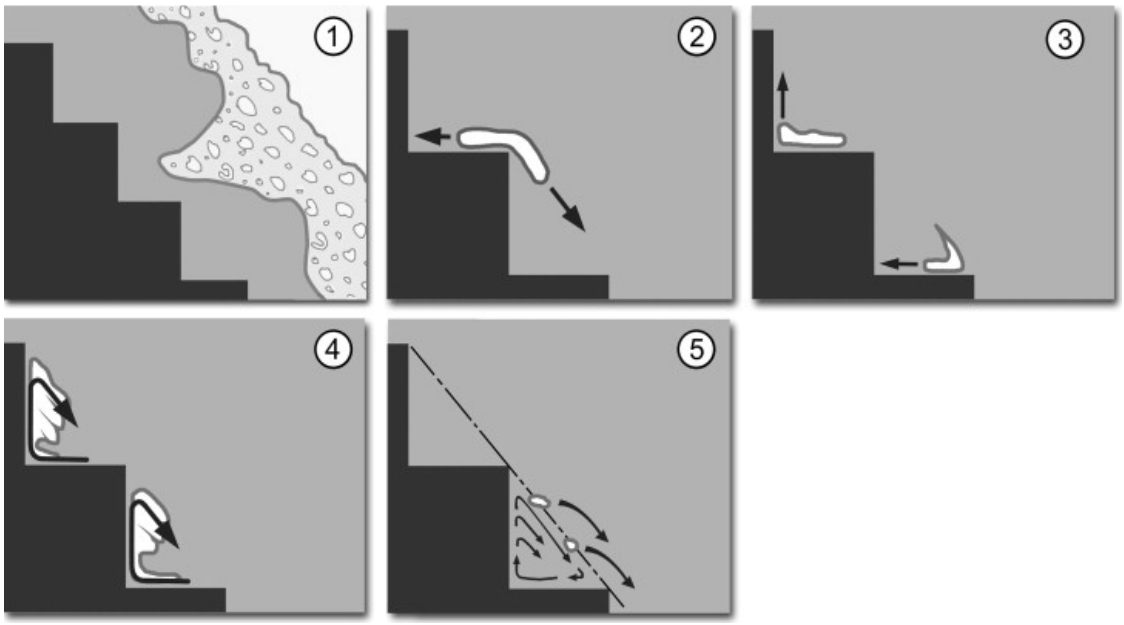

Figure 3-12 (1-5): Schematic view of pseudo-bottom air inception (Pfister & Hager, 2010)

1. The flow at this point is fairly turbulent, with significant surface waves, combined with a bubbly flow. The troughs of the surface waves occasionally protrude to the pseudo-bottom. When the pseudo-bottom is reached, the trough impinges onto the horizontal step edge. Due to the velocity gradient, the trough is cut off from the flow surface (not shown), and it is covered by non-aerated flow, with the result being an air pocket that remains at the step edge. The air pocket on the step edge is shown in picture no. 2.

2. The air pocket that impinged onto the horizontal step is separated, and the air migrates to both step niches.

3. Air is entrained into the niche vortex regions, due to the subatmospheric conditions generated within the vortex.

4. The air is rotated by means of the vortex to the pseudo-bottom, which is also aided by the fact that air bubbles rise. Air is detrained from the step niches over a couple of vortex revolutions by means of instantaneous ejections of air into the mainstream flow (picture no. 5).

The cycle is repeated whenever another surface trough extends to the pseudo-bottom. Due to this phenomenon, it is evident that the bottom inception point varies instantaneously over a range of steps. As a result, the air concentration (C_b) also fluctuates around 1% among aeration cycles, which results in a time-averaged concentration (C_b) of 1%.

3.3.3 Pre-Aeration of Spillway Bottom

Model studies, with a chute aerator placed at the first step, were conducted (Pfister, et al., 2006) to investigate the possibility of aerating the bottom portion of the flow to counter cavitation. The results of this study showed that air concentration increases sharply close to the pseudo-bottom, directly downstream of the aerator, but it dissipates before the natural inception of air is attained. From the inception point, the air concentration within the flow is dictated by normal surface air entrainment. (Refer to **Figure 3-13**.)

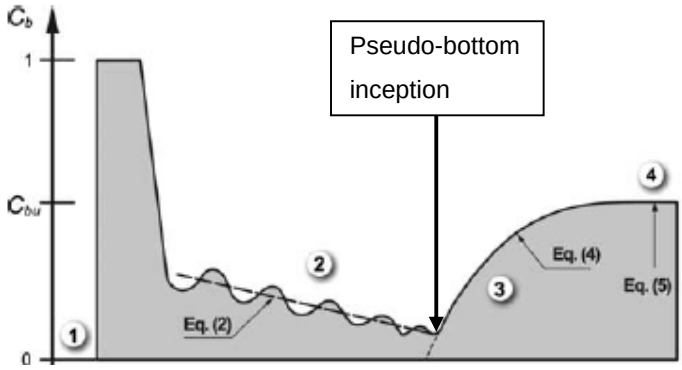

Figure 3-13: Pseudo-bottom air concentration for a stepped spillway with bottom aerator (50º) for model parameters of h = 9.3 cm; q_w max = 0.86 m³/s (Pfister, et al., 2006)

Pfister, et al. (2006) argue that the significant decline of air concentration downstream of the aerator, in the above-mentioned model, can be attributed to the jet impact of the flow on the horizontal step, and to the generation of highly aerated transverse vortices that lose air by means of rolling up on the step riser. It was observed that the 'lost' air bubbles that rose from the air boundary layer at the pseudo-bottom were absorbed by the upper non-aerated flow section, thus removing the entrained air before it could reach the areas prone to cavitation, which are located in the proximity of the inception point.

In summary, the findings of this research regarding the pre-aeration of a stepped spillway show that:

- A large amount of air is entrained directly downstream of the aerator.
- Significant detrainment of air follows initial entrainment.
- Air concentration decreases steadily towards the pseudo-bottom inception point.
- Post pseudo-bottom inception, the air concentration reaches a uniform value that agrees with findings from a stepped spillway with no pre-aeration capabilities.

3.4 PRESSURE

So as to be able to investigate cavitation damage to a stepped spillway chute, the designer has to take into account the role of pressure fluctuations on the vertical and horizontal step faces. The formation of vapour-filled voids, which leads to cavitation, occurs within areas of low pressure. The study of minimum pressures zones that occur along stepped spillway during flow discharge forms part of the current research objective.

3.4.1 Pressure Profile along a Stepped Spillway

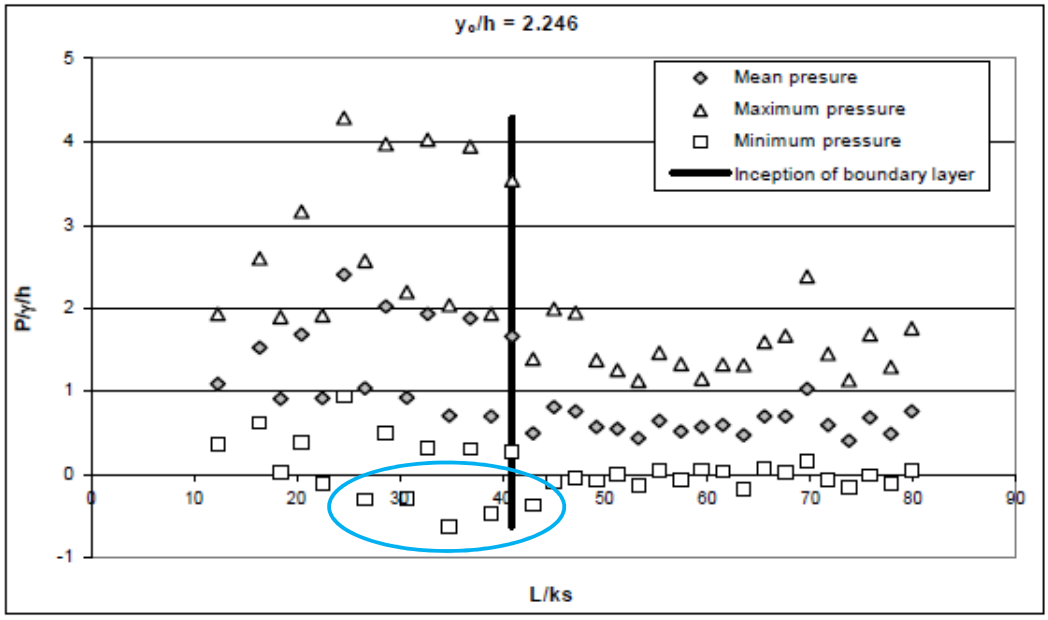

Figure 3-14: Pressure evolution along stepped chute for $y_c/h = 2.26$ (Sànchez-Juny, et al., 2000)

The fluctuating pressure profile along a stepped chute, as indicated in **Figure 3-14**, is separated into two regions, with the point of inception acting as the border between the two regions. The smaller minimum pressures and larger maximum pressures are located upstream of the point of inception. Downstream of the inception point, the fluctuation of pressures is reduced by the introduction of air into the flow.

The presence of air creates a cushioning effect that reduces the fluctuating pressure range over the steps concerned (Amador, et al., 2003).

The blue encircled values in **Figure 3-14** indicate the area where minimum pressure fluctuations occur along the spillways chute. Studies by Amador, et al. (2003; 2009) and Sànchez-Juny, et al. (2000) have shown that such minimum pressures occur in the developing flow region, near the inception point.

Amador, et al. (2009) conducted experiments on a stepped spillway, using pressure taps located on the horizontal outer step edge, and on the upper half of the vertical step. The pressure along the spillway is described in terms of the mean pressure (C_p) and the root mean square pressure (C_p') coefficients to the dimensionless distance from the inception point (s`), which are defined as:

$$s' = \frac{L - L_i}{y_i} \quad \textbf{(3-16)}$$

with C_p defined as:

$$C_p = \frac{p_m/\gamma}{U_m/2g} \quad \textbf{(3-17)}$$

where

C_p = mean pressure coefficient

U_m = mean velocity (m/s)

and C_p' defined as:

$$C_p' = \frac{\sigma_m/\gamma}{U_m{}^2/2g} \quad \textbf{(3-18)}$$

where

C_p' = root mean square pressure coefficient

σ_m = root mean square of pressure fluctuations (Pa)

Figure 3-15 and **Figure 3-16** illustrate the evolution of C_p and C_p' on the horizontal steps along the spillway for a range of discharges, represented as critical flow depth (y_c) over step height (h). It should be noted that the maximum values for each of the two respective graphs are located near the region of air inception (s' = 0). **Figure 3-17** represents the C_p' values along the length of the spillway for the pressure taps located on the vertical steps. A similar trend in the data is observed, compared to the results obtained with the use of the horizontal steps, with the greatest pressure fluctuation occurring close to inception.

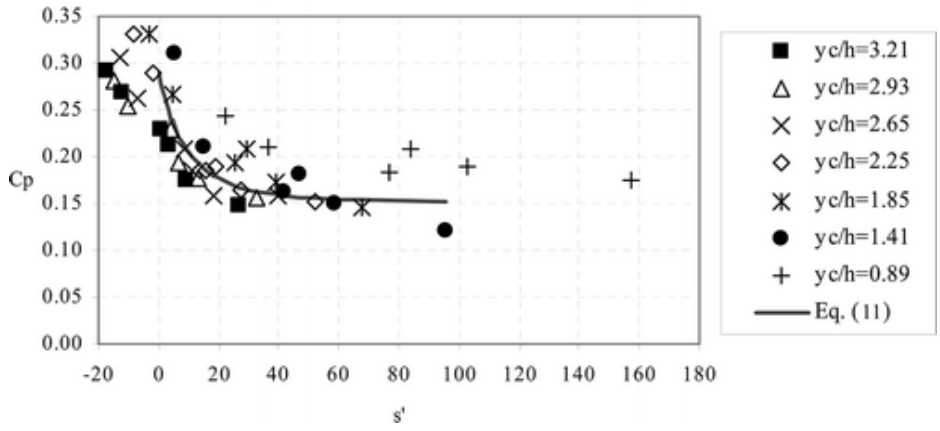

Figure 3-15: Mean pressure coefficient as a function of s', with pressure taps located at the outer edge of the horizontal steps (Amador, et al., 2009)

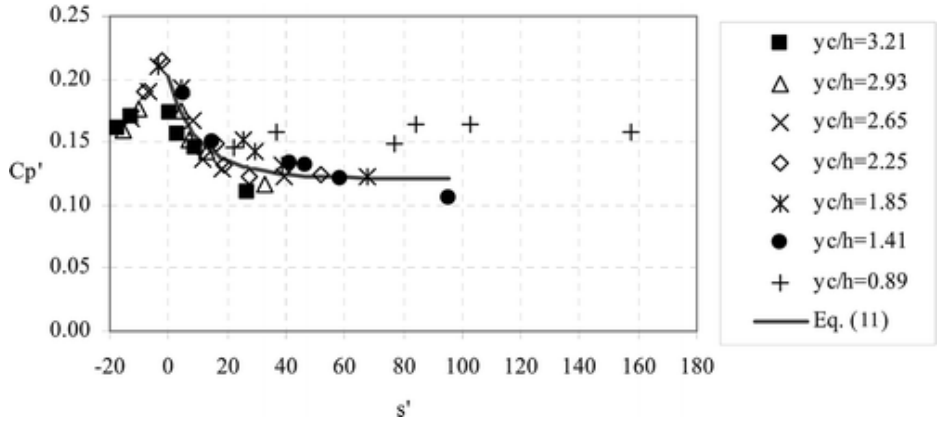

Figure 3-16: Root mean square pressure coefficient as a function of s', with pressure taps located at the outer edge of the horizontal steps (Amador, et al., 2009)

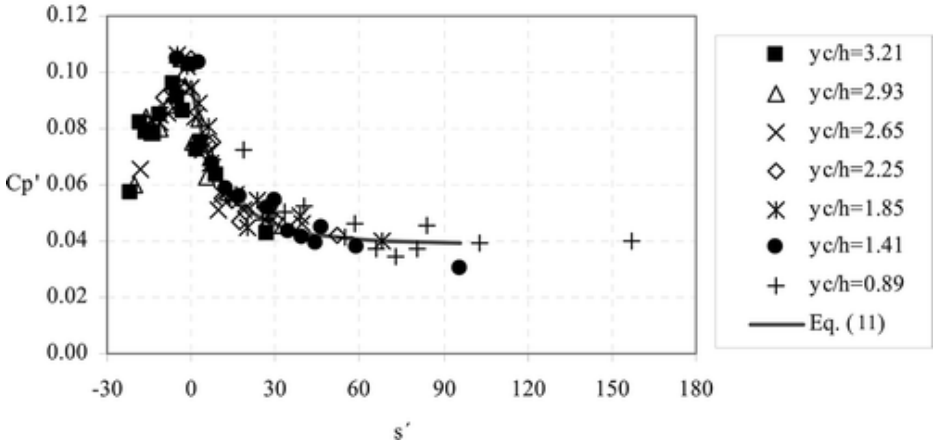

Figure 3-17: Root mean square pressure coefficient as a function of s', with pressure taps located at the upper half of the vertical steps (Amador, et al., 2009)

3.4.2 Pressure Profile on Step Faces

To investigate the pressure distribution for the spillway step riser and tread, a general understanding of the flow behaviour on a stepped profile is required. **Figure 3-18** indicates a typical streamline pattern, and the pressure distribution for a single identified step. A brief description is presented below with the aid of **Figure 3-18** to illustrate the different pressure profiles relating to the skimming flow regime.

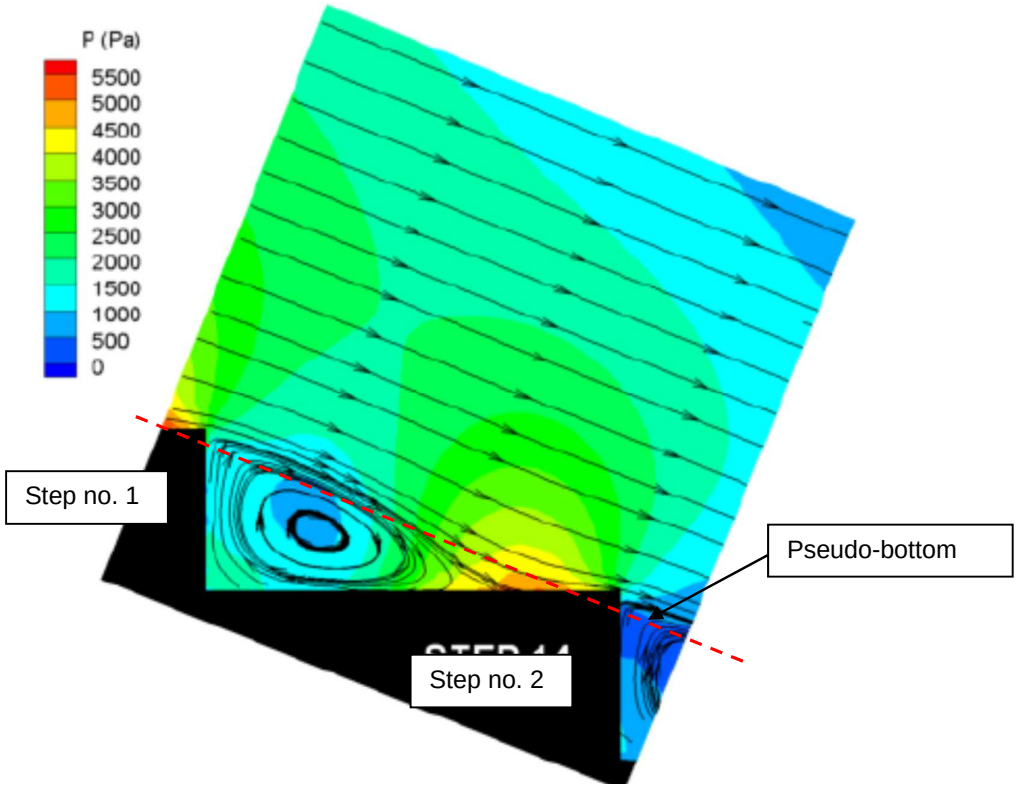

Figure 3-18: CFD stepped chute pressure and streamline simulation result (Frizell, et al., 2013)

Horizontal step face

- The flow along the pseudo-bottom (upstream of step 1) impinges on the horizontal front-end of the lower step (step 2). The impact of flow creates a large positive force on the step face, which is also the location of maximum pressures fluctuation. The slope of the chute depicts the area of impact on the step.
- The impact of flow creates separation of flow. Flow is both ejected into the mainstream flow, and directed into the vortex on step 2.
- The recirculation motion for the vortex that is created by the flow separation is maintained by the transmission of shear stress of the mainstream flow.
- The low-pressure zone on the step face is a result of the subatmospheric conditions within the vortical structure.

Vertical step face

- The area close to the horizontal step experiences positive pressure, due to the impact of the recirculating flow produced by the vortex.
- Near the outer edge of the step riser (step 2), minimum pressures are observed for the vertical step faces. This low-pressure zone occurs due to flow separation over the step edge. It is possible that, for large discharges, the fluctuating pressures within this region can generate negative values.
- The results of a separate numerical simulation study shown in **Figure 3-19** further illustrate the negative pressure zones that can develop on the upper step riser in a fully developed skimming flow regime.

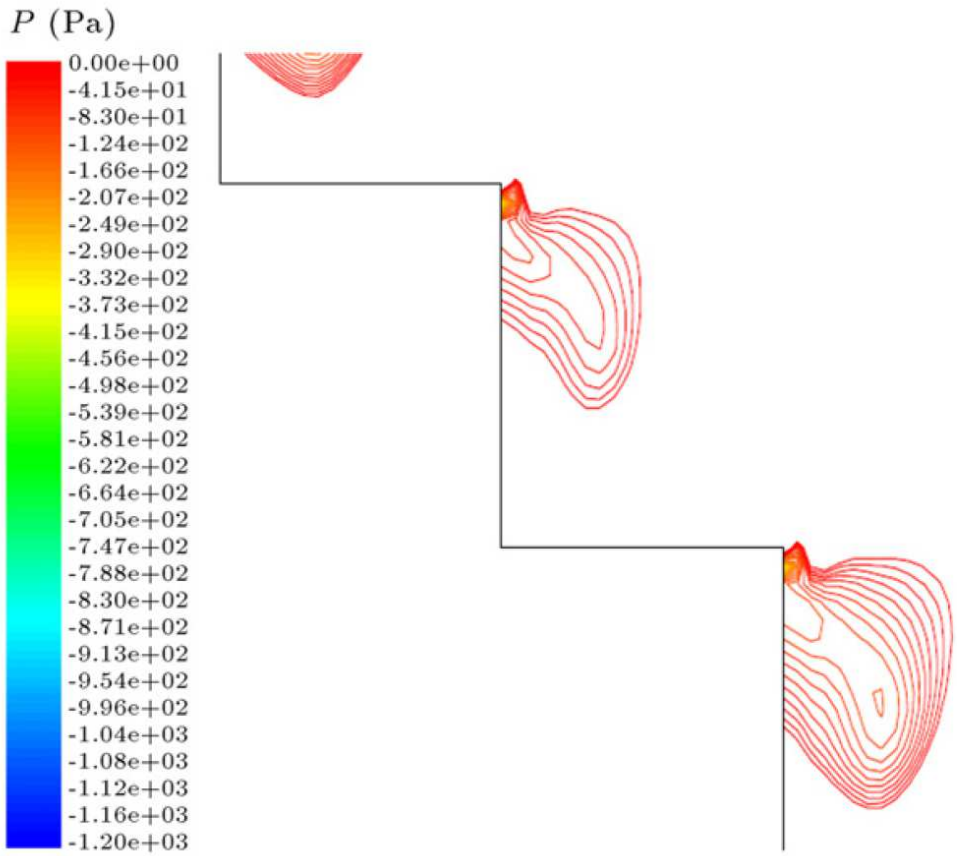

Figure 3-19: Numerical simulation depicting the negative pressure zones on the upper vertical step face for a 45° spillway slope (Nikseresht, et al., 2013)

As described above, the maximum pressures are generated on a stepped spillway surface by means of flow impacting on the horizontal step face, with the occurrence of minimum pressures being due to the flow separation at the vertical step edge.

The phenomenon described is supported by the results of another numerical and separate physical model study. The numerical study simulated the pressures for the horizontal and vertical step faces within the non-aerated zone (i.e. upstream of the inception point), which are shown in **Figure 3-20** and **Figure 3-21**.

Figure 3-22 indicates the minimum and maximum pressures experienced on the vertical (A) and horizontal (B) step faces for the physical model study. The results are presented in dimensionless parameters.

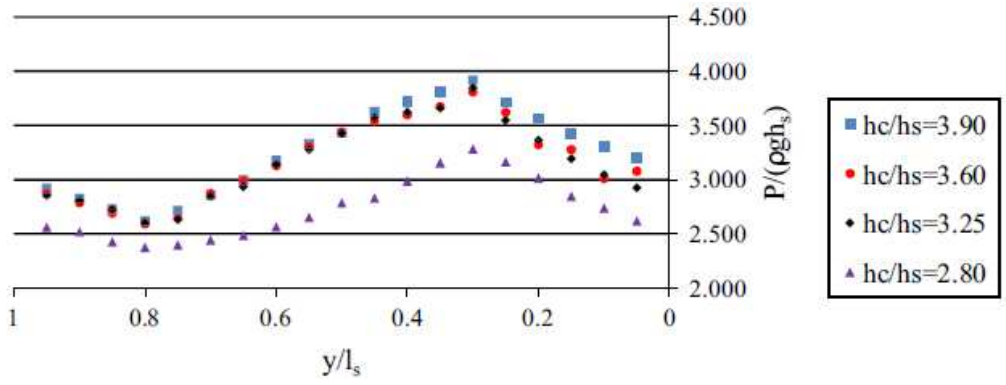

Figure 3-20: Pressure distribution along a horizontal step face, with hc = height above crest weir and hs = step height (Husain, et al., 2014)

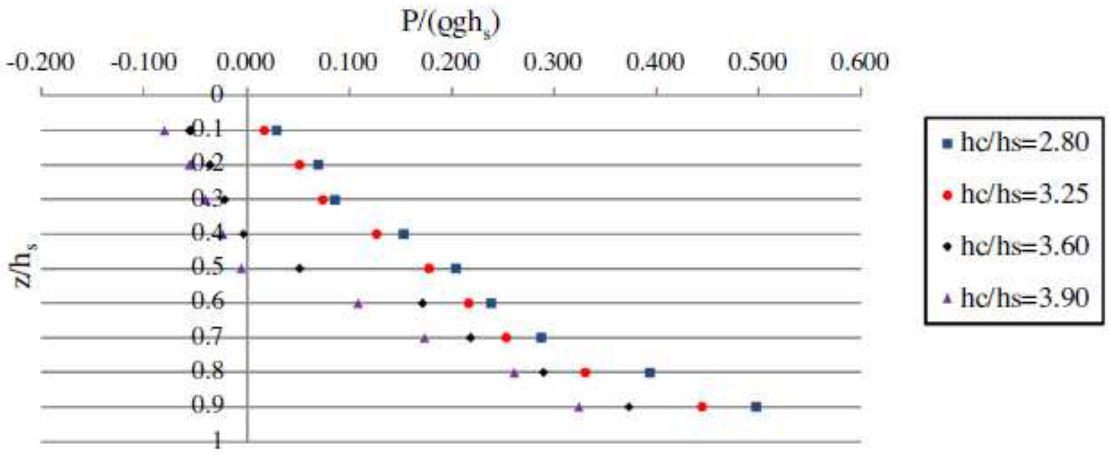

Figure 3-21: Pressure distribution along a vertical step face, with hc = height above crest weir and hs = step height (Husain, et al., 2014)

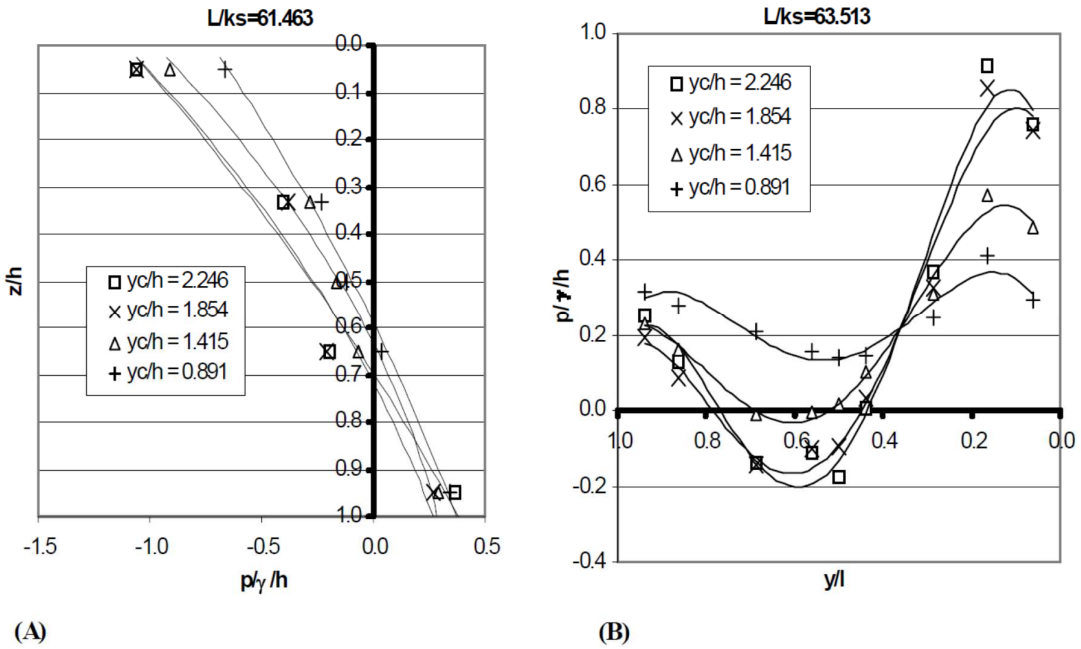

Figure 3-22: Profiles of minimum and maximum pressure on the (A) vertical and (B) horizontal face of a step (Sànchez-Juny, et al., 2000)

It is evident from **Figure 3-20** to **Figure 3-22** that, for an increase in discharge, the pressures on the horizontal step tend to increase, and the pressures at the vertical step edge tend to decrease.

3.5 CAVITATION

3.5.1 Introduction

For large unit discharges on a stepped spillway, low-pressure zones develop within the step cavities, potentially leading to cavitation corrosion. Cavitation occurs whenever the pressure in the water flow drops to a pressure value that is lower than the saturated water vapour pressure at the prevailing temperature. The cavities that form are caused by the evaporation of vapour and gases from the water when the vapour pressure exceeds the pressure in the low-pressure zones in the water body.

When the ‘bubbles' concerned are carried into regions of high pressure, the vapour quickly condenses, and the bubbles implode, resulting in the cavities being suddenly filled by the surrounding water (Novak, et al., 2007).

The implosion of the cavities is not only noisy, but, more importantly, the violent implosion of the cavities on a containment surface, over a sustained period of time, can cause substantial damage, or even failure, to the structure. Low pressures on a stepped chute surface, as were briefly discussed in **Section**

3.4, occur at points of separation of the water flowing alongside fixed boundaries, particularly if the flow velocity is high.

Pre-emptive measures for cavitation protection include:

- Creating as 'smooth' as possible surface boundaries.
- Hardening boundaries by means of polymerised concrete, epoxy resins, and other related materials.
- Introducing air at endangered areas.

The first two preventive measures are expensive, as well as being difficult to apply and maintain for a hydraulic structure. The aeration of flow, however, also poses difficulties in terms of the engineering design, but it has been proven to be very effective in raising instantaneous low pressure, thus reducing cavitation.

3.5.2 Cavitation on Stepped Spillways

To date, no cavitation damage has been documented for an in-service stepped spillway; however, the design practices relating to stepped spillway discharges have been somewhat conservative (Frizell, et al., 2013). The increased popularity of the stepped spillway has directed research towards studying the inception of cavitation in more detail than has been undertaken before. Relevant information from literature on this subject is presented under the subheadings featuring authors' surnames below.

3.5.2.1 Boes and Hager (2003b)

The authors measured the air concentration at the pseudo-bottom within the skimming flow regime using a fibre-optic probe. The model was configured at three different slopes, namely 30°, 40° and 50°. A mathematical relationship was developed between the measured bottom air concentration and the distance beyond the inception point. Based on the experimental research undertaken by Peterka (1953), minimum bottom air concentration values of C_b = 5% and 8% are required to prevent cavitation damage. Using the minimum values stated, the authors employed the mathematical relationship concerned to determine the critical distance from the inception point to where the bottom air concentration reaches the required minimum values. The distance to inception was based on **Equation (3-14)**, which was also derived by the authors. The critical distance downstream from the inception point is:

C_b = 5%

$$L_{cr} = 5.0(\sin\theta)^{-2.3} \quad \textbf{(3-19)}$$

C_b = 8%

$$L_{cr} = 10.0(\sin\theta)^{-3.0} \quad \textbf{(3-20)}$$

Due to the aeration being more pronounced in the prototype than it is in the model, the authors suggest using **Equation (3-19)** for design purposes. With a given spillway slope (θ), the designer can now determine whether critical velocity (at the inception of cavitation) is attained upstream of the calculated critical area (L_{cr}). The authors express a belief that velocities upstream of the critical point should be limited to 13-20 m/s.

3.5.2.2 Amador, et al. (2009)

Pressure measurements were recorded in a model with a bottom inclination of 51.3°. Minimum pressures were observed at the upper half of the vertical step riser. Using a 0.1% probability of minimum pressures occurring within this region, a limiting velocity of 15 m/s at the inception point was recommended.

3.5.2.3 Frizell, et al. (2013)

The authors concerned specifically focused their research on cavitation for stepped spillways by studying flow over a stepped profile in a specialised low-ambient pressure chamber under vacuum conditions. Tests conducted at these low pressures enabled the authors to observe cavitation formation.

The cavitation was found to originate in two areas where subatmospheric conditions were experienced, namely in the upper half of the vertical step riser, and within the vortical structure located in the step cavity. **Figure 3-23** depicts this phenomenon.

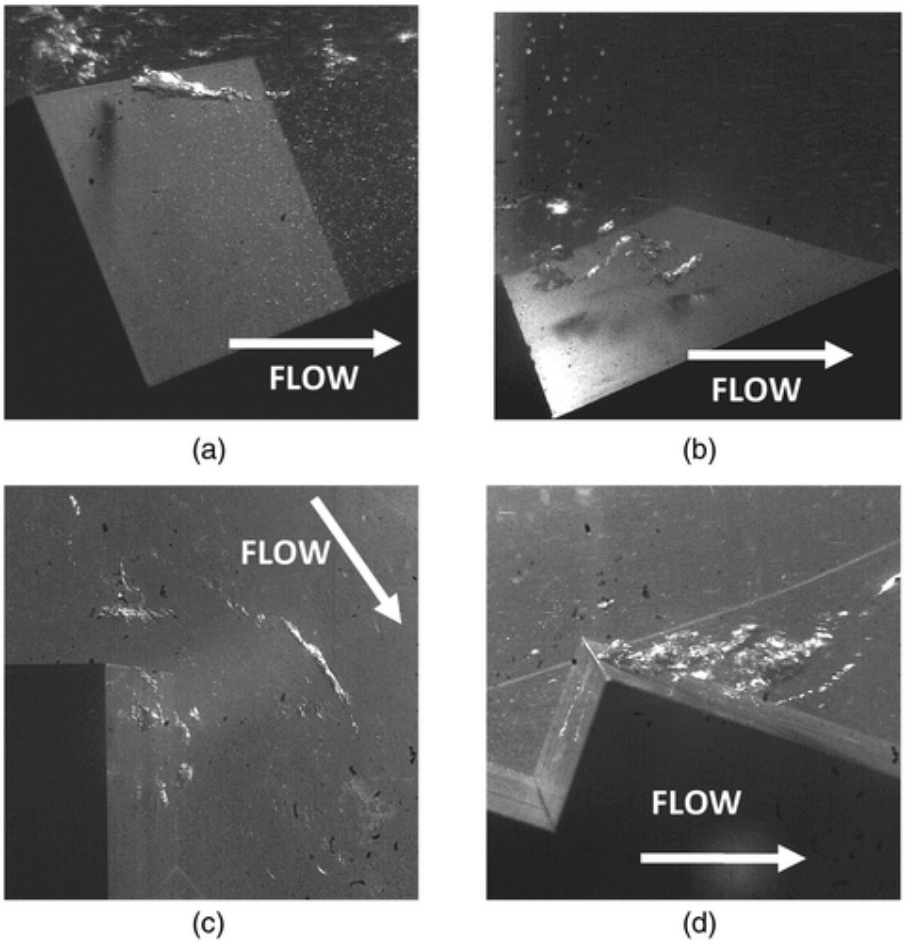

Figure 3-23: Cavitation inception for 21.8° (a, b) and 68.2° (c, d) slopes (Frizell, et al. 2013)

The authors concluded their study by providing a correlation between the spillway friction factor (f) and the cavitation index (σ_{cr}), in the following form:

$$\sigma_{cr} = 4 \times f \quad \textbf{(3-21)}$$

In terms of the model under discussion, the spillway designer is now able to calculate the cavitation index for a range of discharges, by means of using various friction factor formulas that are available in the research field. The formulas concerned are not discussed in the current thesis.

3.5.2.4 Pfister, et al. (2006)

The authors recommend that each step should be treated as a surface irregularity, such as one would normally view at offset on a smooth surface. Based on this approach, it is possible to determine the cavitation index for stepped chutes using conventional methods applied to smooth spillways.

The critical cavitation index (σ_{cr}) is calculated as follows:

$$\sigma_{cr} = \frac{p_g + p_{atm} - p_v}{U_{wi}{}^2/2g} \quad \textbf{(3-22)}$$

where

p_g = gauge pressure (Pa)

p_{atm} = atmospheric pressure (Pa)

p_v = vapour pressure (Pa)

U_{wi} = clear water velocity at inception point (m/s)

The principle underlying this approach was also based on the viewpoint that, downstream of the inception point, cavitation would not occur, due to the self-aeration of the flow. Hence, maximum velocities are obtained at the inception point.

The authors also note that current design guidelines recommend maximum unit discharges of up to 30 m²/s.

3.6 SPILLWAY CREST PIER

3.6.1 General

Piers located on a spillway crest provide structural support either to discharge gates, or to an overhead bridge. The effective width of the spillway is reduced by the number of piers concerned, combined with the respective contraction coefficient of the pier shape. Additional spillway width must be provided to maintain a unit discharge that is similar to that of a spillway containing no piers.

If it is not possible to increase the crest length, while the intended rate of discharge is to be preserved, it must be accepted that the design head over the spillway would, inevitably, increase.

3.6.2 Flow Separation

When a fluid moves past a stationary body, a boundary layer develops around the object's surface, due to viscous shearing forces. **Figure 3-24** depicts a fluid passing a circular obstacle, where a boundary

layer forms at the upstream side of the obstacle. Flow accelerates as it moves around the obstacle that offsets the retarding action of viscous stress acting within the boundary layer. Subsequently, this leads to the boundary layer remaining relatively thin. As the flow approaches the separation point, the viscous stress, in conjunction with the adverse pressure gradient, reduces the energy and forward momentum of the fluid, which causes the thickness of the boundary layer to increase sharply (Webber, 1979).

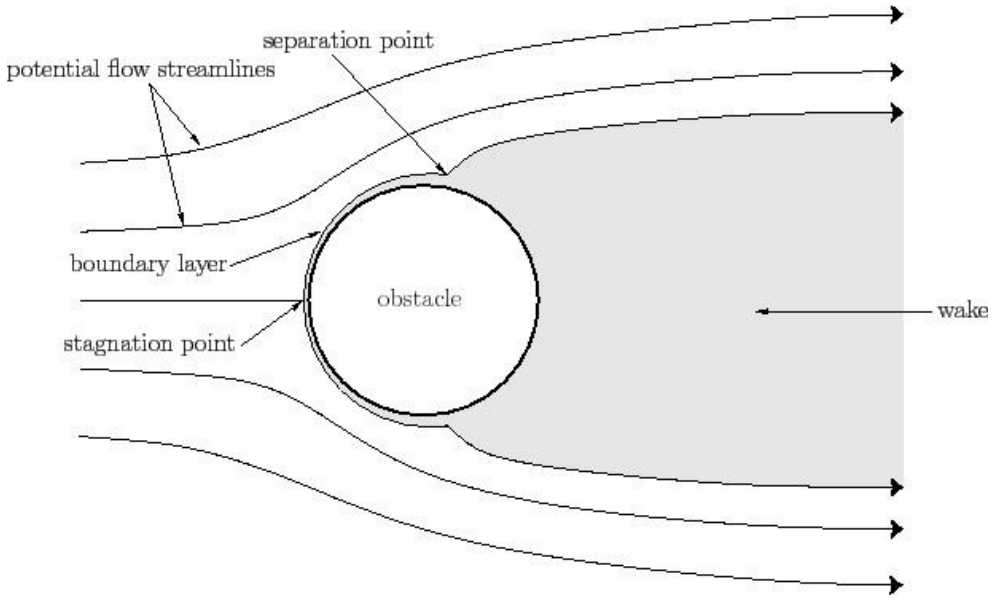

Figure 3-24: Boundary layer flow separation (Fitzpatrick, 2012)

Flow separation occurs when no further retardation of the fluid can take place without the reversal of flow. At this point, the velocity of the boundary layer falls to zero, and fluid becomes detached from the object's surface where turbulent eddies are generated downstream, which is commonly known as the 'wake'.

The shear stress at the separation point is equal to zero, with pressures tending to be lowest at this point of all points, which can lead to cavitation.

3.6.3 Wake Turbulence

For a flow with low velocities and, subsequently, low Reynolds numbers, large and weak vortices form in a symmetrical fashion downstream of the obstacle. With increasing velocity, eddies start to detach themselves from either side of the obstacle, and to form a row of vortices in its wake, known as the 'vortex street'. (Refer to **Figure 3-25**.)

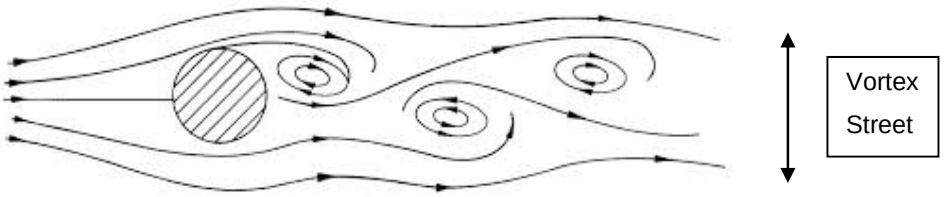

Figure 3-25: Wake known as the 'vortex street' (Turk, 1996)

The alternate shedding of vortices causes the flow separation point to fluctuate in position, correspondingly modifying the pressure distribution around the obstacle, which induces variable lateral thrust. The periodic lateral forces acting on the obstacle can bring about vibration, and, if the frequency of the vibration is similar to the natural frequency of the obstacle, resonance occurs.

3.7 SCALE EFFECT

3.7.1 Hydraulic Similarity

Various design aspects of dam spillways can be tested and modelled for a wide range of conditions with the use of a scaled physical model of the design prototype. Such an exercise at full scale would not be financially feasible; therefore, model studies were performed on a smaller scale to enable the evaluation of the expected hydraulic performance of the prototype.

Recent advances in computer technology have promoted more widespread use of numerical analysis that has been aimed at conducting preliminary investigations of the proposed prototype. Computer-aided models, which can be produced at full scale, can be used to solve complex hydraulic equations without the financial and laboratory constraints that are normally experienced with physical models. However, the results of a numerical model have to be compared to those of a physical model, so as to verify the computed results.

The results of the model study, critically, should represent the expected performance of the prototype. The laws of hydraulic similarity govern the relationship between the model and the prototype's performance. As simultaneous compliance with the laws of similitude is impossible, some discrepancies are unavoidable when extrapolating the results from the model scale to the full scale, with such discrepancies being known as scale effects (Webber, 1979).

The laws of hydraulic similarity encompass three different laws, namely those of geometric, kinematic and dynamic similarity, which are discussed in more detail below.

3.7.1.1 Geometric Similarity

Geometric similarity is similarity of shape that is obtained when the model and prototype, although being similar in shape, differ in size, according to the linear scale adopted. The ratio of any two dimensions in the model, therefore, corresponds to the ratio in the prototype (Webber, 1979). The geometric relationship can be expressed as follows:

$$\frac{(L_1)_m}{(L_2)_m} = \frac{(L_1)_p}{(L_2)_p} \quad \textbf{(3-23)}$$

where

L = linear dimension (m)

m = model

p = prototype.

The ratio between a linear dimension in the model and the corresponding dimension in the prototype is defined as the 'scale factor', and it is expressed as 1:x. The scalar relationship for the area is $1:x^2$, and for the volume is $1:x^3$ (Webber, 1979).

To achieve complete geometric similarity, the boundary roughness of the model should correspond to the prototype, as per the chosen linear scale. Obtaining the required boundary roughness of the model that corresponds to the linear ratio between model and prototype is not always possible, due to the nature of commercially available material for the model (Webber, 1979). However, for a stepped spillway chute, the scalar roughness, instead of being defined by the surface finish, is, rather, defined by the stepped profile of the spillway.

3.7.1.2 Kinematic Similarity

Kinematic similarity is the similarity of motion that implies that velocities and acceleration at homologous points and at homologous times for both systems should have the same ratio. The ratio for kinematic similarity is provided by the following relationship:

$$\frac{(v_1)_m}{(v_2)_m} = \frac{(v_1)_p}{(v_2)_p} \; and \; \frac{(a_1)_m}{(a_2)_m} = \frac{(a_1)_p}{(a_2)_p} \quad \textbf{(3-24)}$$

where

v = velocity (m/s)

a = acceleration (m^2/s)

Fulfilment of kinematic similarity produces flow patterns that are geometrically similar at corresponding times.

3.7.1.3 Dynamic Similarity

Dynamic similarity is the similarity of forces. To attain dynamic similarity, the forces at congruent points within the model and prototype system must have the same ratio, and they must act in the same direction. Thus, the following equation applies:

$$\frac{(F_1)_{\mathrm{m}}}{(F_2)_{\mathrm{m}}} = \frac{(F_1)_{\mathrm{p}}}{(F_2)_{\mathrm{p}}} \quad \textbf{(3-25)}$$

where

F = force (kN)

The component forces acting on a fluid system are pressure, gravity, viscosity, or surface tension. Algebraically, the conditions for dynamic similarity can be expressed as follows (Webber, 1979):

$$\frac{(F_{\mathrm{p}})_{\mathrm{p}}}{(F_{\mathrm{p}})_{\mathrm{m}}} = \frac{(F_{\mathrm{G}})_{\mathrm{p}}}{(F_{\mathrm{G}})_{\mathrm{m}}} = \frac{(Fv)_{\mathrm{p}}}{(Fv)_{\mathrm{m}}} = \frac{(F_{\mathrm{st}})_{\mathrm{p}}}{(F_{\mathrm{st}})_{\mathrm{m}}} \quad \textbf{(3-26)}$$

where

F_p = pressure force (kN/m^2)

F_G = gravity force (kN/m^2)

F_{ν} = viscosity force (kN/m^2)

F_{st} = surface tension force (kN/m^2)

The component forces are presented in dimensionless numbers that are known as Froude (gravity), Reynolds (viscosity), Webber (surface tension), and Euler (elasticity). To achieve perfect hydraulic similarity, the ratio between all the forces must be the same. In practice, however, this cannot be realised, due to the presence and significance of various forces that differ for different hydraulic structures. To achieve dynamic similarity, therefore, the dominant forces present must be identified, and the forces must conform to the similarity laws concerned.

3.7.2 Similarity Laws

3.7.2.1 Euler Law

The Euler law, which depicts the relationship between velocity and pressure, can be shown as:

$$E = \frac{V}{\sqrt{\frac{2\Delta p}{\rho}}} \quad \textbf{(3-27)}$$

where

E = Euler number (dimensionless)

V = velocity (m/s)

Δp = change in pressure (kN/m^2)

The Euler law is of particular relevance to enclosed fluid systems where turbulence is fully developed. Viscous forces are, then, insignificant in relation to the inertial forces. Subsequently, gravity and surface tension forces are entirely absent (Webber, 1979).

3.7.2.2 Froude Law

The Froude law applies to systems where the force of gravity and inertia force are the dominant factors influencing fluid motion. Typical application of the Froude law relates to spillways, weirs and open channels. The Froude law can be expressed as (Webber, 1979):

$$Fr = \frac{V}{\sqrt{gL}} \quad \textbf{(3-28)}$$

where

Fr = Froude number (dimensionless)

V = velocity (m/s)

L = characteristic length (m)

To comply with the Froude law, the corresponding velocities must be related, so that:

$$\frac{V_{\mathrm{p}}}{V_{\mathrm{m}}} = \frac{(gL_{\mathrm{p}})^{0.5}}{(gL_{\mathrm{m}})^{0.5}} = x^{0.5} \quad \textbf{(3-29)}$$

where

x = scale factor

3.7.2.3 Reynolds Law

As all real fluids have viscosity, the potential influence of viscous shear drag requires consideration. Reynolds law is applicable to systems where the forces of viscosity and inertia are the only forces acting on the system (Webber, 1979). Reynolds law can be expressed as:

$$Re = \frac{VL}{v} \quad \textbf{(3-30)}$$

where

Re = Reynolds number (dimensionless)

V = velocity (m/s)

$\boldsymbol{v}$ = kinematic viscosity (m/s^2)

L = length (m)

To comply with Reynolds law, the corresponding velocities must be related, so that:

$$\frac{V_{\mathrm{p}}}{V_{\mathrm{m}}} = \frac{v_{\mathrm{p}} L_{\mathrm{m}}}{v_{\mathrm{m}} L_{\mathrm{p}}} = \frac{v_{\mathrm{p}}}{v_{\mathrm{mp}}} \frac{1}{x} \quad \textbf{(3-31)}$$

where

x = scale factor

3.7.2.4 Weber Law

The Weber law depicts the relationship between surface tension and velocity. Surface tension is significant only when an air-water interface is present in a structure with small dimensions (Webber, 1979). The Weber law can be expressed as:

$$We = \frac{V}{\sqrt{\frac{\sigma}{\rho L}}} \quad \textbf{(3-32)}$$

where

We = Weber number (dimensionless)

V = velocity (m/s)

σ = surface tension (N/m)

ρ = specific density (kg/m^3)

L = length (m)

To comply with the Weber law, the corresponding velocities must be related, so that:

$$\frac{V_p}{V_m} = \frac{\sigma_p^{0.5}\rho_m^{0.5}L_m^{0.5}}{\sigma_m^{0.5}\rho_p^{0.5}L_p^{0.5}} = \frac{\sigma_p^{0.5}\rho_m^{0.5}\,1}{\sigma_m^{0.5}\rho_p^{0.5}x^{0.5}} \quad \textbf{(3-33)}$$

where

x = scale factor

Equation (3-33) states that if the fluid in the model and prototype is the same, then the model velocities must be $x^{0.5}$ times those in the prototype (Webber, 1979).

3.7.3 Scale Model Acceptance Criteria for a Stepped Spillway Aeration Study

3.7.3.1 General

The stepped spillway model study is an open channel with a free surface, and a highly turbulent air-water flow. As gravitational and inertia forces are the dominating forces within the system, the Froude similarity law applies. Turbulent air-water flow cannot be modelled without the scale effects that can only be attained by applying the Froude similitude criteria. The air bubbles within the scale model would, otherwise, be proportionally too large, resulting in a lower transport capacity, and in a higher detrainment rate, when compared to prototype conditions (Boes & Hager, 2003b).

So as to obtain true similarity, the Froude, Reynolds (viscosity) and Weber (surface tension) laws would have to be satisfied simultaneously, which, however, cannot be achieved in practice (Boes & Hager, 2003b). As a result, it is important to ensure high Reynolds and Weber numbers for the model discharges, so as to mitigate the scale effects involved.

Taking into account the above-mentioned factors that contribute to the scale effects, the required geometric scale factor, and the minimum Reynolds and Weber numbers that are relevant to this thesis are discussed in the following subsections.

3.7.3.2 Geometric Scaling

- Pinto (1984, cited in Boes & Hager, 2003b) suggests that a model scale should not be less than 1:15 for spillway aerators.
- A model family with different scale factor ranges of 1:18.75 to 1:30 was investigated by Eccher and Siegenthaler (1984, cited in Boes & Hager, 2003b). Prototype aerations rating up to 1.5 times larger than the model results were recorded for scale factors below 1:25.
- Vischer, et al. (1982, cited in Boes & Hager, 2003b) deduced that a scale factor less than, and equal to, 1:15 should be used for correct aeration in model studies.

- The study of different model scales with various step heights conducted by Pegram, et al. (1999, cited in Boes & Hager, 2003b) found that model scales of 1:20 and larger will accurately represent prototype behaviour, including decreasing scale effects for scales larger than 1:15.
- Boes and Hager (2003b) concluded that, for spillways with a prototype step height of h = 0.6 m, the scale factor should not be below 1:15.
- Pfister, et al. (2006) and Pfister and Hager (2010) conducted numerous model studies on stepped spillways using a scale of 1:12.9 for prototype step heights of h = 1.2 m.

3.7.3.3 Reynolds and Weber Criterion

- Kobus (1984, cited in Boes & Hager, 2003b) proposes Reynolds numbers of at least 1×10^5. The flow depth was used as the referenced length for the research undertaken in the current research.
- A minimum Weber number of 110 is suggested by the findings of Rutschmann (1988) and Speerli (1999), both of whom are cited in Boes and Hager (2003b).
- The stepped spillway model study by Wahrheit-Lensing (1996, cited in Boes & Hager, 2003b) found that Reynolds numbers, defined as Reynolds = $q_w/\boldsymbol{\nu}$, should exceed 7.5×10^4.
- Boes and Hager (2003b) recommend a minimum Reynolds number ($R = q_w/\boldsymbol{\nu}$) of 1×10^5, and a Weber number of 100 should be adopted for stepped spillway model studies.
- A Reynolds number ($R = q_w/\boldsymbol{\nu}$) of 1×10^5 was recorded for multiple model studies conducted by Amador, et al. (2006, 2009) on the non-aerated flow region and pressure fluctuations of stepped spillways.
- Felder and Chanson (2011) calculated Reynolds numbers ranging between 8.2×10^4 and 8.2×10^4 for a model studying the air-water flow properties in a step cavity on a stepped spillway.

3.8 REVIEW OF LITERATURE AND DEFINITION OF THESIS SCOPE RELATING TO LITERATURE

For this section, the scope of the current study is established by applying the information from the reviewed literature for the setting of the objectives and parameters of the model study.

3.8.1 Inception Point

Various equations have been developed to determine the point of inception, as has been discussed in **Subsection 3.2.3**. For the purpose of this thesis, the respective equations have been reworked to compare the length to inception point in a nondimensional format of inception length divided by roughness height (L_i / k).

Figure 3-26 and **Figure 3-27** summarise the nondimensional locations of the inception point versus the Froude number, as calculated with formulas from different authors for a stepped spillway with a slope of 51.3°, and a step height of 1.5 m.

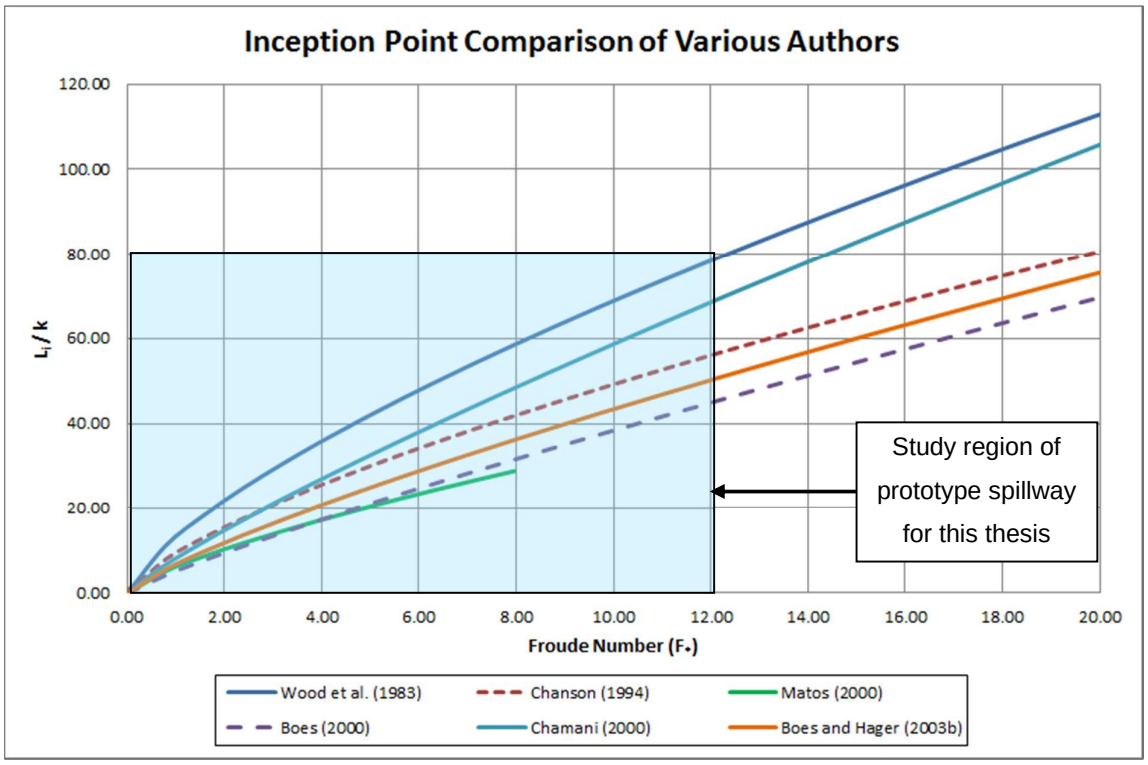

Figure 3-26: Comparison of inception point in relation to Froude number, after various authors, for a spillway angle of 51.3° and a step height of 1.5 m

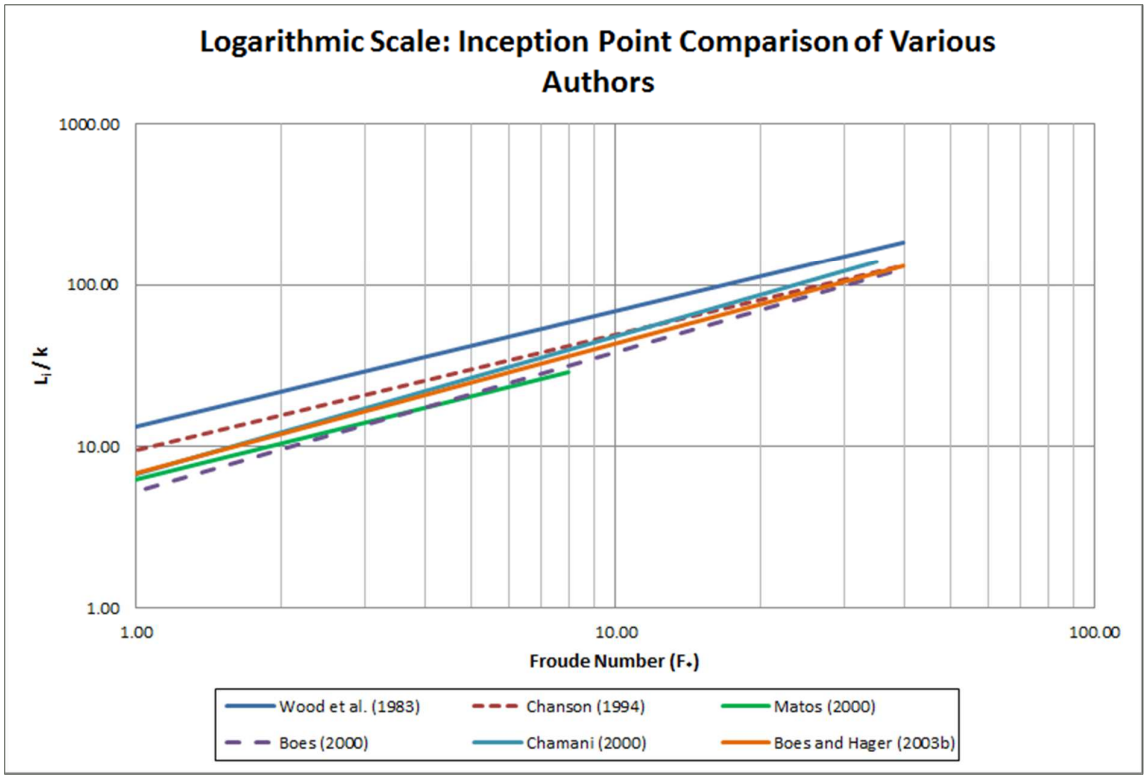

Figure 3-27: Logarithmic scale: inception point comparison relation to Froude number, after various authors, for a spillway angle of 51.3° and a step height of 1.5 m

3.8.1.1 Discussion of Inception Point Equation Relating to the Froude Number

The maximum unit discharge of the experimental model of this thesis was limited to a prototype value of 30 m²/s. With a spillway slope of 51.3° and a prototype step height of 1.5 m, the Froude number (Fr_*) for the maximum unit discharge does not exceed 12, as can be seen in **Figure 3-28**. The region relating to the inception distance for the experimental model used in the current study is shown in a light blue rectangle in **Figure 3-26**.

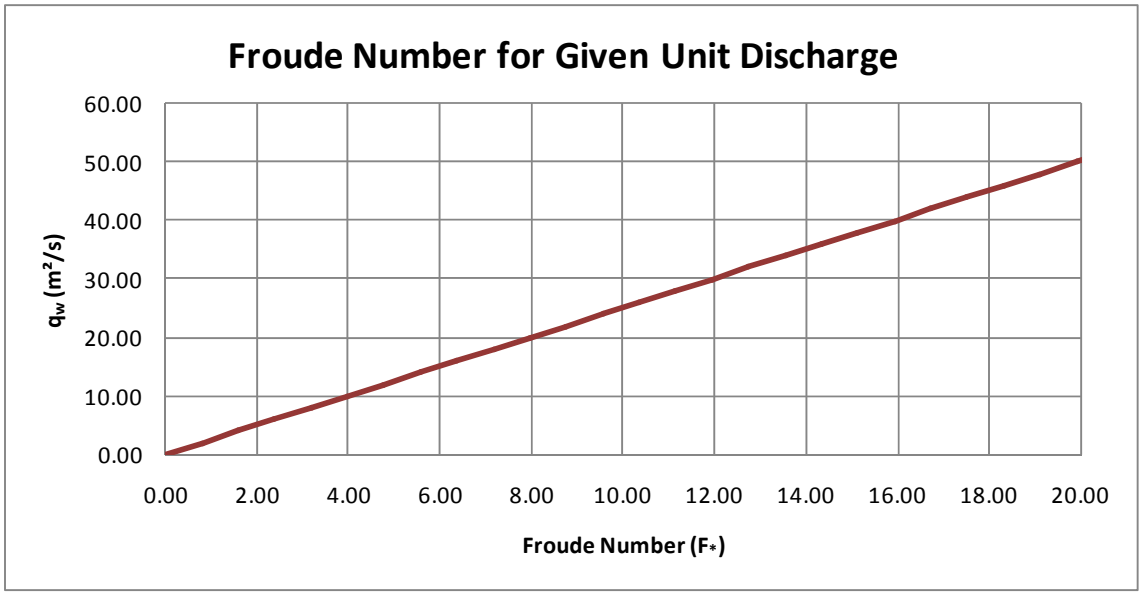

Figure 3-28: Froude number versus unit discharge for a spillway angle of 51.3° and a step height of 1.5 m

Froude number criteria for the various formulas regarding distance to inception are summarised below:

- Wood, et al. (1983) has been derived for smooth concrete spillway, and it is, therefore, not applicable to the study. However, when compared to the remaining formulas, it clearly illustrates that the distance that is required to entrain air into the flow is shorter for stepped spillways.
- A maximum Froude number obtained by Matos (2000) during experimental tests was $Fr_* \approx 8$.
- Chamani (2000) achieved maximum Froude numbers of approximately $Fr_* \approx 35$.
- The model studies conducted by Boes and Minor (2000), Chanson (1994) and Boes and Hager (2003b) all exceeded $Fr_* > 50$.

Excluding Wood, et al. (1983) from the list of equations, it can be seen from **Figure 3-26** that the approximation provided by Chamani (2000) yields the largest inception length from the spillway crest, whereas the flow becomes aerated further upstream, according to Matos (2000). The data of Chanson (1994) and Boes and Hager (2003b), which show close agreement, can be viewed as representing the average inception length.

3.8.1.2 Applicable Length to Inception Formula for the Study

Although various formulas, as proposed by the different authors discussed above, can be employed to determine the length to inception, most of such formulas were based on visual observations, on equations derived from first principles, and from depth-averaged air concentration measurements. The equation developed by Boes and Hager (2003b) involves the statistical analysis of air concentration data obtained from model studies performed at the pseudo-bottom. A primary aim of this thesis was to investigate the concentration of air at the pseudo-bottom, especially in terms of cavitation; therefore, a

suitable length to inception equation had to be adopted for the study. The equation derived by Boes and Hager (2003b) was adopted for the study for the following reasons:

- The length to inception has specific reference to the pseudo-bottom air concentration.
- Compared to equations from other authors, the length to inception can be viewed as a representation of the average length to inception (refer to **Figure 3-26** and **Figure 3-27**).
- The Froude number exceeded 50 for all of the model studies conducted to produce the equation.

In conclusion, all references made to the inception point from this point on, except if otherwise stated, will be considered as referring to the pseudo-bottom inception point, as determined by Boes and Hager (2003b).

3.8.2 Air Concentration

Studies from the literature have found that, downstream of the pseudo-bottom inception point, the required pseudo-bottom air concentration of 5-8% is reached that is sufficient to prevent cavitation damage to a spillway surface. The distance beyond the pseudo-bottom inception point, to where sufficient air percentage is achieved, is known as the critical distance (Boes & Hager, 2003b), with the length being defined by **Equation (3-19)** in **Subsection 3.5.2.1**, using a 5% air concentration value. The point at the end of the critical distance is known, in the current thesis, as the critical point. The air concentration downstream of the critical point increases to a uniform value; therefore, when considering cavitation, the area to be studied extends upstream from the critical point to the spillway crest.

Air concentration along the pseudo-bottom was, therefore, measured from the critical point upstream to the spillway crest. Measurements were conducted for two stepped spillway configurations, namely for:

i. The conventional stepped spillway.
ii. The spillway model (a) above, with a pier being introduced at the ogee crest.

Air concentration data relating to (b) was compared to those relating to (a), in an effort to investigate:

1. A possible earlier onset of air entrainment down the spillway length, meaning the enhanced boundary layer growth set to reduce the length to the inception point.
2. Whether, and, if so, where air concentration along the pseudo-bottom and upstream of the critical point was affected.
3. Whether adjustments to the crest pier design had any effects to the experimental objectives listed in points 1 to 2 above.

In addition to the air concentration investigations listed in points 1 to 3 above, the following behavioural patterns of air along the pseudo-bottom were investigated:

i. The method of air entrainment for two different pier designs.
ii. Whether the aeration properties of a stepped spillway with crest piers follow the same pattern as indicated in the research of Pfister, et al. (2006) which focuses on the pre-aeration of the spillway bottom, by means of adding a chute aerator at the first step (refer to **Subsection 3.3.3**).

3.8.3 Pressure

In view of the findings on pressure distributions along stepped spillway, and within step, cavities, the model study of this thesis was focused on minimum pressure zones in respect of cavitation:

i. At the critical point.
ii. Upstream of the critical point along the spillway.
iii. At the upper edge of the vertical steps, within the flow region specified in (i) & (ii).

From the findings of literature studies on the horizontal and vertical steps, the smallest minimum pressures were found to be at the upper edge of the vertical riser. (Refer to **Figure 3-21** and **Figure 3-22 (A)** in **Subsection 3.4.2**.)

3.8.4 Cavitation

Downstream of the critical point, the presence of an adequate percentage of air in the mixture near the solid surfaces is expected to prevent cavitation (Peterka, 1953, cited in Amador, et al., 2009). Hence, the velocities that are upstream of, and at, the critical point require evaluation, so as to avoid cavitation. Recommendations regarding the velocity and discharge limits that are required for preventing the inception of cavitation are summarised below:

- Boes and Hager (2003b) recommend a maximum velocity of 20 m/s at the inception point.
- Velocity limited to 15 m/s at the inception point was proposed by Amador, et al. (2009), so as to prevent cavitation.
- Pfister, et al. (2006) suggest a unit discharge of not more than 30 m²/s.
- Frizell, et al. (2013) established a correlation between the cavitation index and friction factor, so as to enable the determination of the areas along the spillway that are prone to cavitation.

3.8.4.1 Incipient Cavitation Number

Figure 3-29 represents the cavitation indices for unit discharges, as proposed by Pfister, et al. (2006) and by Frizell, et al. (2013). The data of Frizell, et al. (2013) suggest that any relevant stepped spillway friction formula can be utilised to determine the cavitation index. Two different friction factors were evaluated for a 51.3° spillway with a step height of 1.5 m:

- The bottom friction factor (f_{bi}) at the inception point (Boes & Hager, 2003a).
- The mean friction factor (f_i) at the inception point (Tozzi, 1994).

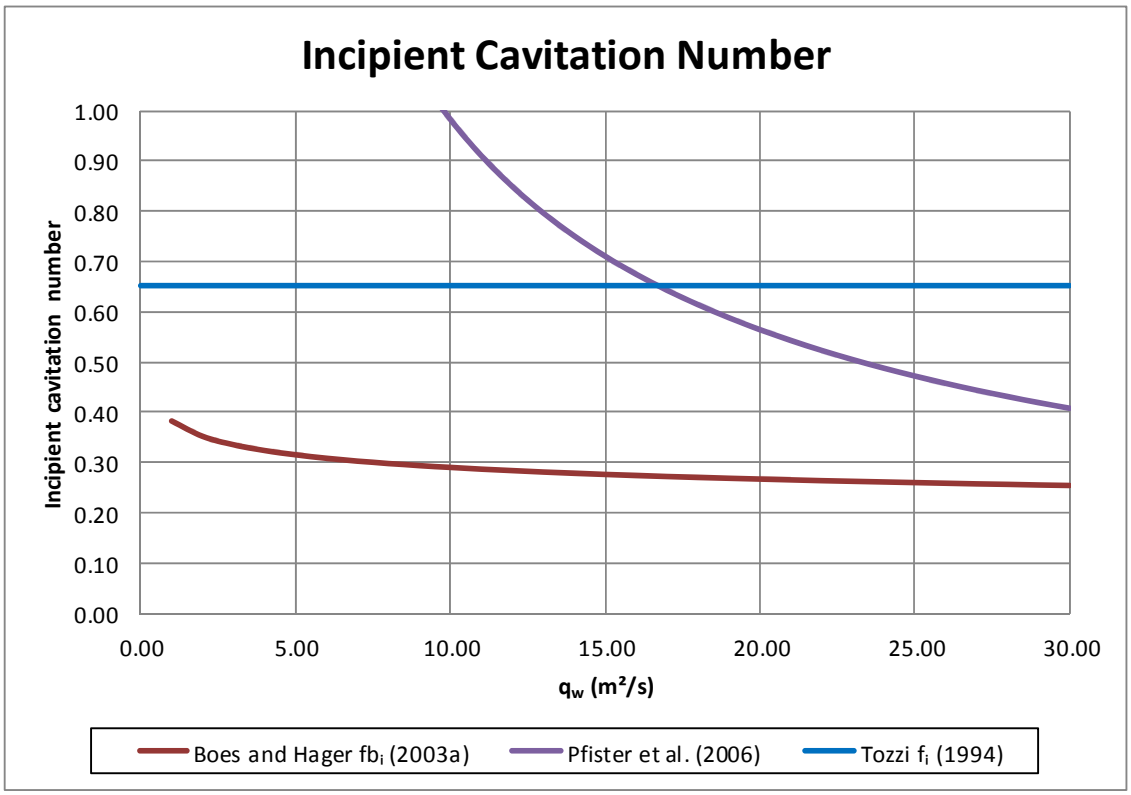

Figure 3-29: Incipient cavitation number vs. unit discharge for a stepped spillway, 51.3° and h = 1.5 m, after various authors

Given the maximum prototype unit discharge of 30 m²/s for this thesis, the incipient cavitation number equals 0.65, 0.40 and 0.26 for Tozzi (1994), Pfister, et al. (2006) and Boes and Hager (2003a), respectively. The method recommended by Frizell, et al. (2013), combined with the bottom friction factor determined by Boes and Hager (2003a), is considered the most conservative approach, as can be seen in **Figure 3-29**.

The critical index data of Frizell, et al. (2013) can be used with **Equation (3-22)** to determine the minimum allowable gauge pressure at the inception point before cavitation sets in. **Figure 3-30** illustrates this fact by presenting the regions of no and probable cavitation. Cavitation seems imminent for velocities exceeding 18 m/s at the inception point, and for corresponding unit discharges exceeding 18 m²/s.

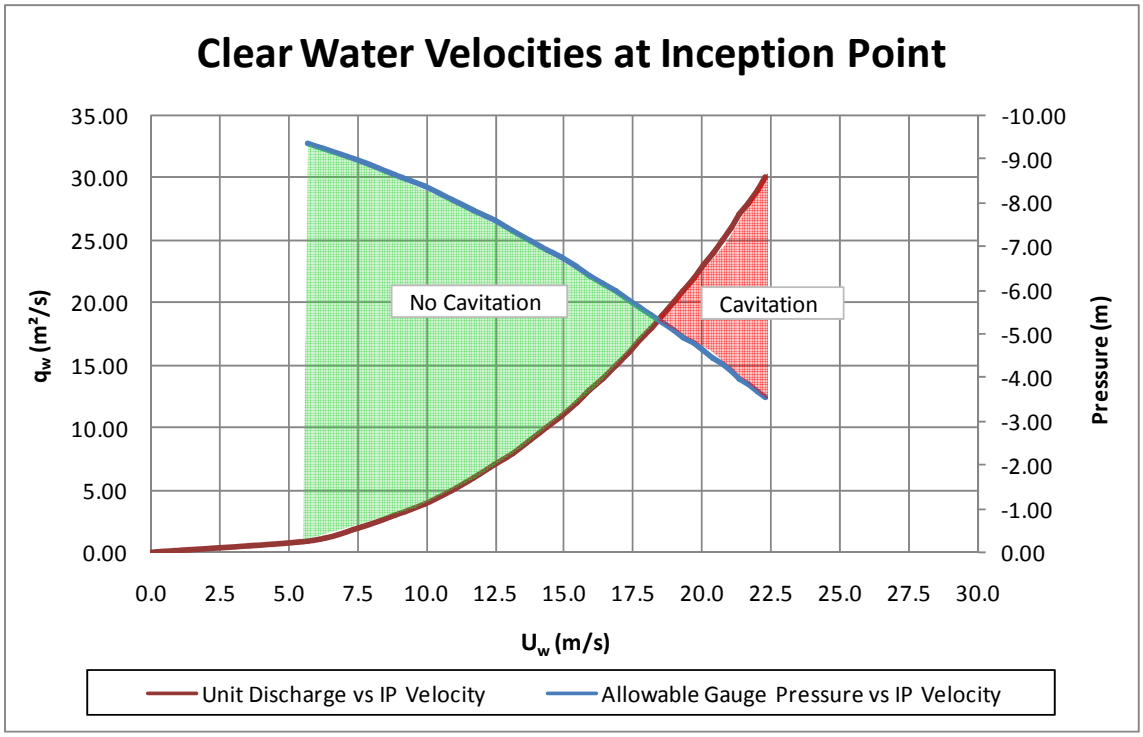

Figure 3-30: Allowable pressure at inception point (IP) vs. velocity for a stepped spillway, 51.3° and h = 1.5 m, after Frizell, et al.

In summary, a clear water velocity of 15 m/s, as at the inception point, appears to be a safe design criterion when considering a stepped spillway with an ogee-shaped crest, a slope of 51.3°, and a step height of 1.5 m, as proposed by Amador, et al. (2009). A velocity reaching 20 m/s at the inception point might initiate cavitation damage, and it can be considered the upper velocity limit, as recommended by Boes and Hager (2003b).

3.8.5 Modelling Criteria Considering Scale Effects

3.8.5.1 Scaling Aeration Effects

In **Subsection 3.7.3.2**, it was stated that Pinto (1984), Vischer, et al. (1982) and Boes and Hager (2003b) all concluded that a model scale of 1:15 and less is to be adopted for experimental research involving aeration studies, so as to prevent the distortion of the aeration characteristics within the two-phase flow. Consequently, a model scale of 1:15 was adopted for the currently employed model.

3.8.5.2 Satisfying Reynolds and Weber Criteria

The air-water relationship within the flow down a stepped spillway requires a scale that is large enough to exclude scale effects, as was discussed in **Subsection 3.7.3.1**. **Figure 3-31** illustrates that a model scale of 1:15 with prototype unit discharges exceeding 6 m^2/s will satisfy the minimum Reynolds and Weber numbers of 1×10^5 and 100 respectively, based on the Froude similitude criterion.

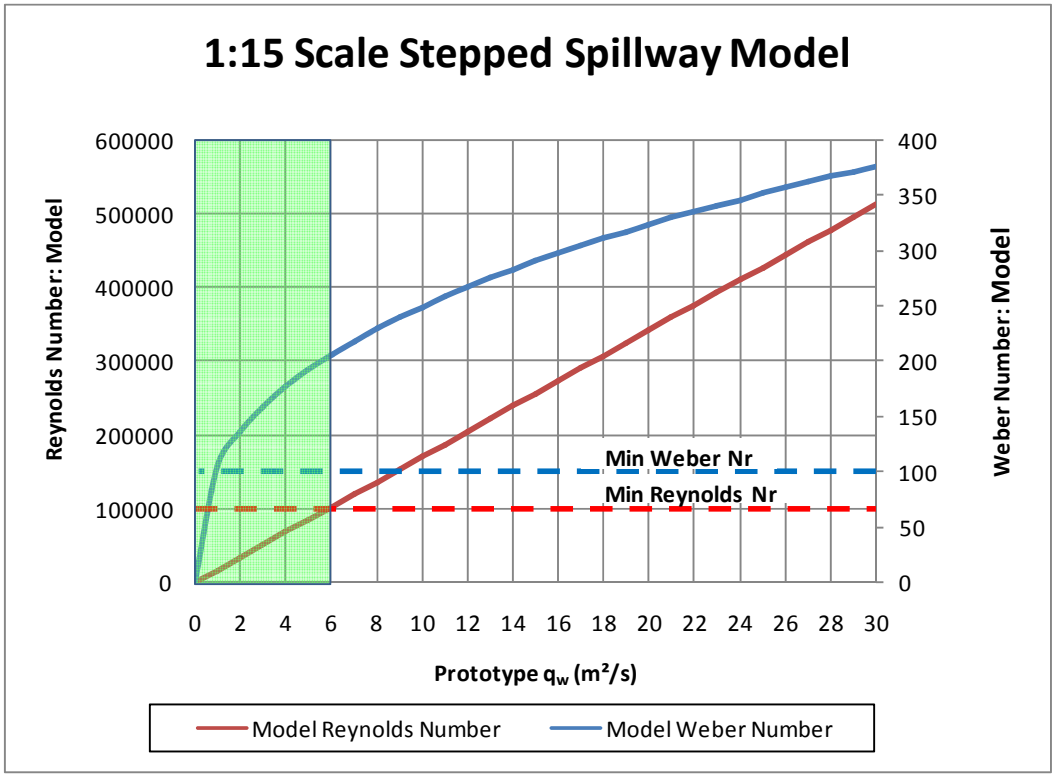

Figure 3-31: Reynolds and Weber numbers for 1:15 stepped spillway model, with a 51.3° slope

3.8.6 Spillway Crest Pier

The research that was conducted for this thesis is focused on the comparison of a stepped spillway with, and one without, crest piers. The principal aim of employing a crest pier is to introduce turbulence at the overflow crest, so as to explore the possibility of either:

- Accelerating the growth of the boundary layer along the spillway, or
- Enhancing air entrainment at the beginning of the spillway.

In addition, two different crest pier designs were studied. The distance that a pier extends down a spillway can affect the air entrainment characteristics of the flow concerned. Visual observations, coupled with pressure and air concentration measurements, were used to investigate the relationship between different pier designs and downstream turbulence across the spillway width.

4. EXPERIMENTAL MODEL

The current chapter provides details of the design of the stepped spillway model, information regarding the instrumentation used to capture the data, and a detailed account of the test procedures employed to achieve the study objective. It should be noted that preliminary experimental work was conducted to aid with the refinement of the pier design and the test procedures. The details of the preliminary experimental work are provided within this chapter.

4.1 PHYSICAL STEPPED SPILLWAY MODEL

4.1.1 Spillway Layout and Dimensions

A 1:15 scale model was constructed to satisfy the minimum Reynolds and Weber criteria, and to mitigate the scaled aeration effects, as were discussed in **Subsection 3.8.5**.

The model consisted of a DN 600 inlet pipe elbow, a stilling basin, an uncontrolled ogee, crest and a stepped chute. **Figure 4.1** illustrates the plan layout of the model, whereas **Figure 4-2** shows a sectional view of the model.

Detailed as-built plans of the spillway model are provided in **Appendix 1**.

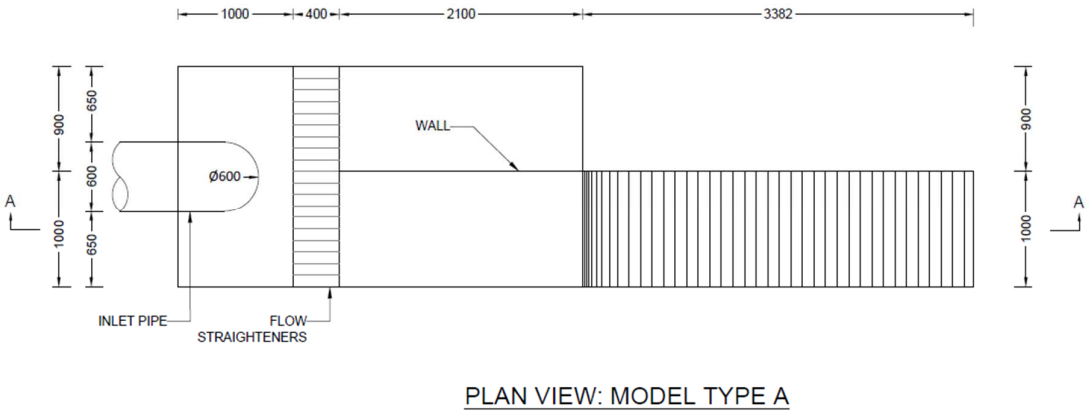

Figure 4-1: Plan view of spillway model (i.e. representation of the spillway centre)

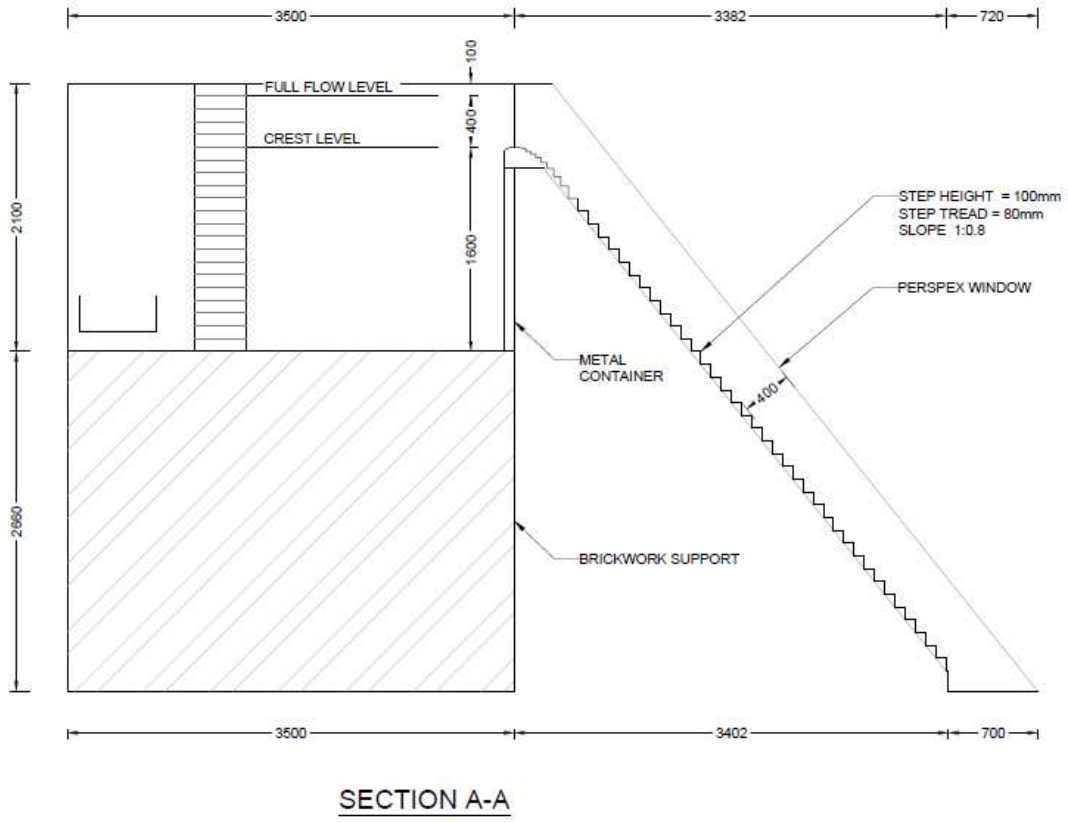

Figure 4-2: Section A-A of spillway model

The inlet pipe was connected to a 3 500 × 1 900 × 2 100 mm metal container that acted as the stilling basin for the model. The metal container was supported with 2 660 mm high brickwork. Flow straighteners, 300 mm long, were placed downstream of the inlet pipe that extended the full cross-sectional width of the metal container.

A 1 000 mm wide rectangular stepped chute with an ogee crest was attached to the metal container. The stepped channel was 4 260 mm high (from crest to ground), with a step height of 100 mm and a bottom inclination of 51.3°, corresponding to a slope of 1:0.8 (V:H), typical of RCC dams. The 400 mm spillway walls were constructed from perspex to allow for visual inspection of the flow. Photographs of the model are shown in **Figure 4-3** and **Figure 4-4**.

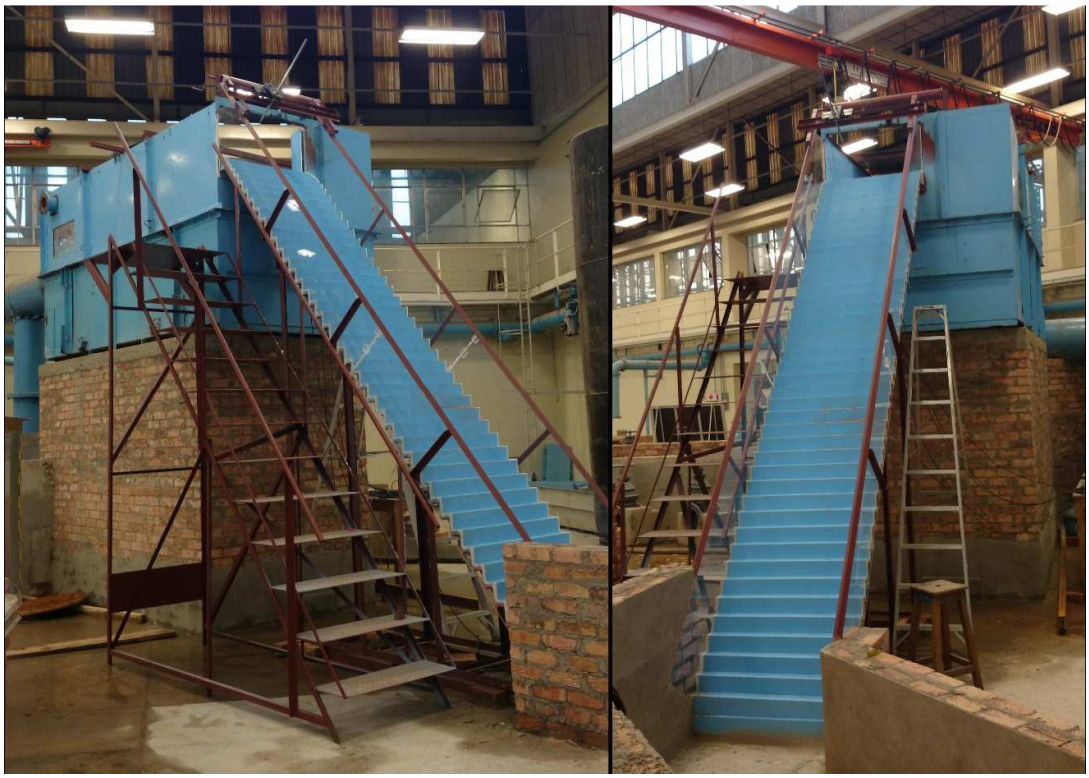

Figure 4-3: Stepped spillway model

Figure 4-4: Flow straightener wall

4.1.2 Laboratory Apparatus

The laboratory set-up and apparatus is described with the aid of **Figure 4-5**.

Water is pumped via a DN 600 steel pipe that connects to the stilling basin of the stepped spillway. Water flows into the stilling basin, over the spillway crest, and down the stepped chute. Downstream of the chute, the water runs into a drainage channel. It collects in an underground reservoir that then feeds water back to the pumps, effectively completing the cycle.

Within the stilling basin, water is directed through a flow straightener (i.e. a hollow brick wall) upstream of the crest, so as to ensure a stable approaching flow. Flow into the stilling basin is controlled by means of the upstream gate valve, and it is monitored using a flow meter. The instrumentation and process to monitor the flow is discussed in **Subsection 4.2.1**.

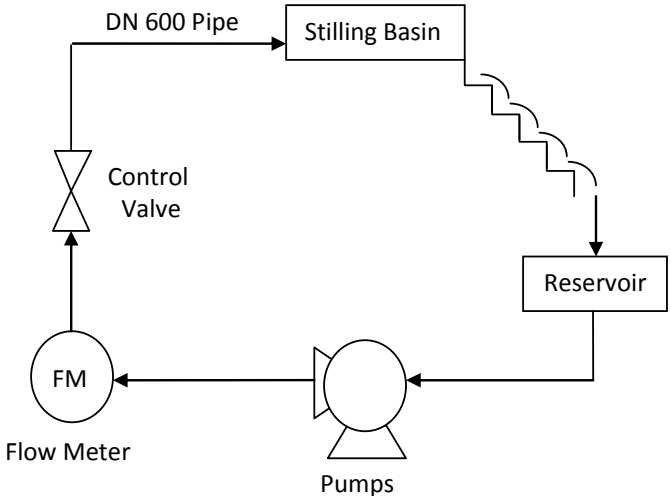

Figure 4-5: Laboratory flow diagram

4.1.3 Crest Design

The design of the overflow crest is based on an ogee profile with a vertical upstream face, and no spillway piers. Steps varying in step tread and riser length are provided downstream of the crest apex to facilitate a smooth flow transition between the ogee profile and the constant slope stepped chute.

The design of the crest is discussed in the following order: 1) the calculation of the design head; 2) the design of the ogee profile; and 3) the modification to the ogee profile to include the transitional steps.

4.1.3.1 Calculation of Design Head

The discharge over an ogee crest is given by the equation:

$$Q = C_e L H_e^{1.5} \quad \textbf{(4-1)}$$

Table 4-1 summarises the calculation of the design head over the prototype spillway and the chosen 1:15 scaled experimental physical model.

Table 4-1: Design summary of ogee profile

Description (refer to Figure 4-6)	Unit	Prototype	Model (1:15)
H_e/H_d	m/m	1.333	1.333
C_e/C_o		1.04	1.04
P (from the bottom of the tank to the crest)	m	24.00	1.600
H_d	m	4.20	0.280
H_e	m	5.60	0.373
P/H_d	m/m	5.71	5.714
C_o		2.18	2.18
C_e		2.27	2.27
Effective crest length	m	15.00	1.000
Maximum q_w	m²/s	30.00	0.516
Design q_w	m²/s	18.76	0.323

4.1.3.2 Ogee Profile

The design of the ogee profile was done according to the design guidelines stipulated in United States Bureau of Reclamation (USBR) (1987). **Figure 4-6** shows the geometry characteristics of a nappe-shaped ogee profile. Note that the coordinate system shown is different to the one presented in **Subsection 4.1.4.3**.

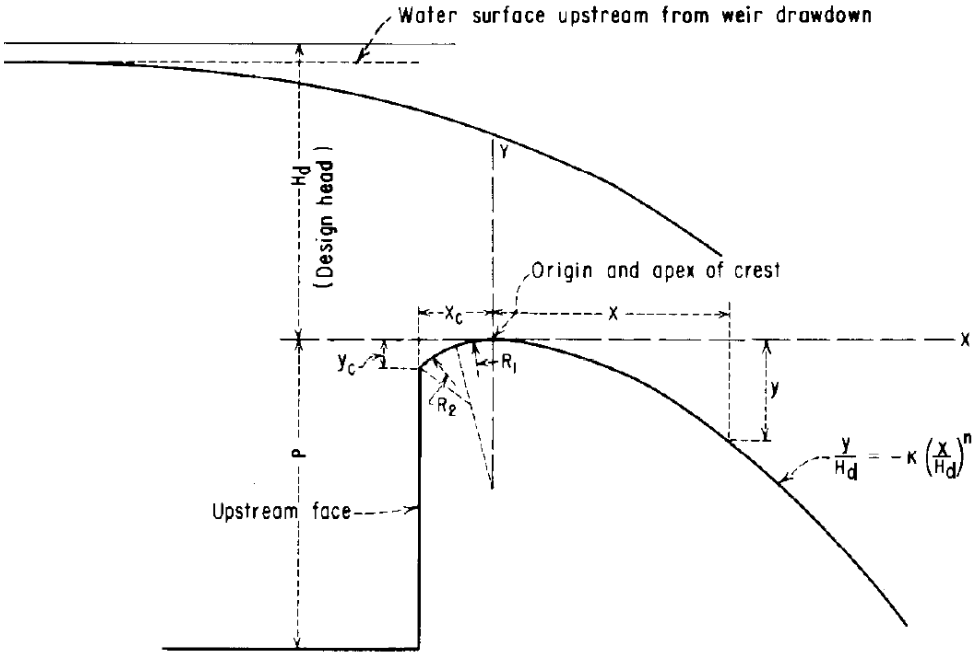

Figure 4-6: Nappe-shaped ogee profile (USBR, 1987)

The basic shape of the ogee spillway was derived from the lower envelope of the overall nappe flowing over a high vertical rectangular notch with approach velocity equal to 0 m/s (Novak, et al., 2007). The shape of the nappe is described by the following equation (refer to **Figure 4-6** for crest origin and symbols):

$$\frac{Y}{H_d} = \mathrm{K}\left(\frac{\mathrm{X}}{\mathrm{H_d}}\right)^{\mathrm{n}} \quad \textbf{(4-2)}$$

where

Y = y-coordinate

X = x-coordinate

K, n = constants obtained from USBR (1987)

The parameters used to calculate the ogee profile using **Equation (4-2)** are shown in **Table 4-2**.

Table 4-2: Design summary of ogee profile

Description	Unit	Prototype	Model (1:15)
H_d	m	4.200	0.280
h_a/H_d	m/m	0.005	0.005
K		0.500	0.500
n		1.869	1.869
R_1 (defined as per **Figure 4-6**)	m	2.226	0.148
R_2 (defined as per **Figure 4-6**)	m	0.987	0.066
X_c (defined as per **Figure 4-6**)	m	1.184	0.079
Y_c (defined as per **Figure 4-6**)	m	0.533	0.036
Point of tangency (x-coordinate)	m	5.984	0.399
Point of tangency (y-coordinate)	m	4.041	0.269

4.1.3.3 Transitional Steps

A spillway where the stepped profile starts at the point of tangency (i.e. at the end of the ogee curve) is inclined to cause flow detachments at the first step for small discharges. When the flow strikes the step tread, it tends to jump, thereby missing subsequent steps and impacting the steps that are lower downstream. As soon as the discharge increases to a critical value, the jump disappears.

To resolve this specific problem for low discharges, a varied step profile was developed by the CEDEX (Centro de Estudios y Experimentación de Obras Públicas) laboratory in Spain that connects the stepped chute with the ogee crest profile, with the result being known as the transitional steps. Each of the transitional step treads is based on the design head, as is illustrated by **Figure 4-7**.

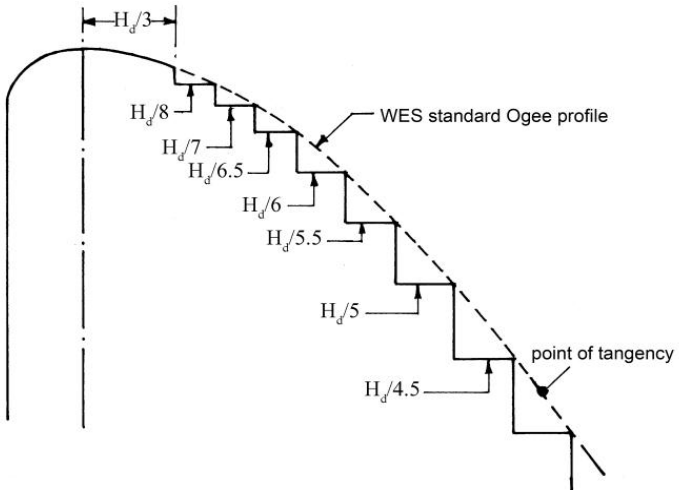

Figure 4-7: Transitional steps proposed by CEDEX, Spain

4.1.3.4 Model Spillway Crest

The ogee profile, in combination with the adopted CEDEX transition steps, was used for the physical model. This is shown in **Figure 4-8** and the crest of the physical model in **Figure 4-9**. An additional step with $H_d/3.73$ (the step with step height of 94 mm – see **Figure 4-8**) was added downstream of $H_d/4.5$ (step height of 77 mm) to prevent an abrupt change from the last transitional step to the start of the constant design steps on the 1V:0.8H slope.

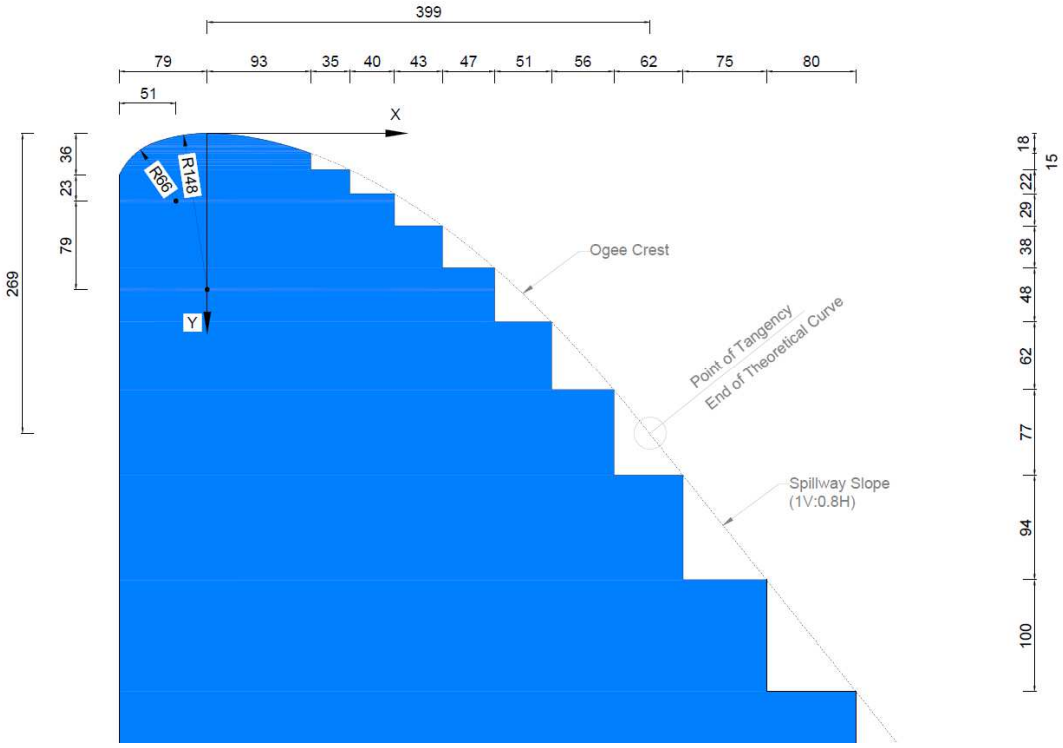

Figure 4-8: Model crest (design) – dimensions shown in mm

Figure 4-9: Model crest (photograph)

4.1.4 Spillway Pier

4.1.4.1 Design of Crest Pier

The design of the crest pier was based on a Type 2 'Bullnose' pier, according to the guidelines provided by the American Society of Civil Engineers (ASCE) (1995). **Figure 4-10** describes a typical Type 2 pier based on the design head H_d.

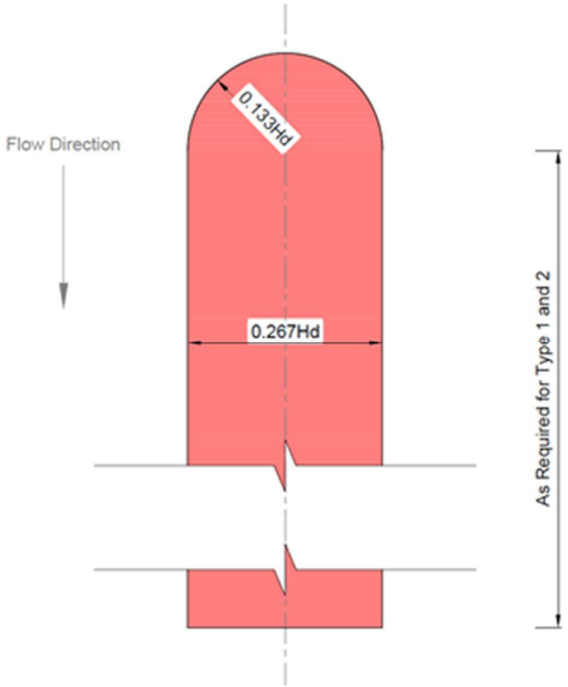

Figure 4-10: Type 2 crest pier (ASCE, 1995)

4.1.4.2 Model Crest Pier

The dimensions of the different crest piers are shown in **Figure 4-11** and **Figure 4-12**. Two different spillway types were considered for use in the study. The piers differed only in the length that they extended downstream of the spillway crest. For the purposes of this research, the different piers were classified as Types 1 and 2.

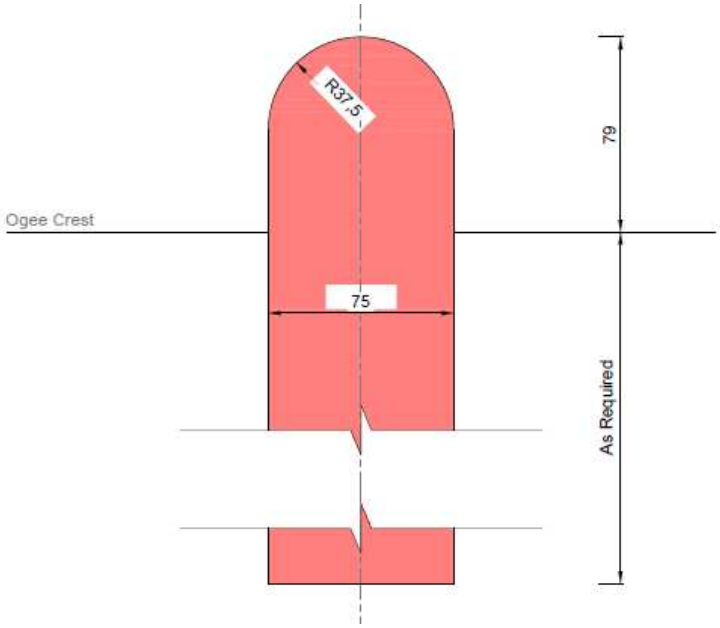

Figure 4-11: Plan view of model crest pier

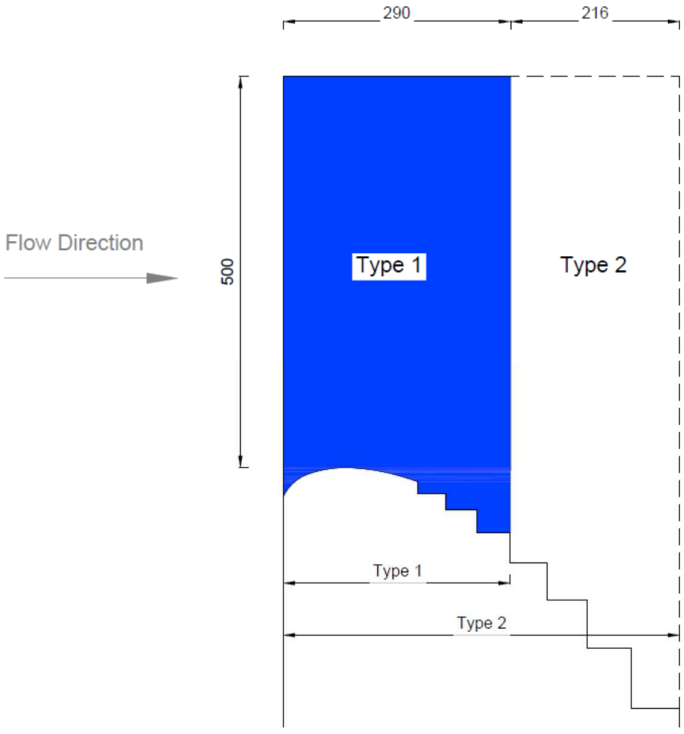

Figure 4-12: Side view of model crest piers (Types 1 and 2)

4.1.4.3 Model Coordinate System

The coordinate system, and the respective notation that was adopted for the model, are shown in **Figure 4-13**. The streamwise distance parallel to the pseudo-bottom was denoted as *L*, and the axis perpendicular to the pseudo-bottom as *y*. Notation *x* was used to define the distance across the width of the channel, with the origin being at the right side of the spillway.

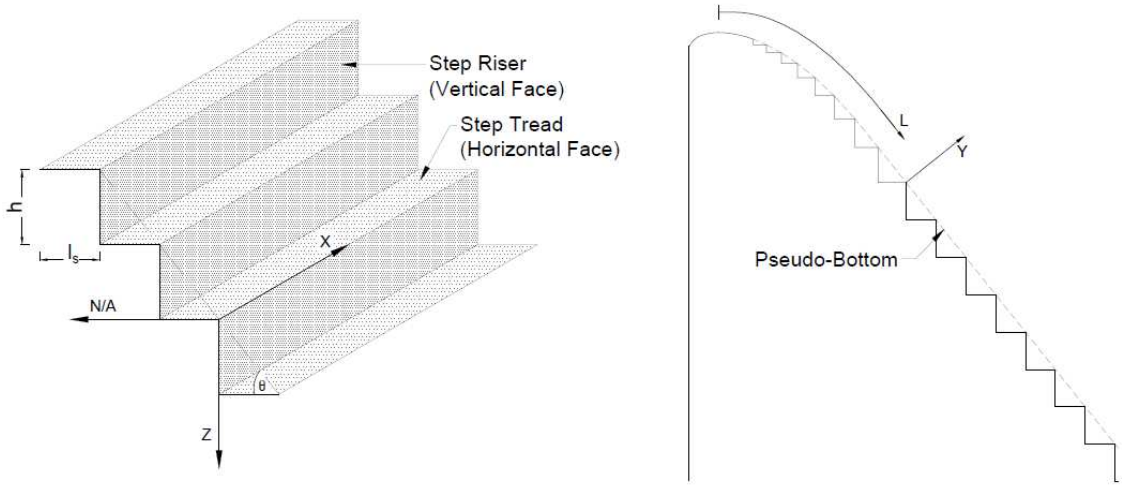

Figure 4-13: Model coordinate system

4.1.4.4 Model Setups

Experimental tests were conducted on different model configurations, which was termed 'model setups' for the purposes of this thesis. The different model configurations were based on the following:

- Testing for a standard stepped spillway with no piers (control test).
- Testing for a standard stepped spillway equipped with piers of different designs (crest pier Types 1 and 2).

All crest pier types were to be located in the centre of the spillway, meaning at x-coordinate = 500 mm. The different model setups are shown in **Table 4-3**.

Table 4-3: Model configurations

Model setup	Pier type	No. of piers	Pier x-coordinate (mm):
1	–	No piers	–
2	1	1	500
3	2	1	500

4.2 INSTRUMENTATION

The following equipment was used to record the spillway discharge, as well as the air concentration and the pressure:

- A flow meter was used to measure the flow into the stilling basin. The readings were recorded manually from the flow meter display.
- The water level upstream of the crest was manually recorded with a measuring needle.
- The air concentration was recorded electronically at 10 kHz, using a conductive needle probe.
- Pressure transducers were used to record the pressure on the step face electronically at 100 Hz.

4.2.1 Spillway Discharge

The discharge over the spillway crest was measured using two different instrumentation devices. The first flow indicator was a SAFMAG electromagnetic flow meter installed on the inlet pipe, upstream of the stilling basin, which meter recorded with an accuracy of ±5% for all flows. The second device was a measuring needle that was used to document the water level within the stilling basin, upstream of the crest. The variation in the water levels was found to be ±0.7% for all tested discharges. The empirical ogee crest discharge formulas, as discussed in **Subsection 4.1.3**, were reworked for each recorded water level, so as to obtain the expected discharges.

Photographs of the electromagnetic flow meter and the measuring needle are shown in **Figure 4-14** and **Figure 4-15**, respectively.

Figure 4-14: Electromagnetic flow meter (SAFMAG)

Figure 4-15: Measuring needle in stilling basin

4.2.2 Air Concentration

The air concentration within the flow down the stepped spillway was measured using an intrusive conductive needle probe with a tip diameter of ø = 0.1 mm at a signal acquisition frequency of 10 kHz.

The probe concerned operates on the electrical inductance principle, which, for the application of this study, measured the conductivity of water and air. A high frequency amplifier excites the probe, which then returns a voltage signal to a data acquisition module, indicating the current water-air phase at the probe tip.

The acquisition unit registers the output voltage within a certain conductivity range, with water being the upper limit, and air the lower. A steep signal drop corresponds to an air bubble being pierced by the probe tip. Although the signal is theoretically rectangular, the probe response is not square, due to the finite size of the tip, the wetting/drying time of the interface covering the tip, and the response time of the probe and electronics involved (Chanson & Carosi, 2007).

The probe and combined amplifier and data acquisition unit (in the TNP module) was supplied and calibrated by the German-based company, HZDR Innovation.

The probe was fixed to a travelling trolley that was mounted on the spillway sides. The trolley support was able to travel parallel to the spillway bottom, and it could be adjusted in the x- and y- coordinate direction. The probe tip was orientated to the direction of flow to ensure best bubble penetration. Photographs illustrating the probe, including the TNP unit and the support trolley system are shown in **Figure 4-16** to **Figure 4-20**.

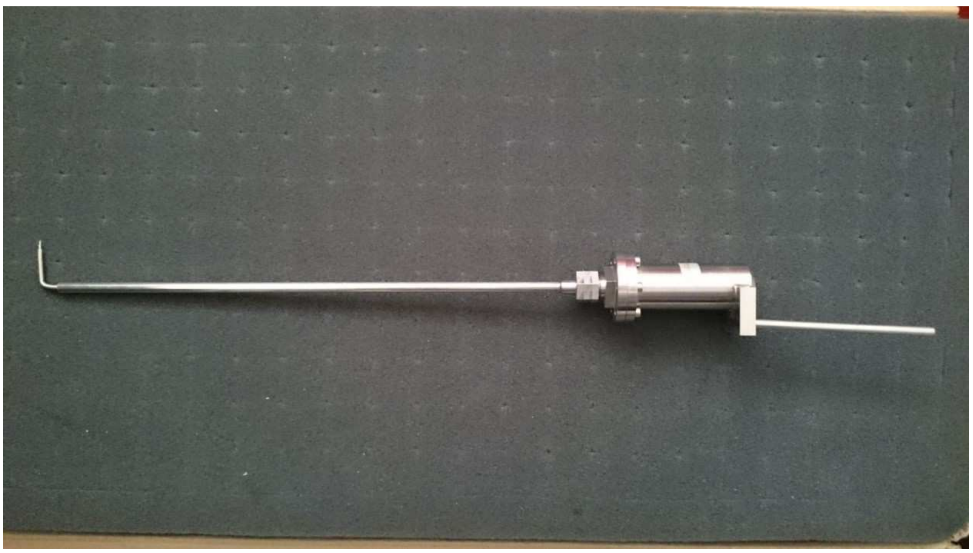

Figure 4-16: Conductive needle probe (HZDR Innovation)

Figure 4-17: Conductive needle probe tip (0.1 mm)

Figure 4-18: Thermal Needle Probe (TNP) device

Figure 4-19: Conductive needle probe support system

Figure 4-20: Conductive needle probe support system (side view)

Raw data captured by the acquisition unit were analysed with the use of a software product called VoidWizard, which was also supplied by HZDR Innovation. The software was able to generate reports depicting the void fractions, the conductivity and the number of bubbles encountered over a preselected time step.

Figure 4-21 presents an illustrative example of the Void Wizard interface. The raw data are 'smoothed' into a binary format that portrays the air and liquid phase, whereby the upper conductivity threshold represents a liquid phase, and the lower threshold the air phase. The accuracy of the binary data can be altered by adjusting the time period over which the data are averaged. As preliminary investigations showed that an averaging time step of more than 0.1 sec would not increase the accuracy of the data, a time step of 0.1 sec was employed for all binary data analyses. The average void fraction (i.e. the air concentration %) is calculated by dividing the total air phase time periods by the sampling time.

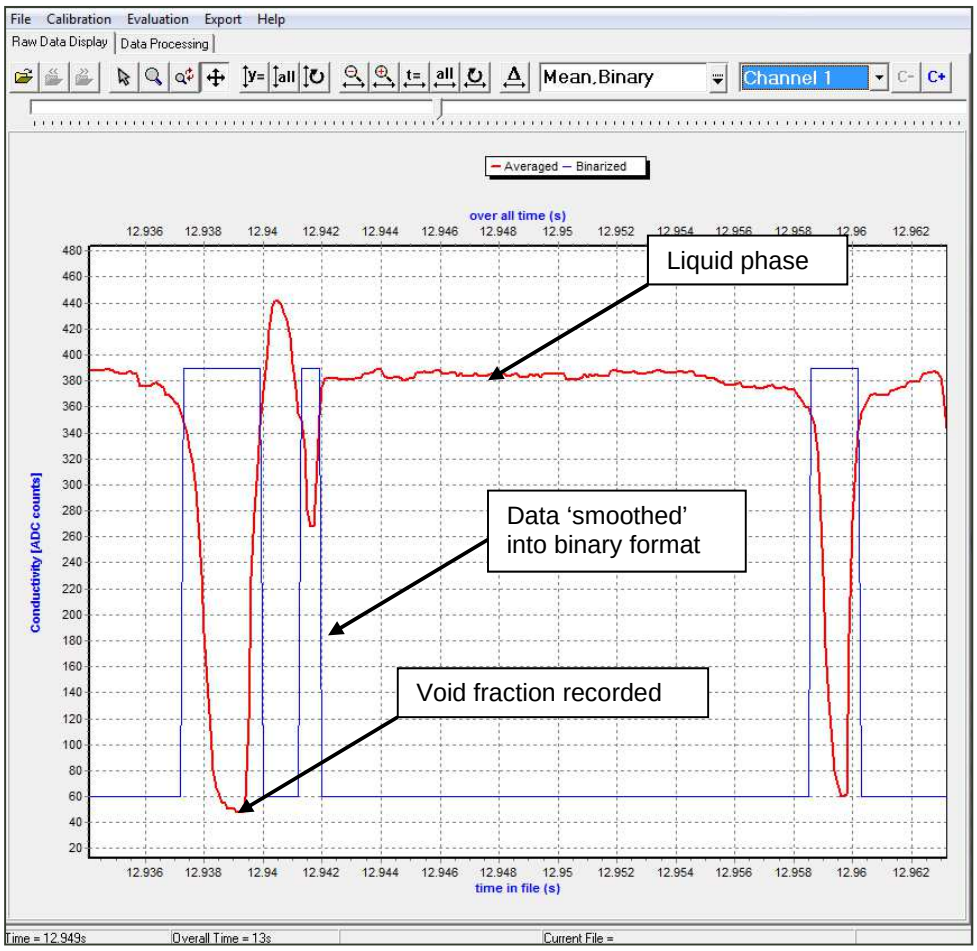

Figure 4-21: Void Wizard software (HZDR Innovation)

4.2.3 Pressure

Fluctuating pressures were measured using WIKA S-10 pressure transducers, with a linear working range of -1 to +1 bar, and an output range of 4 to 20 mA or DC 10 to 30 V. The sensors were connected to pressure taps by means of 6 mm rigid tubes, at an average length of 100 mm. The taps were installed flush to the vertical step face, 90 mm above the step tread.

The diameter of the pressure cell transducers was 17.5 mm, with a combined nonlinearity, hysteresis and repeatability error of 0.5% for the span range. A 12-channel analogue to digital data logger (PicoLog) was used to record the voltage output of the sensors at 100 Hz. A photograph of the pressure sensors, and of a typical installation underneath the model spillway, is shown in **Figure 4-22**.

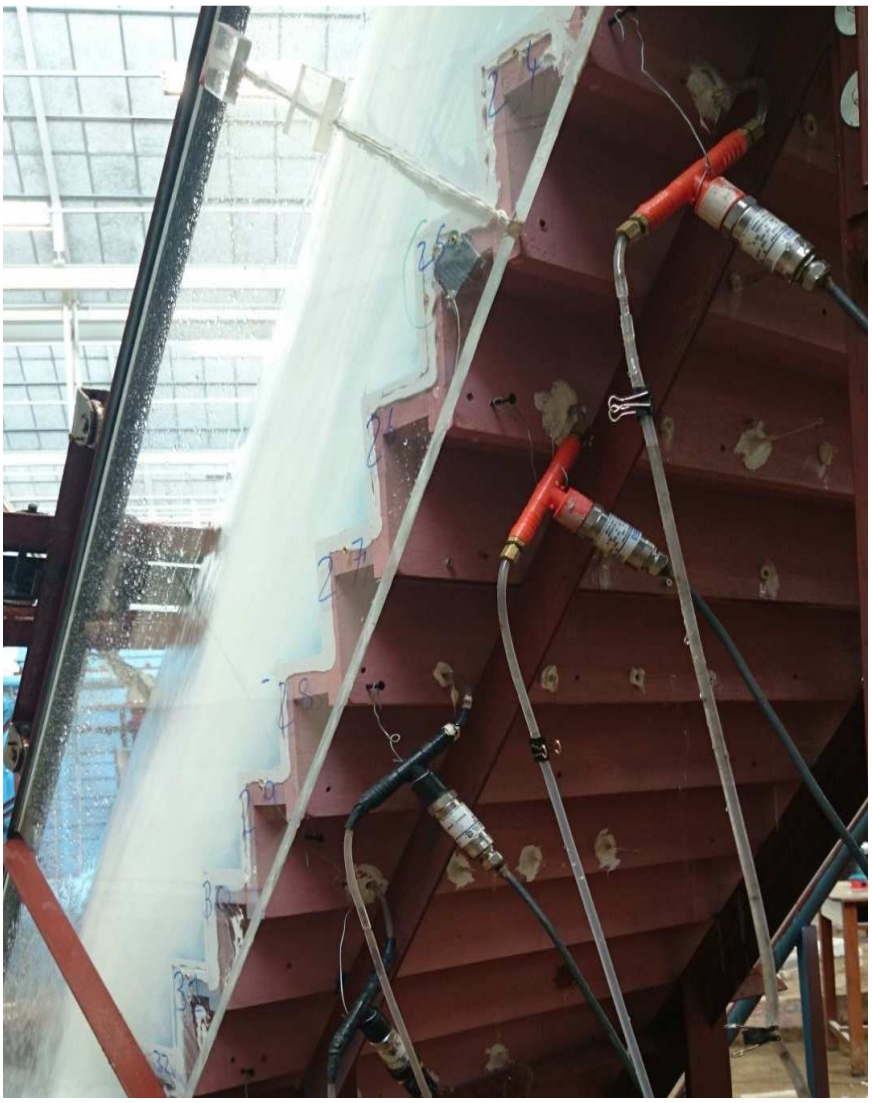

Figure 4-22: Pressure sensors installed beneath spillway

The pressure sensors measure the pressures in milliampere, which were then converted to volt by means of a 120 Ω resistor. The voltage readings were converted to metres head by means of the following equation:

$$\mathrm{H} = \frac{(+1\ \mathrm{m}) - (-1\ \mathrm{m})}{(20\ \mathrm{mA} - 4\ \mathrm{mA})} \times \left(\frac{\mathrm{x(V)}}{120\ \Omega} \times 1000 \right) - 1.5 \qquad \textbf{(4-3)}$$

where

H = metres head (m)

x = DC output voltage (V)

4.3 STATISTICAL ANALYSIS OF EXPERIMENTAL DATA

4.3.1 Air Concentration

The raw data captured by the acquisition unit were analysed using the applicable software, as described in **Subsection 4.2.2**. The data were transformed into a binary format, with the result being registered as either a liquid or air phase for a certain time period. The average void fraction for a sampling period was calculated on the basis of the results obtained with the software.

The analysis of the air concentration data was performed using the software, and no further statistical analysis was required.

4.3.2 Pressure

4.3.2.1 Mean Pressure

The calculated average of each data set represented the mean pressure for the specific location measured on the spillway.

4.3.2.2 Maximum and Minimum Pressures

The maximum and minimum pressure for this study were defined as the pressures located three standard deviations above and below the mean respectively, meaning a 0.15% probability, assuming normal distribution of the sample data. (Refer to **Figure 4-23**.) The applicable confidence interval was selected to eliminate outliers of the data set, and also to ensure that the maximum and minimum pressures could be presented with a high level of confidence. A reliable representation of the minimum pressures is important when evaluating cavitation on a spillway.

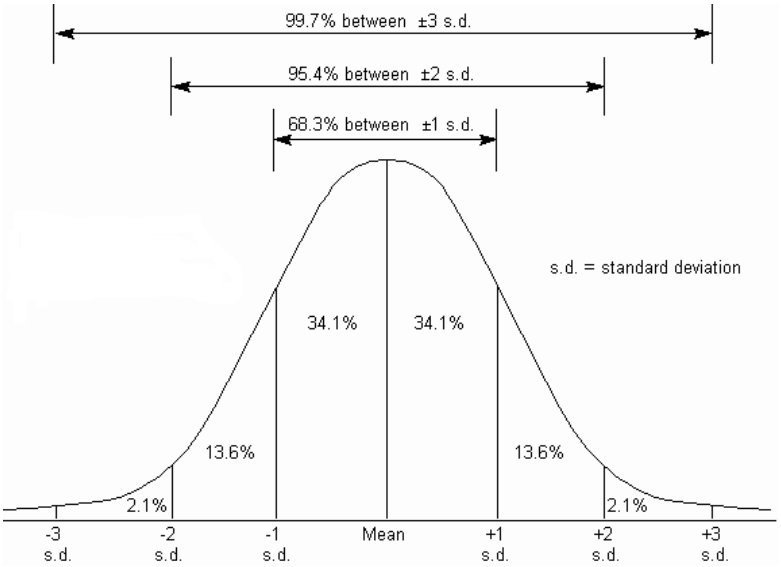

Figure 4-23: Normal bell curve (Syque, 2014)

When using the central limit theorem to determine the maximum and minimum pressures, it is assumed that the data set is normally distributed. To qualify the approach discussed above, data from two different sensors were statistically analysed by:

1. Using a normal probability plot to determine whether the data departed from normality.
2. Visually plotting the data against a normal distribution bell curve.

For the investigation, data were used from pressure sensors located at steps 16 and 22 at the centre of the spillway with no crest piers (x = 500 mm) at the upper vertical step (h = 90 mm) for a unit discharge of 25 m²/s. Data were recorded over a period of 10 minutes. The voltage output from the sensors was not converted to pressure, as doing so was not required for this analysis. A set of descriptive statistics for each sensor is shown in **Table 4-4**.

Table 4-4: Descriptive statistics for pressure sensors at steps 16 and 22

Sensor	Mean (V)	Standard deviation (V)	Maximum (V)	Minimum (V)	Skewness	Data samples
Step 16	1.507	0.076	1.734	1.280	0.570	60000
Step 22	1.569	0.118	1.922	1.216	0.875	60000

From **Table 4-4**, it can be seen that the positive skewness for both sensors is an indication that the data is skewed to the right.

Normal probability plot

The normal probability plots for steps 16 and 22 are illustrated in **Figure 4-24** and **Figure 4-25**, along with the probability plots from the pressure sensor data.

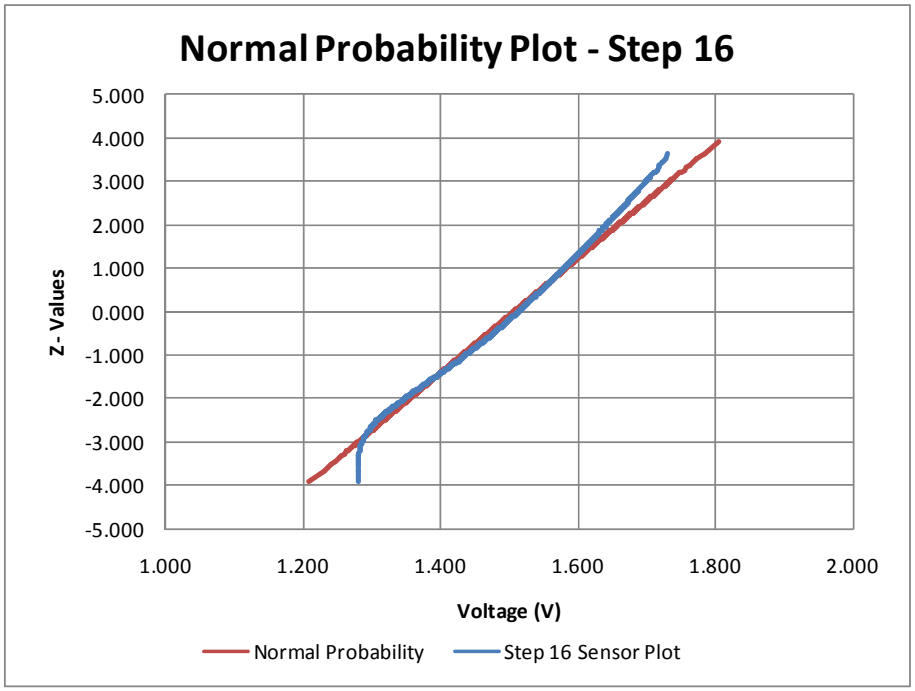

Figure 4-24: Normal probability plot – pressure sensor at step 16

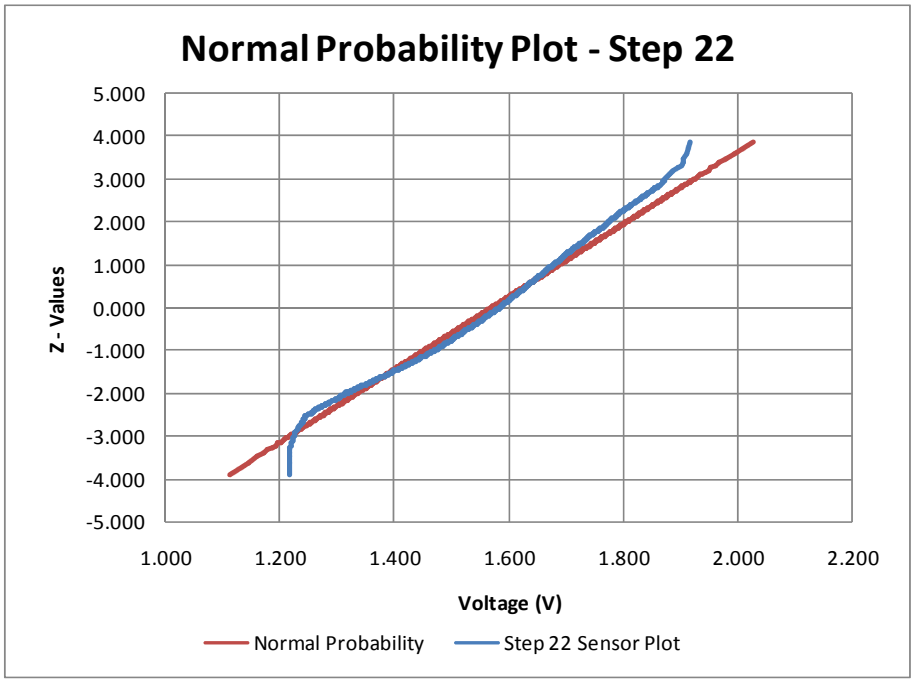

Figure 4-25: Normal probability plot – pressure sensor at step 22

From **Figure 4-24** and **Figure 4-25**, it is evident that the data from the pressure sensors plot well with the expected normal probability plot, with only slight departures from the normal when approaching the maximum and minimum values presented in **Table 4-4**.

Normal distribution curve (bell curve)

The normal distribution curve for steps 16 and 22 is illustrated in **Figure 4-26** and **Figure 4-27**, along with the histograms from the pressure sensor data. Note that, for both curves, the data only range from the minimum and maximum values shown in **Table 4-4**.

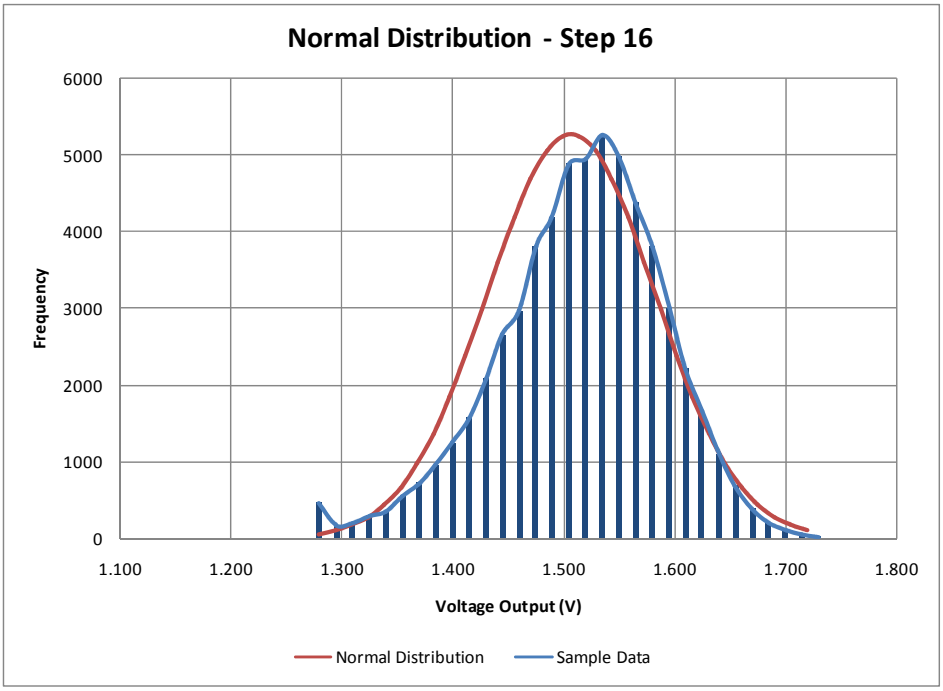

Figure 4-26: Normal distribution and histogram for pressure sensor at step 16

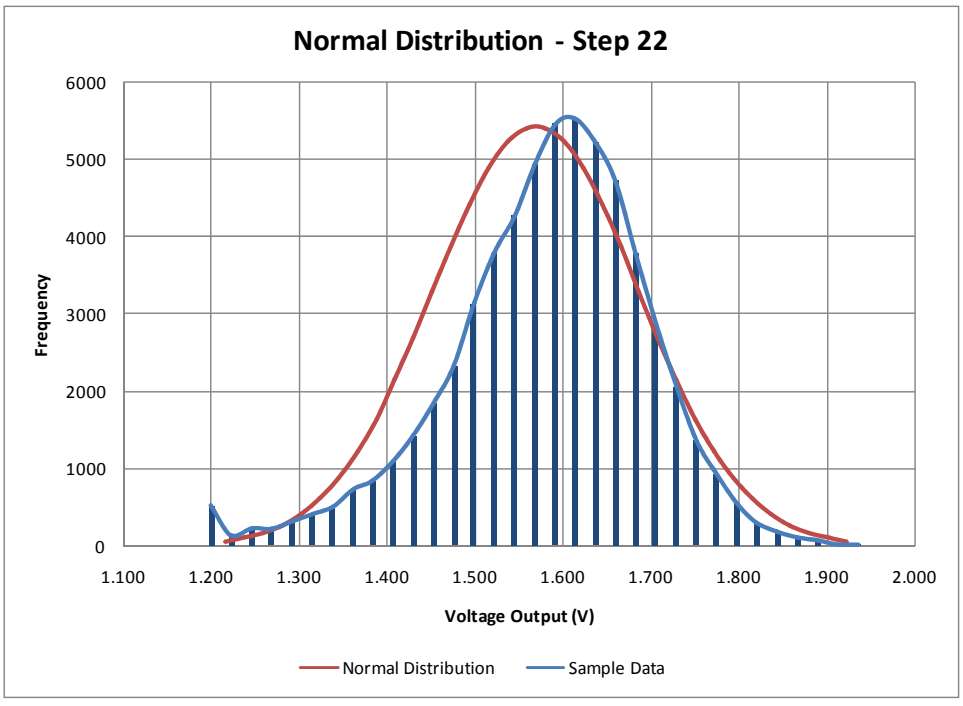

Figure 4-27: Normal distribution and histogram for pressure sensor at step 22

Figure 4-26 and **Figure 4-27** show that the pressure data plot well with the expected normal distribution curve, although skewed to the right, as was expected.

In conclusion, the graphical analysis of the pressure sensor data has proven that the data can be assumed to be distributed normally, which verifies the approach taken in using a certain confidence interval to represent the maximum and minimum pressures involved.

However, the skewing of the pressure data to the right should be noted. Note was taken of all the recorded pressure sensor data. In general, the average pressure of the sample data would, accordingly, tend to lean more to the positive side, meaning that more positive than negative pressures would be likely to be encountered.

Consideration must be given to how a 0.15% probability to represent the minimum pressures compares with the probability found in previous research. Amador, et al. (2009) suggest that a minimum pressure of 0.1% probability should be used to evaluate possible cavitation. The probability of 0.1% is in good agreement with the 0.15% chosen for this study.

Note that all references to maximum and minimum pressures for experimental results were based on the maximum and minimum pressures defined in this section.

4.4 SAMPLING TIME

The required acquisition period (i.e. sampling time) for air concentration and pressure data was determined to apply to all future experiments. Tests with different sampling times were conducted and evaluated to obtain a data set representative of the actual hydraulic conditions of the model.

The statistical mean and standard deviation were calculated for each data set, so as to establish the sample period in which the results start to converge, with emphasis being on the standard deviation. Convergence of the calculated standard deviation at a specific sampling time and onwards highlights the fact that the sample size recorded was large enough to include the variation of data, and that any extended sampling period (i.e. entailing the capturing of additional data) would not improve the results.

The elected sampling times for the air concentration and pressure tests differed, due to the different instrumentation and acquisition frequencies used to measure each. **Table 4-5** showcases the different sampling times investigated for each subject with a cross (x). All experiments were conducted using the model setup with no crest piers for a prototype unit discharge of 15 m²/s.

Table 4-5: Sampling times investigated

Description	Minutes								
	0.25	0.5	1.0	2.0	4.0	6.0	8.0	10.0	20.0
Air concentration	x	x	x	x	x	x	–	–	–
Pressure	–	x	x	x	x	x	x	x	x

4.4.1 Air Concentration

All air concentration tests were conducted at the outer edge of step 22, in line with the pseudo-bottom of the spillway at the centre of the 1 000 mm-wide model spillway (x = 500 mm). The specific tested discharge over the spillway produced an inception point at step 17, which was expected when using **Equation (3-14)**, as developed by Boes and Hager (2003b), and which was confirmed by visual observation during the model experiments. Hence, step 22 was selected as a point where frequent bubbles would be detected by the conductive probe, providing a good statistical data set of the void fractions encountered.

Figure 4-28 illustrates the average void fraction, the standard deviation and the number of bubbles detected for each sampling period. Note that the average void fraction and the standard deviation of all sampling times does not vary, remaining consistent throughout, including the fact that the number of bubbles detected increases linearly with each acquisition period.

An acquisition period of 30 s was selected as the representative sampling time for all future air concentration tests. A sampling time of 15 s would also show similar results, but as the majority of the tests were to be conducted within the non-aerated developing flow region, an extended time period was considered to be appropriate.

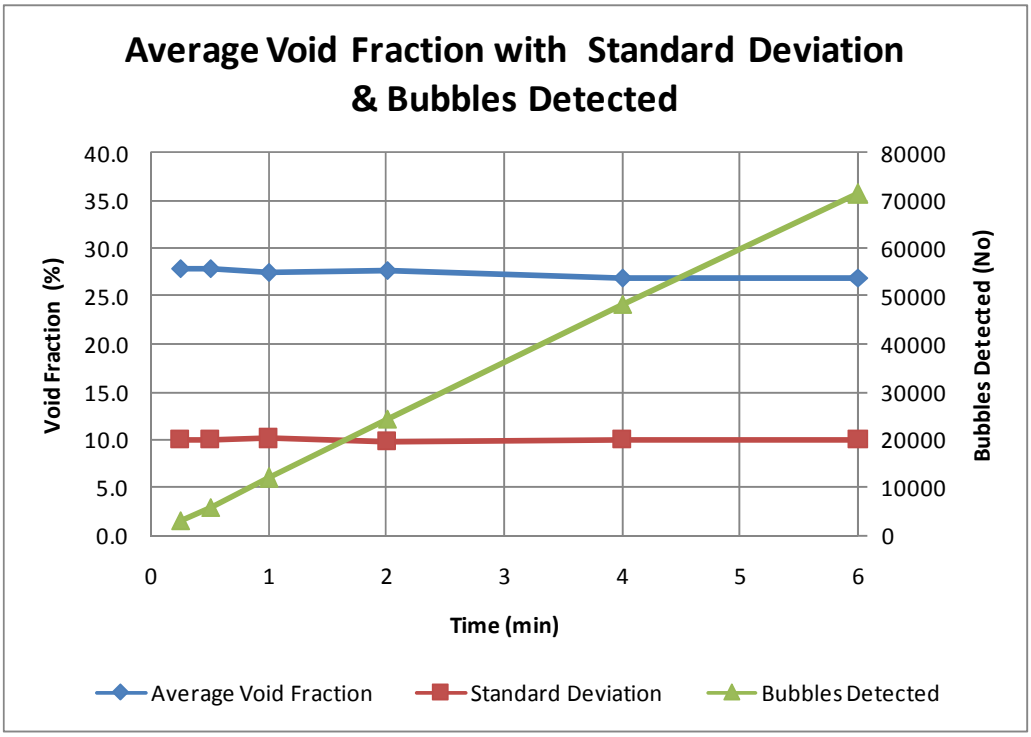

Figure 4-28: Average void fraction, with standard deviation and bubbles detected for different sampling periods

4.4.2 Pressure

Pressure transmitters were positioned in the centre spillway (x = 500 mm) on the upper vertical step faces (h = 90 mm) of steps 8, 15, 16 and 17. As stated, the entrainment of air occurs at step 17 for this specific discharge. The literature survey undertaken for the purposes of this thesis showed that the maximum fluctuation of negative pressures can be found at, and slightly upstream of, the inception point (refer to **Section 3.4**). Measurement in this zone would ensure that sufficient variation of data was recorded.

The minimum pressure and standard deviation recorded for each pressure sensor with the respective sampling periods is shown in **Figure 4-29** and **Figure 4-30**, respectively.

Both **Figure 4-29** and **Figure 4-30** illustrate that the data start to converge from a sampling time of 10 min and more. A sampling time of 10 min was chosen as the representative sampling time for all future pressure tests.

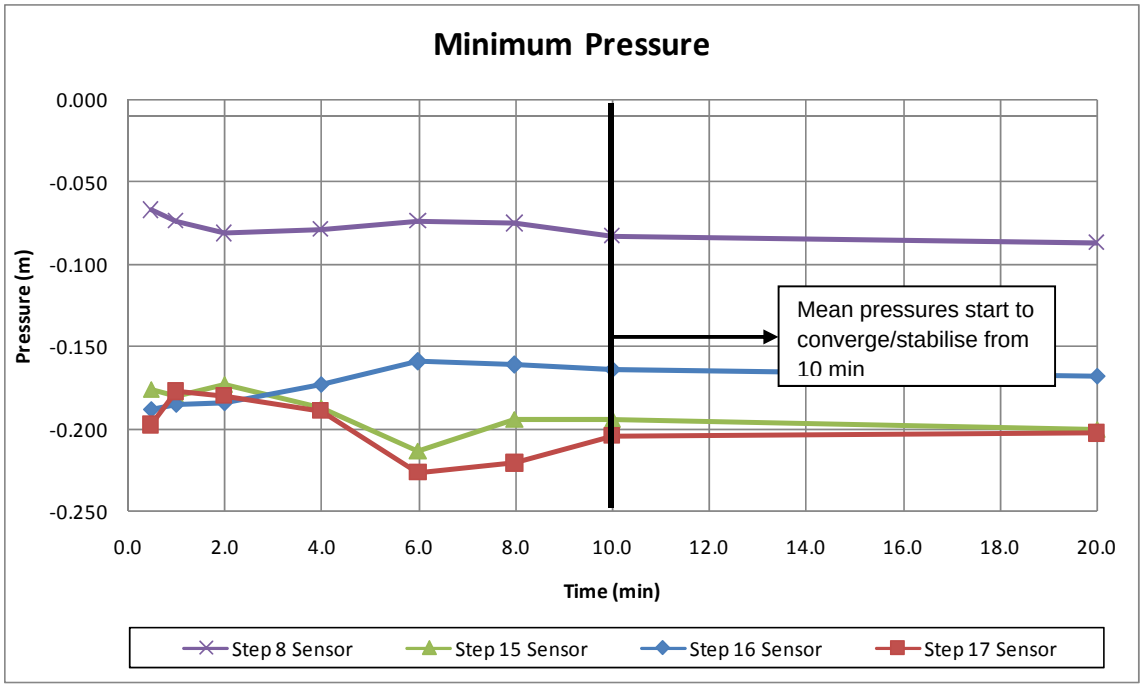

Figure 4-29: Average pressure for different sampling periods

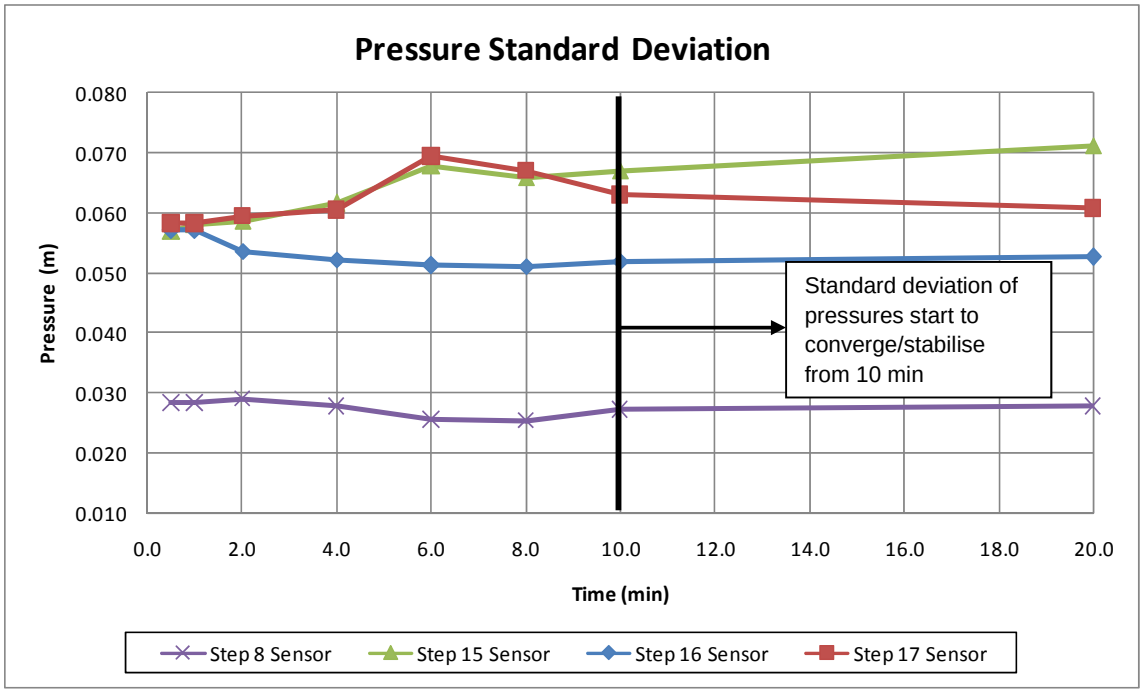

Figure 4-30: Pressure standard deviation

4.5 NORMALISING PARAMETERS TO A DIMENSIONLESS NUMBER

The results of the following measured parameters are all presented as a dimensionless number in this study. The different dimensionless variables were used to represent all the experimental data from this point forward in the document.

4.5.1 Air Concentration

The average void fraction was calculated over the selected sample period, which is discussed in **Subsection 4.4.1**. All air concentration results shall be expressed as a percentage (%) for this document.

4.5.2 Pressure

The results obtained from the pressure experiments will be expressed as a dimensionless number, as described below:

$$Pressure\ Dimensionless\ Number = p/\gamma/h \quad \textbf{(4-4)}$$

where

p = pressure (N/m²)

γ = specific weight of water (N/m³)

h = step height (m)

4.5.3 Location along Spillway

The equation used to present the location along the spillway as a dimensionless number is shown below:

$$s_i = \frac{L - L_i}{H_e} \quad \textbf{(4-5)}$$

where

s_i = dimensionless number

L_i = distance to pseudo-bottom inception point from crest along spillway profile (m)

L = distance to specific point from crest along spillway profile (m)

H_e = energy head upstream of crest (m)

Note that the abbreviations shown above for the different dimensional variables have already been defined, but it is repeated as these parameters are used to represent the experimental results.

4.6 PRELIMINARY EXPERIMENTAL WORK

A set of pilot experimental tests regarding the air concentration and pressures was conducted on the prototype model spillway, so as to determine the performance of the crest pier prior to the refinement of the pier design, and so as to evaluate the proposed testing procedures. The testing procedures are discussed in **Section 4.8**.

This section briefly discusses the experimental set-up, and results of the preliminary experimental work. The conclusion drawn from these experiments was used to improve the design of the pier and the test procedures.

4.6.1 Experimental Set-Up

Three separate tests were conducted to establish the influence of the piers on the following:

1. The discharge head.
2. The air concentration and pressure results for a constant discharge of 20 m^3/s.

The following parameters were common to all the different tests:

- Three different model setups were used, as were defined in **Subsection 4.1.4.4**.
- The sampling time for air concentration and pressure measurements was according to the times established in **Section 4.4**.
- All air concentration and pressure measurements were conducted at the spillway centre (x = 500 mm)

4.6.2 Discharge Head

The discharge head was evaluated with three different prototype flows. The prototype discharge head for each model setup is provided in **Table 4-6**. The table also indicates the percentage increase in discharge head for model setups 2 and 3, compared to model setup 1.

The model setups for this thesis were defined as follows:

- Model setup 1 - Control test for a spillway with no pier
- Model setup 2 - Spillway equipped with a Type 1 pier
- Model setup 2 - Spillway equipped with a Type 2 pier

Table 4-6: Discharge head for preliminary experimental work

Q (m^3/s)	Discharge Head [H_e] (m)		
	Model setup 1	Model setups 2 & 3	Increase in H_e
20.00	4.46	4.64	4.0%
25.00	5.07	5.31	4.7%
30.00	5.63	5.94	5.6%

The unit discharge for model setups 2 and 3 was calculated with the recorded discharge head values. The unit discharge for each model setup with corresponding increase in discharge for model setups 2 and 3, compared to model setup 1, is shown in **Table 4-7**.

Table 4-7: Unit discharge for preliminary experimental work

Q (m^3/s)	Unit discharge [q_w] (m^2/s)		
	Model setup 1	Model setups 2 & 3	Increase in q_w (in %)
20.00	20.0	21.8	8.8
25.00	25.0	27.2	9.0
30.00	30.0	32.7	9.2

From the above-mentioned results, it is evident that the increased discharge head of model setups 2 and 3 would subsequently result in a higher unit discharge, which would lead to higher velocities down the chute.

The increased discharge head and corresponding increased velocity was reflected within the air concentration and pressure results of model setups 2 and 3. As an approach to normalising the variables could not be established, it was accepted that the results between model setup 1 and model setups 2 and 3 could not be accurately compared.

4.6.3 Air Concentration and Pressure Results

As discussed, the results could not be represented faithfully, due to the increase in discharge head when a pier is introduced at the crest. Nevertheless, obvious differences between the results of the model setups were noticed once plotting on a graph took place.

4.6.3.1 Air Concentration

Figure 4-31 shows the air concentration along the spillway for all the model setups, at a prototype flow of 20 m^3/s.

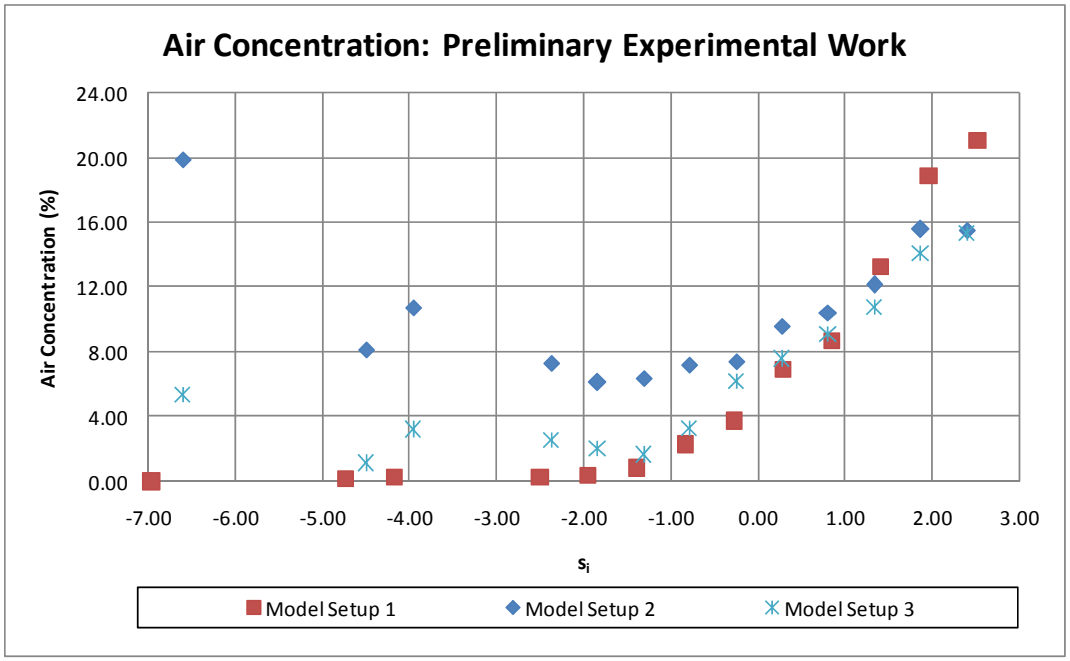

Figure 4-31: Air concentration results for preliminary experimental work at a prototype flow of 20 m³/s

The air concentration upstream of the inception point for both model setups 2 and 3 is higher compared with that of model setup 1, with model setup 2 producing the uppermost result. Downstream of the inception point, the values of model setups 2 and 3 approach the conventional norm (in terms of the results of model setup 1).

Similar behaviour of air concentration along the spillway was observed for the model studies on the piers, and in the case of the findings of Pfister, et al. (2006), as discussed in the literature (refer to **Subsection 3.3.3**). The large amount of air that is entrained immediately downstream of the pier then dissipates gradually along the spillway towards the percentage of air concentration that was observed for the spillway with no pre-aeration capabilities. This phenomenon was attributed to the highly aerated vortices that lose air by rolling up the step face, in which case the 'lost' air bubbles are then absorbed by the upper flow region.

4.6.3.2 Pressures

The maximum and minimum pressures along the spillway for all the model setups at a prototype flow of 20 m³/s are illustrated in Figure 4-32.

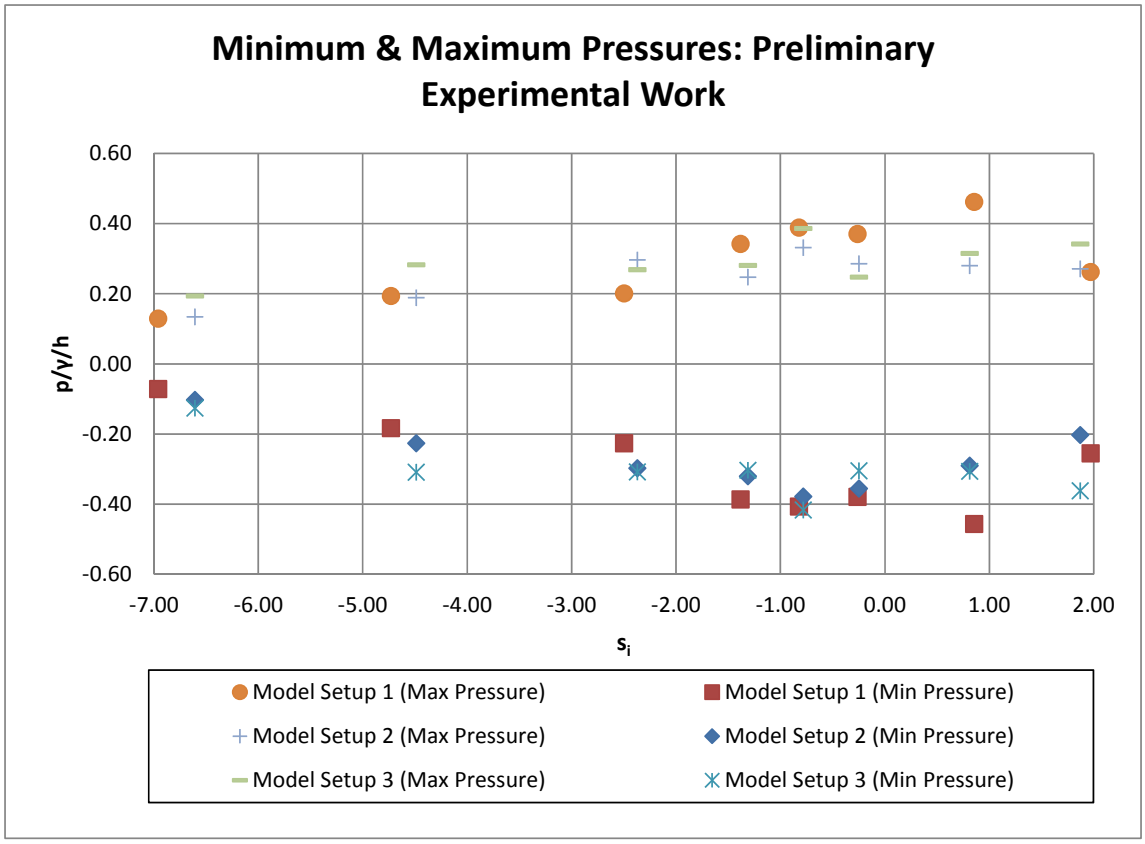

Figure 4-32: Maximum and minimum pressure results for preliminary experimental work, at a prototype flow of 20 m³/s

The results obtained clearly show that the pressure fluctuation increases from the spillway crest to the inception point. Further downstream of the inception point, a reduction of the pressure fluctuations is observed. The smallest minimum pressures were recorded within the proximity of the inception point.

Fewer pressure fluctuations can be seen for model setups 2 and 3 just upstream of the inception point, when they are compared to model setup 1. Although this might be credited to the increased air concentration, it could not be confirmed in relation to the preliminary experimental work.

4.6.4 Additional Experimental Observations

An interesting visual observation was made with regard to the air being entrained at the pseudo-bottom, downstream of the piers.

For the Type 1 pier, the jet flow develops directly downstream of the pier (see **Figure 4-33** to **Figure 4-35**). This was noticed for all prototype flows tested, which consisted of 20 m³/s, 25 m³/s and 30 m³/s. A Type 1 pier extends from the crest to step 3, which is still within the ogee profile of the crest.

Flow separation is created downstream of the pier that extends across the full flow depth, down to the step surfaces. Air is entrained into the flow through the separation gap, and onto the step niches. It is

then believed to be transported across the spillway width, which is made possible either by the negative pressure envelope that exists at the bottom of the ogee profile, or by the rolling vortices that exist on the steps.

Figure 4-33: Jet flow for Type 1 pier at prototype flow of 30 m³/s

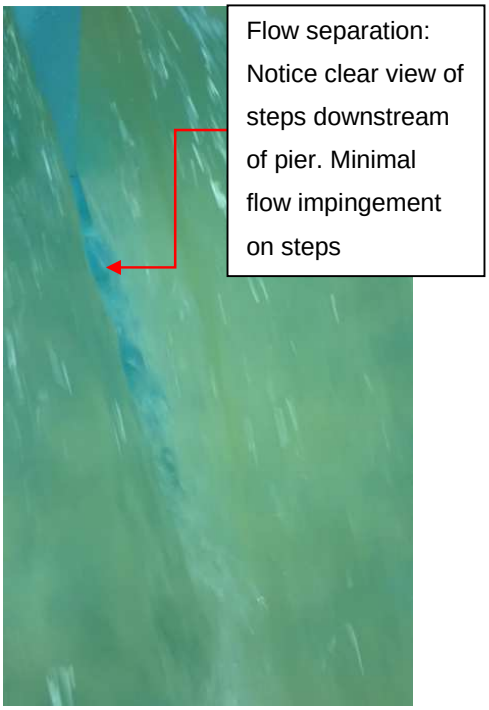

Figure 4-34: Flow separation downstream of Type 1 pier at prototype flow of 30 m³/s – preliminary experimental work

Figure 4-35: Detail A of Figure 4-33

The jet flow that develops on the ogee profile does not project onto the horizontal step faces to the same measure that can be seen with the skimming flow within the downstream uniform flow region. Less impingement by the jet flow on the horizontal step was observed as the discharge was increased.

In line with the belief that the flow over the ogee still adheres to the shape of a lower nappe, minimal impingement on the horizontal step was observed for the jet flow, especially for discharges greater than, or equal to, the design discharge (H_d). This theory also supports the observation that the separation of flow directly downstream of the pier extends all the way down to the spillway surface.

No jet flow was observed for the Type 2 pier (see **Figure 4-36** and **Figure 4-37**). However, it can be seen that flow impinges on the horizontal step downstream of the pier, typical to a skimming flow regime, and that it also entrains air directly behind the pier. Note that the pier extends to step 7, past the point of tangency, where the spillway slope is constant.

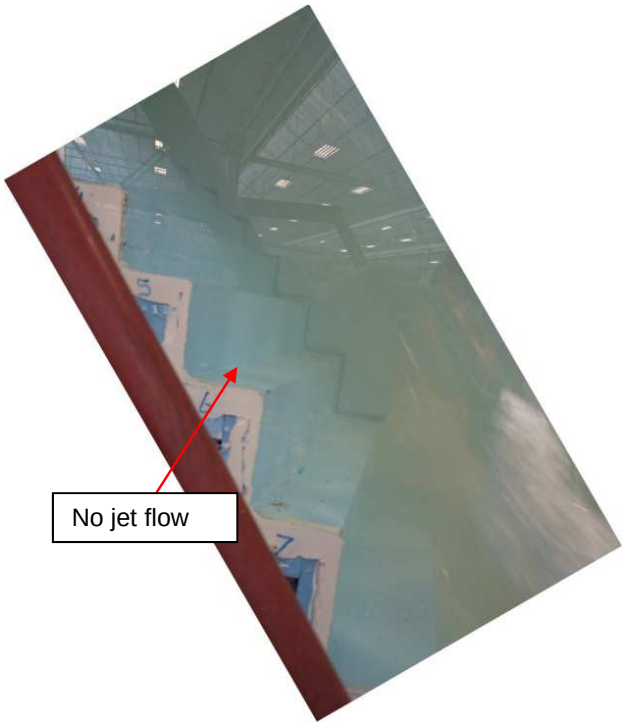

Figure 4-36: Flow alongside a Type 2 pier at prototype flow of 20 m³/s

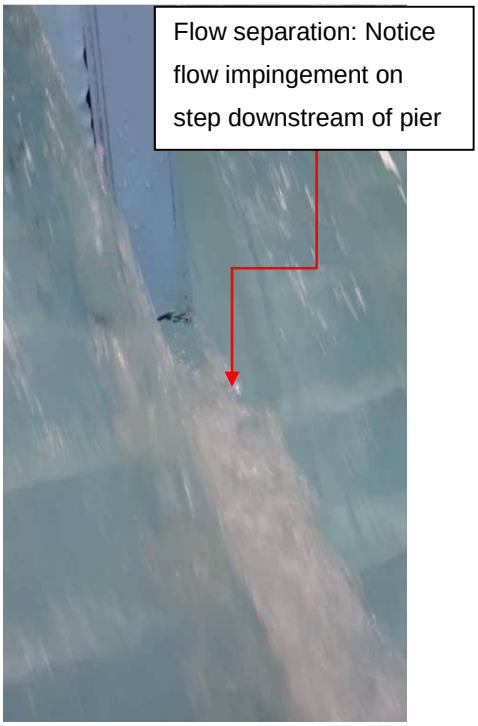

Figure 4-37: Flow separation downstream of Type 2 pier in prototype flow of 20 m³/s – preliminary experimental work

In conclusion, it appears that the entrainment of air downstream of a pier is subject to the length that the pier extends down the spillway. A pier that terminates within the ogee profile crest zone could produce severe jet flow, whereas no jet flow is created downstream of a pier that extends past the point of tangency.

Subject to the slope of the chute, the horizontal step tread downstream of the point of tangency seems to be large enough for sufficient flow impingement, in order to facilitate aerated skimming flow directly downstream of the pier.

4.6.5 Conclusion of the Preliminary Experimental Work

Regarding cavitation on spillways, to which spillways are more prone upstream of the inception point, the results indicate that, by introducing piers at the spillway crest, the air concentration along the pseudo-bottom at the spillway centre (i.e. x-coordinate = 500 mm) can be increased. The results also show that a slight reduction of pressure fluctuations can be expected around the inception point, due to the presence of a crest pier.

Increased air concentration upstream of the inception point was observed for a Type 1 pier, due to the occurrence of jet flow, whereas less, albeit more than that in the case of a spillway with no piers, air concentration was recorded for a Type 2 pier, where skimming flow develops downstream of the pier.

4.6.6 Recommendations Arising from the Preliminary Experimental Work

From the conclusions drawn from the preliminary experimental model studies, the following recommendations were put forward to be incorporated into the testing of the final prototype model.

- The discharge head for each selected unit discharge should be the same between all model setups, so as to eliminate varied velocities down the chute. The modifications that were made to the flow for each model setup are discussed in **Subsection 4.7.1**.
- A pier design should be adapted to minimise, or to eliminate, the effect on the discharge head. In addition, two different pier designs are recommended for studying the flow behaviour downstream of the pier, with one terminating within the ogee profile crest zone, and with one extending past the point of tangency. The piers, which were designed in line with the above remarks, are discussed in **Subsection 4.7.2**.
- Increased points of measurement across the spillway width are required to quantify the impact of the spillway piers on the development of air concentration and pressure along, and across, the spillway chute. The experimental procedures are discussed in **Section 4.8**.
- A prototype unit discharge above the design discharge of 18.8 m^2/s should be used to ensure that negative pressures are generated on the crest ogee. The selected unit discharge for the experimental model is discussed in **Subsection 4.8.2**.

4.7 ALTERATIONS TO PROTOTYPE CREST PIER

Modifications were made to the original proposed pier design, so as to incorporate the recommendations that followed from the preliminary experimental work. The following subsection will discuss the modified design of the crest pier.

4.7.1 Discharge Head with Consideration to Crest Piers

4.7.1.1 Modified Pier Concept

For a constant flow over the spillway crest, the model pier design and the position on the crest did affect an increase in the discharge head, when compared to the performance of a spillway containing no piers.

A modified pier concept was proposed that was based on the existing pier design of the Gariep Dam shown in **Figure 4-38**. The piers are positioned slightly downstream of the crest and below the critical flow depth, so as to eliminate any effect on the discharge head when compared to spillway with no piers, or so as to produce only a minimal increase in discharge head.

Figure 4-38: Gariep Dam piers (Anonymous, 2010)

4.7.1.2 Position of Modified Pier

Experimental tests were conducted using the existing Type 1 pier to determine the best position downstream of the crest where the discharge head would not be affected were the flow to be kept constant.

The point closest to the crest at which no change was observed for the discharge head, was when the front end of the pier was located at step 4.

Figure 4-39 and **Figure 4-40** illustrate the position and downstream effects of a Type 1 pier with the front end positioned on steps 1 and 4, respectively.

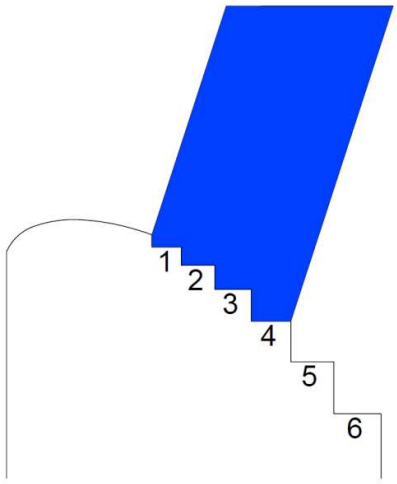

Figure 4-39: Type 1 pier with front end located at step 1 for a prototype flow of 30 m³/s

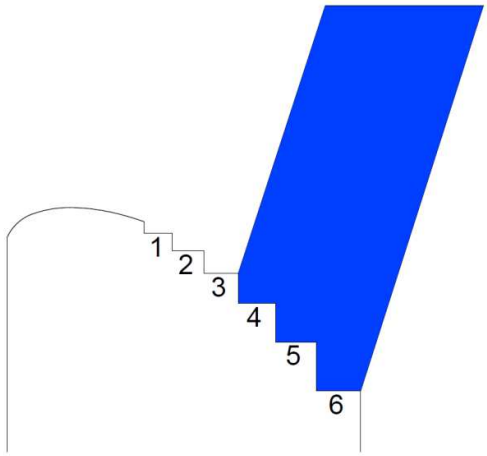

Figure 4-40: Type 1 pier with front end located at step 4 for a prototype flow of 30 m³/s

The downstream turbulence created once the front end of the pier was positioned at steps 2 to 4 was deemed to be too severe for a typical spillway. The practical implications associated with the unsteady flow downstream of the pier would outweigh the initial positive intentions of a constant discharge head with a constant flow. The front end of the new pier design, would, therefore be located at step 1

With the new pier positioned at step 1, a higher discharge head would be recorded for the spillway with the pier, compared to what would be recorded in terms of the discharge head for a spillway with no pier, provided that the flow were to be similar for both.

To accurately compare the air concentration and pressure experimental results, the energy height at the spillway crest should be the same across all model setups. It was, therefore, decided to keep the discharge head constant for all model setups, by means of adjusting the model flow.

4.7.2 Design of Modified Pier

The design of the new crest pier remained exactly the same as the design for the previous crest pier, except that the pier was angled slightly, and for it being positioned downstream of the crest. The Type 1 pier extends downstream to step 4, still within the ogee profile zone, while Type 2 pier terminates at step 7, which is beyond the point of tangency. The dimensions and photographs of the two piers are shown in **Figure 4-41** to **Figure 4-44**.

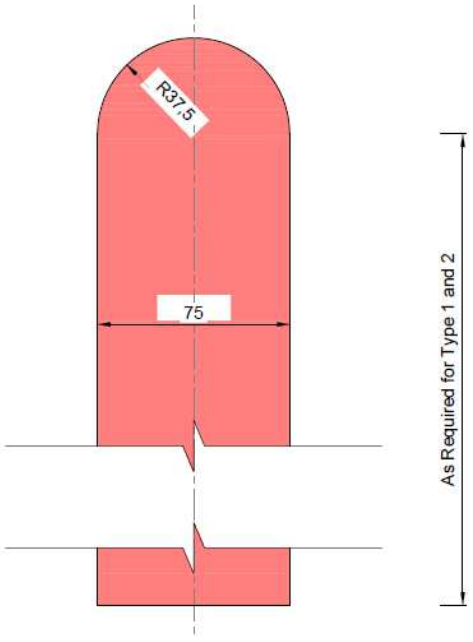

Figure 4-41: Plan view of model crest pier – dimensions shown in mm

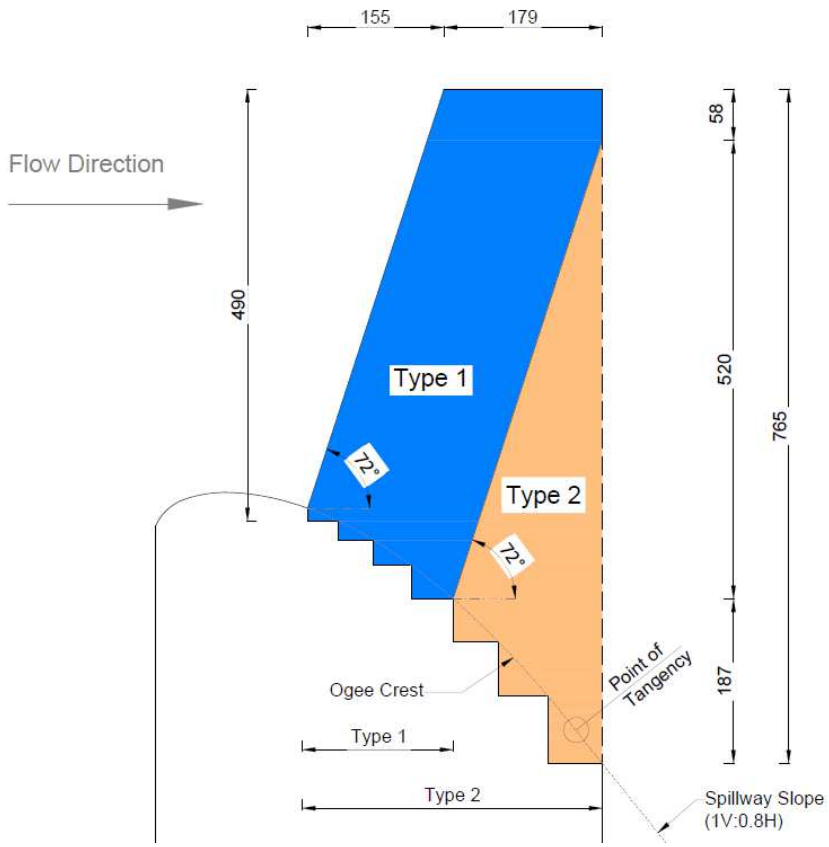

Figure 4-42: Side view of new model piers (types 1 and 2) – dimensions shown in mm

Figure 4-43: Type 1 pier installed on spillway

Figure 4-44: Type 2 pier installed on spillway

4.8 EXPERIMENTAL TEST PROCEDURES

4.8.1 Introduction

The principal aim of the study was to determine whether an earlier onset of air entrainment could be achieved by introducing piers at the spillway crest. The spillway area to be studied would, therefore, be the region between the crest and the pseudo-bottom inception point, known as the developing and rapidly varied flow regions (flow regions 1 and 2, respectively) as described in **Subsection 3.1.4**.

The results of the preliminary experimental work showed that the concentration of air at the pseudo-bottom is increased directly downstream of a crest pier, but still little is known about how the air concentration develops across the spillway width. The set of experimental tests was devised to investigate the air concentration properties across the spillway width within Flow Regions 1 and 2. The minimum pressures, with regard to cavitation, were also measured across the same study region, so as to determine the influence of surface pressures when a spillway is pre-aerated.

The critical point was defined in **Subsection 3.8.2**, which refers to the point downstream of the inception at which the pseudo-bottom air concentration is sufficient to prevent cavitation damage. The study area was extended downstream of Flow Region 2 to include the critical point as well.

Figure 4-45 illustrates the testing procedure followed for this study. Three different model setups were tested. The test results of model setup 1 were compared to those obtained for model setups 2 and 3, so

as to determine whether the introduction of spillway piers could enable a stepped spillway to convey discharges exceeding the recommended limit, without endangering the structure to cavitation damage.

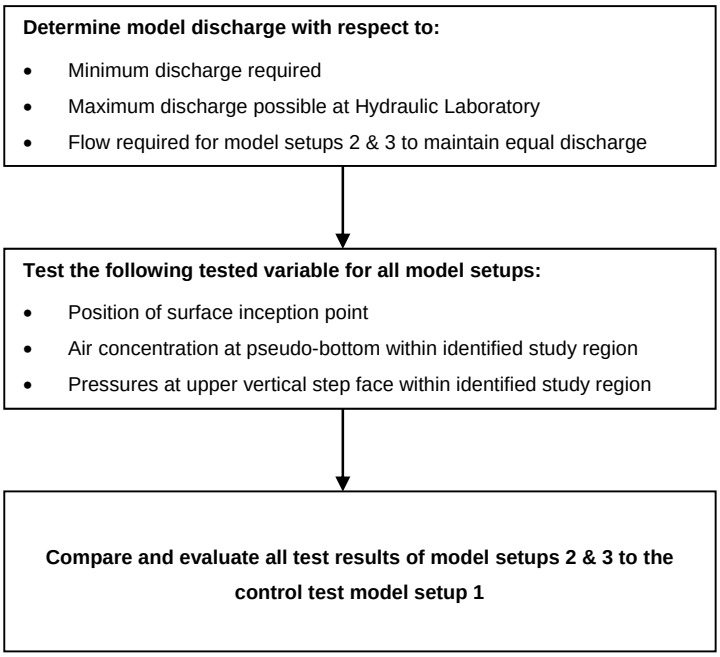

Figure 4-45: Model testing procedure

4.8.2 Experimental Test Parameters

Preliminary sampling tests determined that an average acquisition time of 0.5 min (30 sec) with the conductive needle probe is sufficient to capture a reliable set of data for all ensuing air concentration tests, and that a sampling time of 10 min is required to obtain a realistic average for the fluctuating pressures on the upper vertical step face. **Section 4.4** describes how the different lengths of sampling time were established.

The minimum prototype discharge of the model must be able to satisfy the Reynolds and Weber criterion (refer to **Subsection 3.8.5.1**), to produce skimming flow down the spillway chute (refer to **Subsection 3.1.3.4**), and to exceed the design discharge of the ogee crest, so as to ensure that a negative envelope is created on the ogee profile. In addition, the minimum discharge should also exceed the maximum recommended discharge with regard to cavitation (refer to **Subsection 3.8.4.1**), in order to test whether the aeration produced by the crest piers could be an effective measure of cavitation prevention for discharges above the recommended value.

The different unit discharge values for each criterion are listed below:

- Reynolds and Weber Criterion – 6 m²/s
- Skimming flow regime – 4 m²/s
- Ogee crest design discharge – 18.8 m²/s
- Cavitation discharge limit – 18 m²/s

A minimum prototype unit discharge of 25 m²/s was selected to satisfy all model criteria.

The maximum unit discharge for the model was subjected to the maximum flow obtainable at the Stellenbosch Hydraulic Laboratory, which was 600 l/s. The maximum flow used in the model was 516 l/s, which corresponded to a prototype value of 30 m²/s for a spillway with no pier.

The preliminary experimental work undertaken enabled the conclusion to be drawn that the energy height for each discharge across all the model setups should be the same. The prototype flow was, therefore, adjusted for model setups 2 and 3, so as to ensure that the discharge head and unit discharge corresponded to that of model setup 1. The adjusted prototype flows with corresponding discharge heads are shown in **Table 4-8**.

Table 4-8: Adjusted prototype flows for experimental model

q_w (m²/s)	Model setup 1		Model setup 2 & 3	
	H_e (m)	Q (m³/s)	H_e (m)	Q (m³/s)
25.00	5.07	25.0	5.07	24.2
30.00	5.63	30.0	5.63	28.5

The prototype and model flow used to record the experimental measurements for the different model setups is shown in **Table 4-9**.

Table 4-9: Prototype and model discharge values

q_w (m²/s)	Model setup 1		Model setup 2 & 3	
	Prototype Q (m³/s)	Model Q (l/s)	Prototype Q (m³/s)	Model Q (l/s)
25.00	25.00	430	24.2	417
30.00	30.00	516	28.5	490

Three tests were conducted for all the following model setups:

- **Test A** – Visual observations of the surface inception point.
- **Test B** – Recording of the pseudo-bottom air concentration within the study region.
- **Test C** – Pressure measurements at the upper vertical step face within the study region.

The three tests are described in more detail in the following sections.

4.8.3 Test A: Surface Inception Point

The distance to surface inception was visually recorded for each discharge, and for all model setups. The aim of this test was to create a data set of visual observations by means of which to compare the results of tests that were conducted using air and pressure instrumentation, in terms of tests B and C, respectively.

The length to surface inception was measured from the spillway crest to the point where surface air entrainment was observed. The surface inception point may vary instantaneously over several steps, thus the length to this point was monitored over a period of 1 min to determine the average obtained.

For this test, the point of surface inception was defined as the point where clear water flow ends and turbulent white water commences. (See **Figure 4-46**.) Localised areas of air entrainment occurred across the spillway width, due to the effect of the crest pier(s) and the side walls. As a result, a conservative approach was used, by classifying the general point of surface inception at the most downstream point where air is entrained, meaning where the clear water flow ends.

Figure 4-46: Test A – surface inception point

4.8.4 Test B: Air Concentration

The objective was to measure the air concentration along, and across, the spillway pseudo-bottom within the study region that extended just downstream of the ogee crest to the critical point. The critical point differed for each discharge.

The air concentration was recorded along the spillway with the conductivity needle probe located at the outer step edge for each measuring position. The different measuring positions used for recording the air concentration for each selected discharge are shown in **Table 4-10**. Note that the cells highlighted in orange represent the pseudo-bottom inception point, whereas the cells in blue represent the approximate critical point for each discharge, as determined by Boes and Hager (2003b).

Only half of the spillway width was evaluated, being the half from the centre of the spillway (x = 500 mm) to the end (x = 875 mm). The air concentration recorded for the study area would be a replica of the other half of the spillway, due to the symmetry of the physical model. Results from the study area were, therefore, mirrored so as to showcase the air concentration of the width across the entire spillway.

Table 4-10: Test B – Positions for measuring air concentration

Prototype discharge (m^2/s)	L distance (mm)	Step (no.)	Position 1	Position 2	Position 3	Position 4
			x-coordinate: (mm)	x-coordinate: (mm)	x-coordinate: (mm)	x-coordinate: (mm)
25	663	8	500	625	750	875
	919	10	500	625	750	875
	1175	12	500	625	750	875
	1431	14	500	625	750	875
	1687	16	500	625	750	875
	1943	18	500	625	750	875
	2328	21	500	625	750	875
	2712	24	500	625	750	875
	3096	27	500	625	750	875
	3480	30	500	625	750	875
30	663	8	500	625	750	875
	919	10	500	625	750	875
	1175	12	500	625	750	875
	1431	14	500	625	750	875
	1687	16	500	625	750	875
	1943	18	500	625	750	875
	2328	21	500	625	750	875
	2712	24	500	625	750	875
	3096	27	500	625	750	875
	3480	30	500	625	750	875
	3864	33	500	625	750	875

4.8.5 Test C: Pressures

The objective was to measure the minimum pressures within the study region, so as to determine the influence of pressures on the spillway.

For each measuring position, the pressure was measured on the vertical step face at 0.9*h* with pressure transducers. The positions for recording the pressures for each selected discharges are shown in **Table 4-11**. As discussed, the orange and blue cells highlight the pseudo-bottom inception and critical point, respectively.

As for Test B, the results of the study area were mirrored to present the pressures across the entire spillway width.

Table 4-11: Test B – Positions for measuring pressure

Prototype discharge (m²/s)	L distance (mm)	Step (no.)	Position 1	Position 2	Position 3	Position 4
			x-coordinate: (mm)	x-coordinate: (mm)	x-coordinate: (mm)	x-coordinate: (mm)
25	663	8	500	625	750	875
	1175	12	500	625	750	875
	1687	16	500	625	750	875
	2200	20	500	625	750	875
	2456	22	500	625	750	875
	2712	24	500	625	750	875
	2968	27	500	625	750	875
	3480	30	500	625	750	875
30	663	8	500	625	750	875
	1175	12	500	625	750	875
	1687	16	500	625	750	875
	2200	20	500	625	750	875
	2456	22	500	625	750	875
	2712	24	500	625	750	875
	2968	27	500	625	750	875
	3480	30	500	625	750	875
	3864	33	500	625	750	875

5. EXPERIMENTAL MODEL TEST RESULTS

Within this chapter, the results of the different tests are presented. The visual observed results of Test A will be discussed first, followed by the results of Tests B and C. Detailed discussions regarding the experimental results will be examined in Chapter 6.

5.1 TEST A: Surface inception points

The step at which the surface inception point was observed for all model setups is shown in **Table 5-1** which gives the theoretical pseudo-bottom inception point (after Boes and Hager (2003b) for a spillway with the model's parameters.

Table 5-1: Test A results - surface inception points compared with the theoretical pseudo-bottom inception points

q (m²/s)	Step Number (No.)			
	Theoretical pseudo-bottom inception point	Model setup 1	Model setup 2	Model setup 3
25	24	24	22	23
30	27	27	25	26

The table above clearly shows that the theoretical pseudo-bottom and the observed surface inception point for the physical model with no pier occur at the same position. This implies that the rapidly varied flow region (Region 2) is very small for the tested conditions.

From the results, it can be seen that an earlier point of air entrainment was observed for a spillway with a pier (model setups 2 and 3) when compared to the point that was observed with a spillway with no pier (model setup 1). If the performance of the pier design is to be based on the results of Test A, the Type 1 pier in model setup 2 would be preferred, as the point of surface inception took place further upstream in comparison to the other model setups.

5.2 TEST B: Air Concentration

The air concentration results are presented in a table format, as well as graphically, for each model setup within this section. The scatter plot figures show the actual recordings which was taken for half of the spillway width (x = 500 to x = 875). However the results shown in the tables and contour plots represents the entire spillway width (x = 125 mm to x = 875 mm) due to symmetry of the model as discussed in **Subsection 4.8.4**.

5.2.1 Model Setup 1 (no pier)

The average air concentration results of model setup 1 for the two unit discharges tested are tabulated in **Table 5-2** and **Table 5-3**, and they are illustrated graphically in **Figure 5-2** to **Figure 5-4**. The results are plotted against the dimensionless distance s_i.

Table 5-2: Test B results of model setup 1-25 m²/s

S_i (normalized distance)	Air concentration (%)						
	x = 125	x = 250	x = 375	x = 500	x = 625	x = 750	x = 875
-6.37	0.04	0.00	0.00	0.00	0.00	0.00	0.04
-5.57	0.02	0.00	0.00	0.00	0.00	0.00	0.02
-4.77	0.07	0.01	0.03	0.11	0.03	0.01	0.07
-3.97	0.03	0.02	0.02	0.04	0.02	0.02	0.03
-3.17	0.03	0.01	0.01	0.03	0.01	0.01	0.03
-2.37	0.24	0.15	0.06	0.10	0.06	0.15	0.24
-1.16	1.76	1.28	1.41	1.18	1.41	1.28	1.76
0.04	6.70	5.30	5.70	6.44	5.70	5.30	6.70
1.24	15.01	13.72	14.40	13.11	14.40	13.72	15.01
2.44	24.73	22.75	19.45	23.16	19.45	22.75	24.73

Table 5-3: Test B results of model setup 1-30 m²/s

S_i (normalized distance)	Air concentration (%)						
	x = 125	x = 250	x = 375	x = 500	x = 625	x = 750	x = 875
-6.89	0.00	0.00	0.00	0.00	0.00	0.00	0.00
-6.18	0.11	0.08	0.19	0.31	0.19	0.08	0.11
-5.46	0.01	0.06	0.03	0.00	0.03	0.06	0.01
-4.75	0.09	0.13	0.38	0.02	0.38	0.13	0.09
-4.03	0.02	0.18	0.47	0.08	0.47	0.18	0.02
-3.32	0.03	0.11	0.13	0.80	0.13	0.11	0.03
-2.24	0.13	0.07	0.48	0.41	0.48	0.07	0.13
-1.17	0.95	0.97	1.03	1.81	1.03	0.97	0.95
-0.09	6.04	4.20	4.05	4.11	4.05	4.20	6.04
0.98	11.35	10.04	8.43	10.34	8.43	10.04	11.35
2.05	14.77	13.38	16.82	14.96	16.82	13.38	14.77

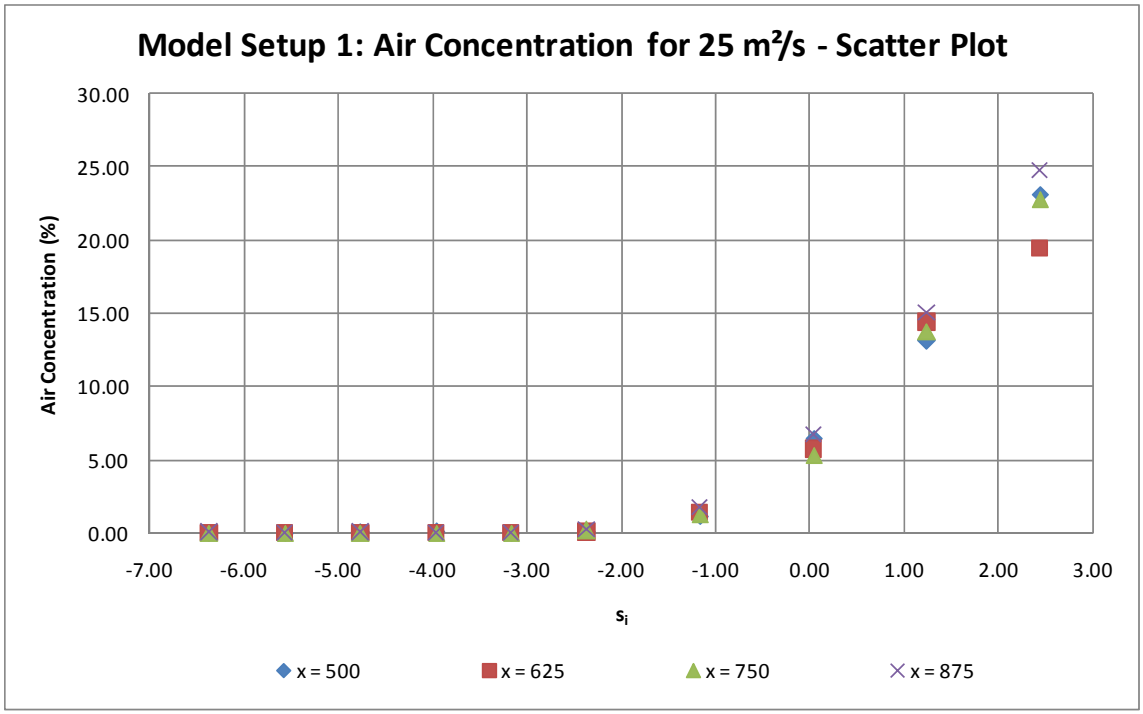

Figure 5-1: Test B results of model setup 1-25 m²/s (scatter plot)

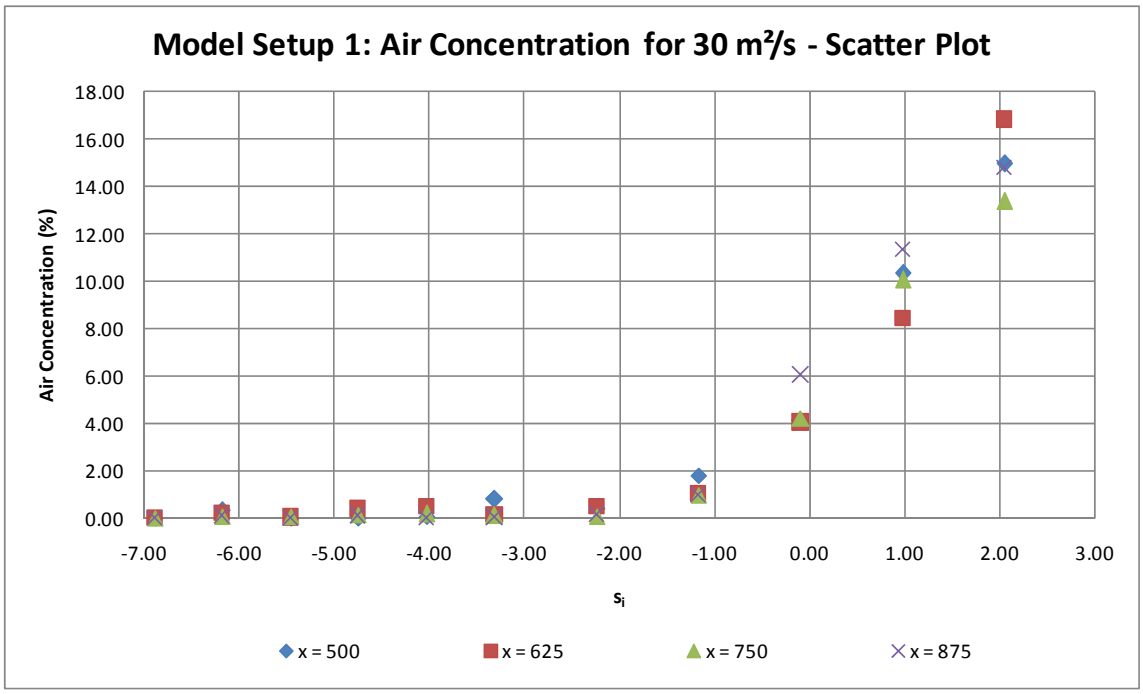

Figure 5-2: Test B results of model setup 1-30 m²/s (scatter plot)

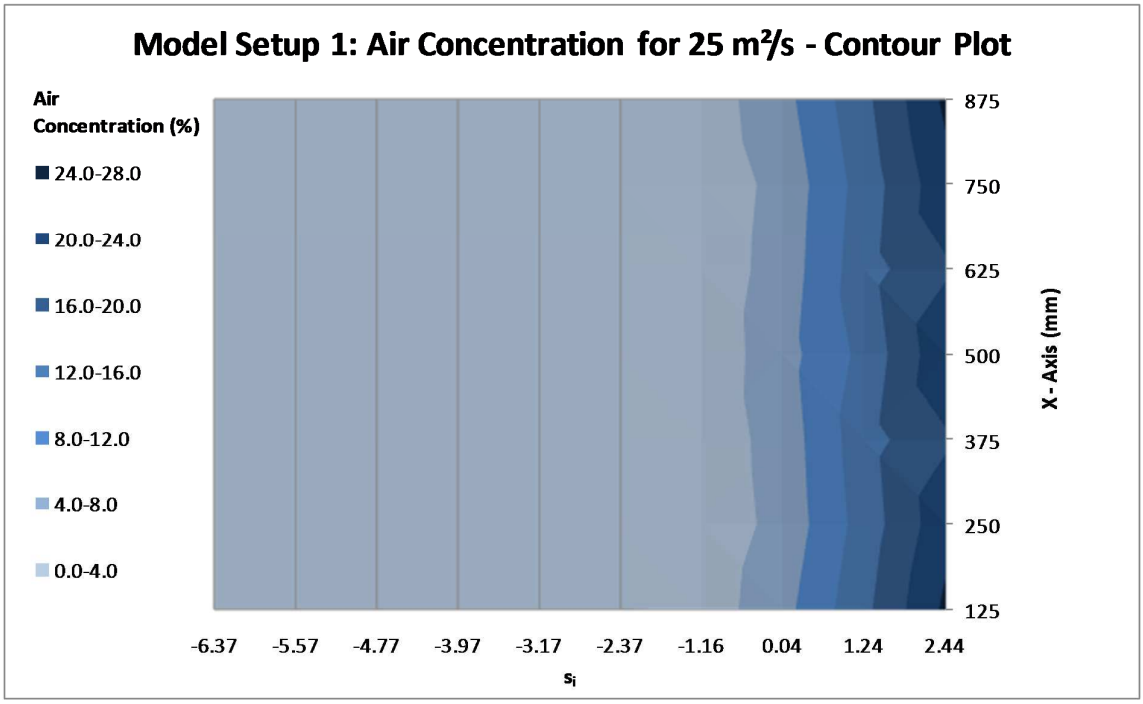

Figure 5-3: Test B results of model setup 1-25 m²/s (contour plot)

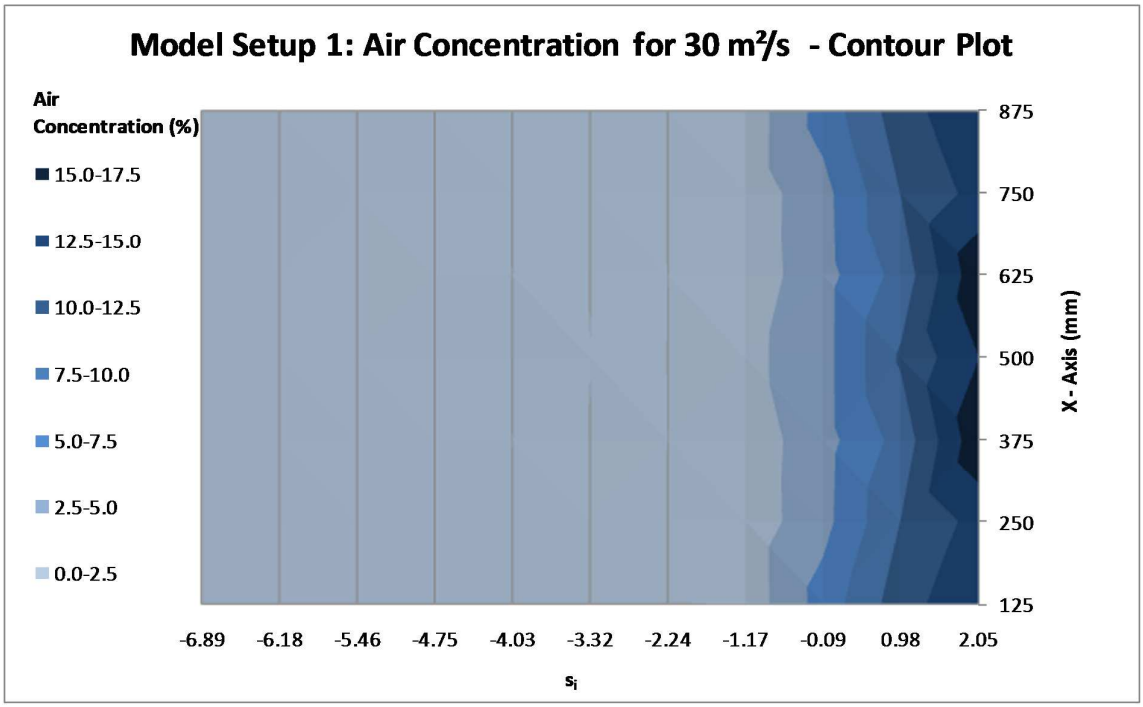

Figure 5-4: Test B results of model setup 1-30 m²/s (contour plot)

5.2.2 Model Setup 2 (Type 1 pier)

The air concentration results of model setup 2 for the two unit discharges are tabulated in **Table 5-4** and **Table 5-5**, and they are illustrated graphically in **Figure 5-5** to **Figure 5-8**. The results are plotted against the dimensionless distance s_i.

Table 5-4: Test B results of model setup 2-25 m²/s

S_i (normalized distance)	Air concentration (%)						
	x = 125	x = 250	x = 375	x = 500	x = 625	x = 750	x = 875
-6.37	1.58	7.33	11.69	23.56	11.69	7.33	1.58
-5.57	1.23	4.33	6.42	14.25	6.42	4.33	1.23
-4.77	1.20	2.88	5.31	11.01	5.31	2.88	1.20
-3.97	0.78	2.36	4.23	7.79	4.23	2.36	0.78
-3.17	0.30	2.18	4.21	6.84	4.21	2.18	0.30
-2.37	0.45	1.56	3.94	6.10	3.94	1.56	0.45
-1.16	1.95	3.40	4.85	8.21	4.85	3.40	1.95
0.04	5.91	9.88	9.24	9.52	9.24	9.88	5.91
1.24	16.80	16.51	18.99	16.17	18.99	16.51	16.80
2.44	28.47	28.65	20.14	23.47	20.14	28.65	28.47

Table 5-5: Test B results of model setup 2-30 m²/s

S_i (normalized distance)	Air concentration (%)						
	x = 125	x = 250	x = 375	x = 500	x = 625	x = 750	x = 875
-6.89	5.47	10.25	17.03	25.41	17.03	10.25	5.47
-6.18	4.37	4.37	7.69	17.79	7.69	4.37	4.37
-5.46	3.47	3.36	4.25	12.62	4.25	3.36	3.47
-4.75	3.08	2.64	3.75	10.54	3.75	2.64	3.08
-4.03	2.06	2.27	3.64	8.35	3.64	2.27	2.06
-3.32	3.83	5.24	3.47	9.30	3.47	3.89	3.83
-2.24	1.59	2.39	5.45	8.11	5.45	2.39	1.59
-1.17	2.10	4.80	6.51	6.95	6.51	4.80	2.10
-0.09	7.95	10.46	13.06	9.20	13.06	10.46	7.95
0.98	15.99	15.95	15.36	14.74	15.36	15.95	15.99
2.05	20.44	24.72	22.66	21.09	22.66	24.72	20.44

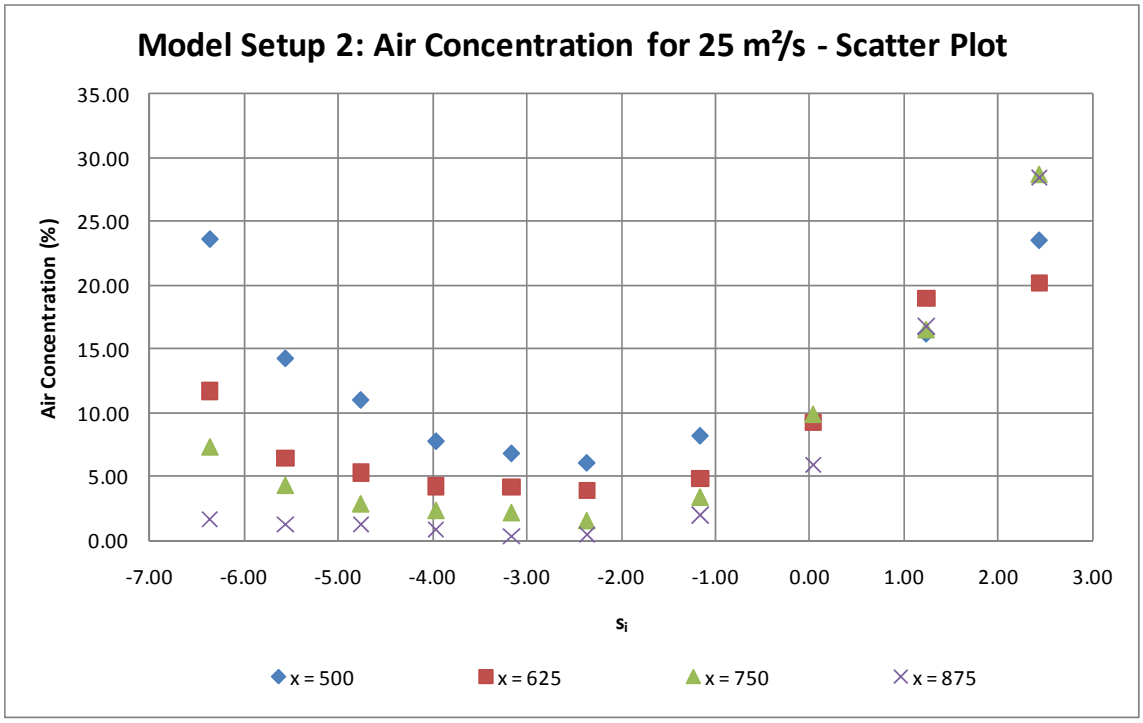

Figure 5-5: Test B results of model setup 2-25 m²/s (scatter plot)

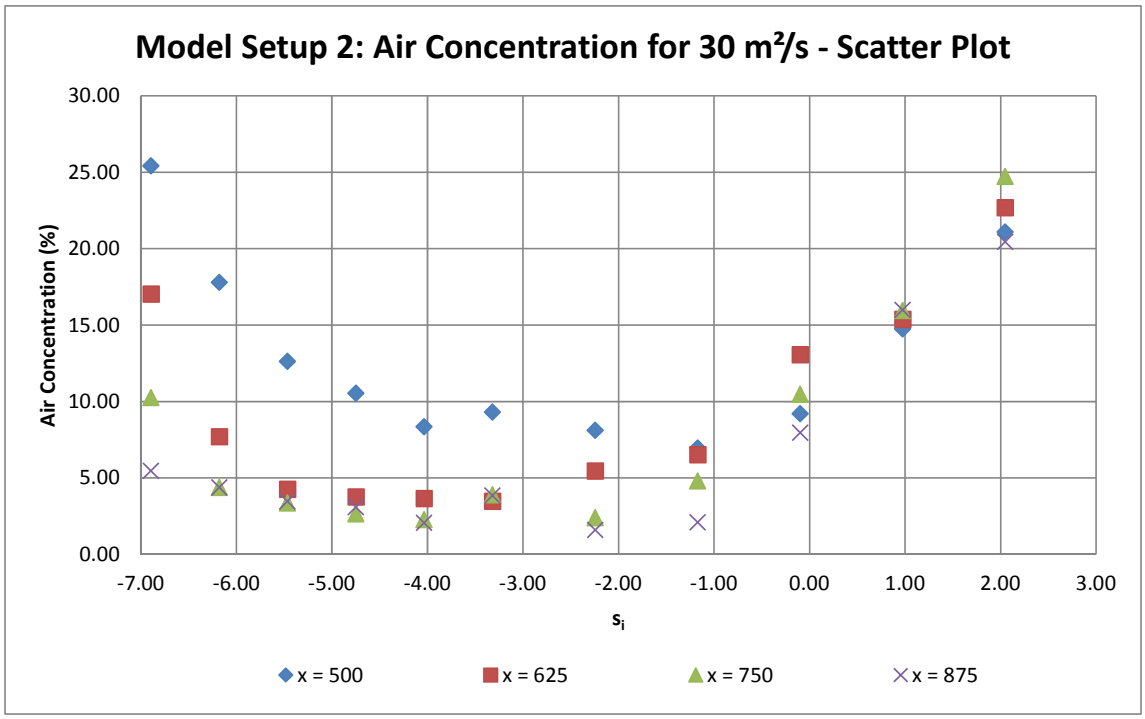

Figure 5-6: Test B results of model setup 2-30 m²/s (scatter plot)

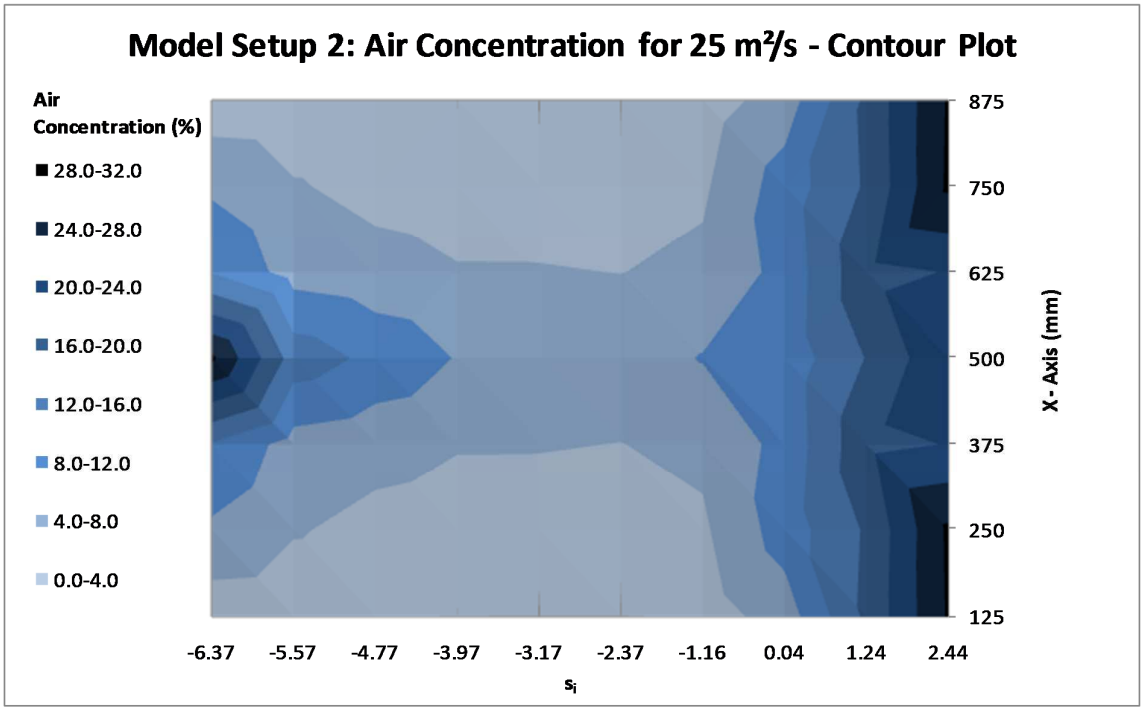

Figure 5-7: Test B results of model setup 2-25 m²/s (contour plot)

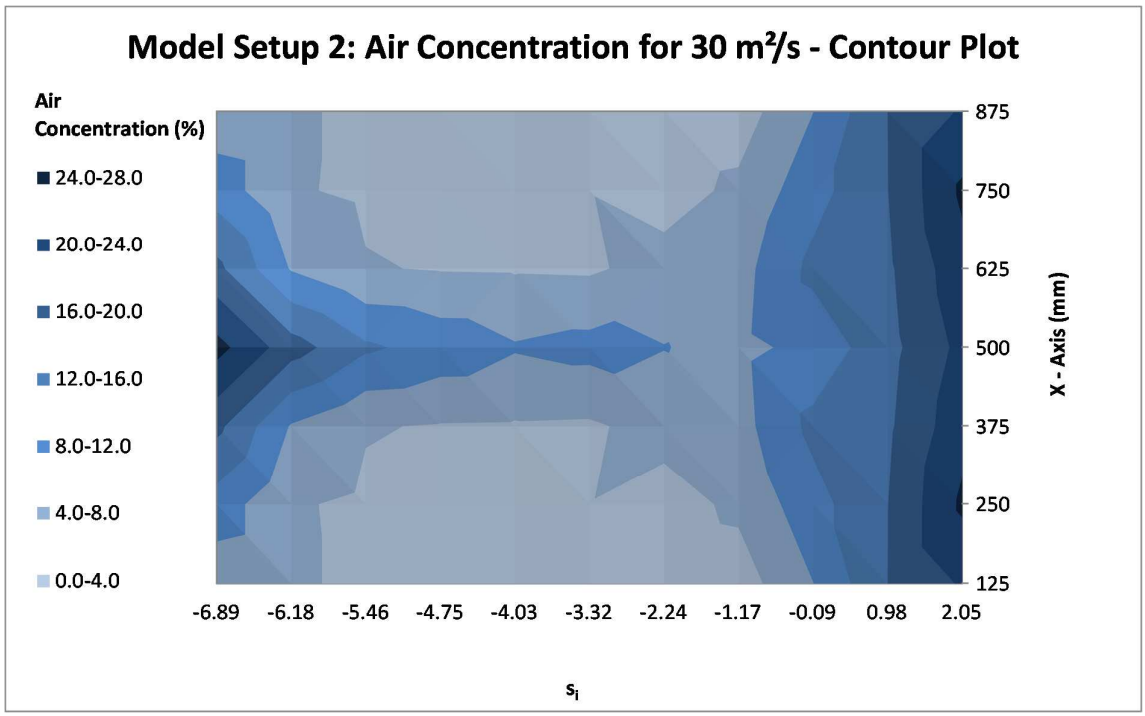

Figure 5-8: Test B results of model setup 2-30 m²/s (contour plot)

5.2.3 Model Setup 3 (Type 2 pier)

The air concentration results of model setup 3 for the two unit discharges are tabulated in **Table 5-6** and **Table 5-7**, and they are illustrated graphically in **Figure 5-9** to **Figure 5-12**. The results are plotted against the dimensionless distance s_i.

Table 5-6: Test B results of model setup 3-25 m²/s

s_i (normalized distance)	Air concentration (%)						
	x = 125	x = 250	x = 375	x = 500	x = 625	x = 750	x = 875
-6.37	0.01	0.01	0.48	7.45	0.48	0.01	0.01
-5.57	0.06	0.08	0.31	2.15	0.31	0.08	0.06
-4.77	0.10	0.40	0.33	2.15	0.33	0.40	0.10
-3.97	0.05	0.19	0.34	2.53	0.34	0.19	0.05
-3.17	0.07	0.07	0.34	1.88	0.34	0.07	0.07
-2.37	0.15	0.14	0.89	2.71	0.89	0.14	0.15
-1.16	1.52	1.65	3.19	5.06	3.19	1.65	1.52
0.04	4.69	7.01	8.64	7.23	8.64	7.01	4.69
1.24	14.41	16.72	16.24	12.10	16.24	16.72	14.41
2.44	26.41	24.06	18.01	18.05	18.01	24.06	26.41

Table 5-7: Test B results of model setup 3-30 m²/s

s_i (normalized distance)	Air concentration (%)						
	x = 125	x = 250	x = 375	x = 500	x = 625	x = 750	x = 875
-6.89	0.01	0.20	1.02	12.62	1.02	0.20	0.01
-6.18	0.02	0.14	0.92	4.12	0.92	0.14	0.02
-5.46	0.08	0.20	0.82	3.00	0.82	0.20	0.08
-4.75	0.05	0.10	0.48	1.96	0.48	0.10	0.05
-4.03	0.03	0.14	0.70	1.66	0.70	0.14	0.03
-3.32	0.01	0.10	0.36	1.19	0.36	0.10	0.01
-2.24	0.31	0.51	1.33	1.15	1.33	0.51	0.31
-1.17	1.40	1.79	3.46	2.46	3.46	1.79	1.40
-0.09	4.43	5.42	5.04	4.11	5.04	5.42	4.43
0.98	10.78	11.06	7.68	7.88	7.68	11.06	10.78
2.05	13.45	12.24	12.93	10.32	12.93	12.24	13.45

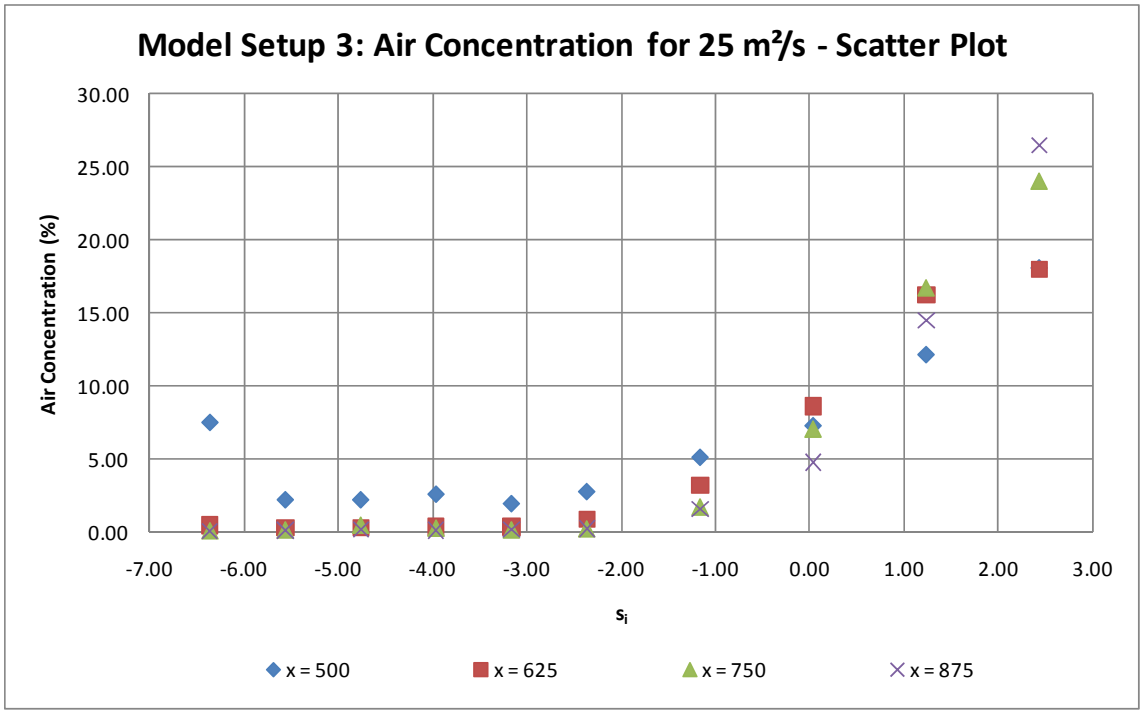

Figure 5-9: Test B results of model setup 3-25 m²/s (scatter plot)

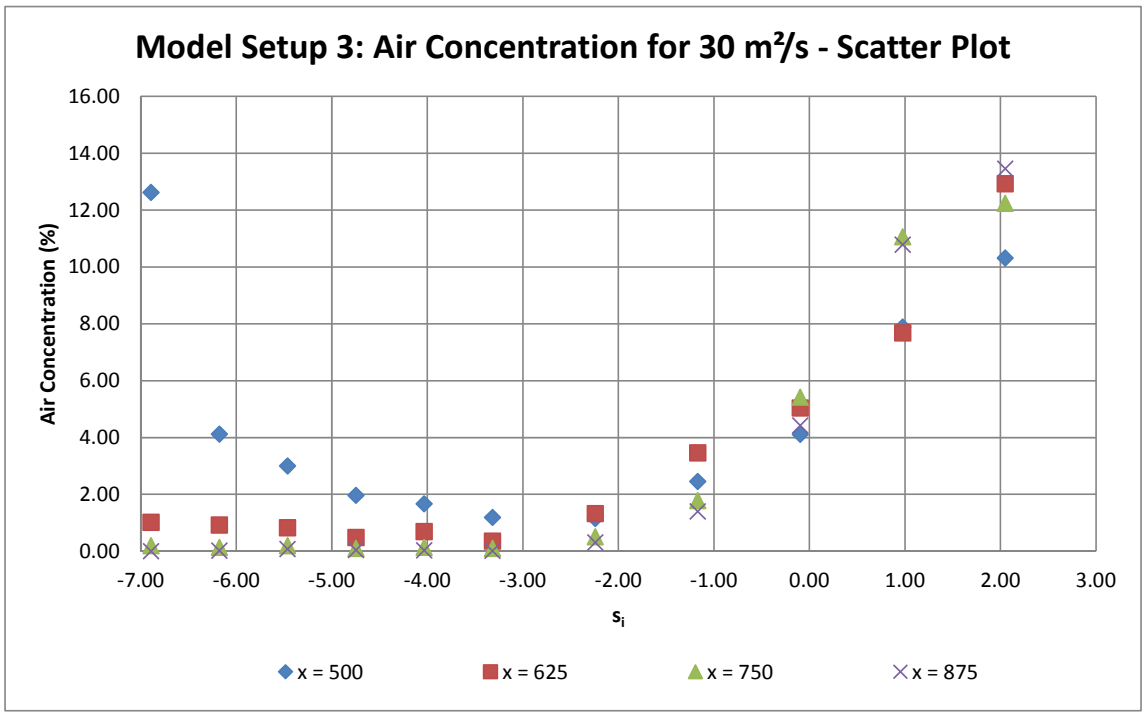

Figure 5-10: Test B results of model setup 3-30 m²/s (scatter plot)

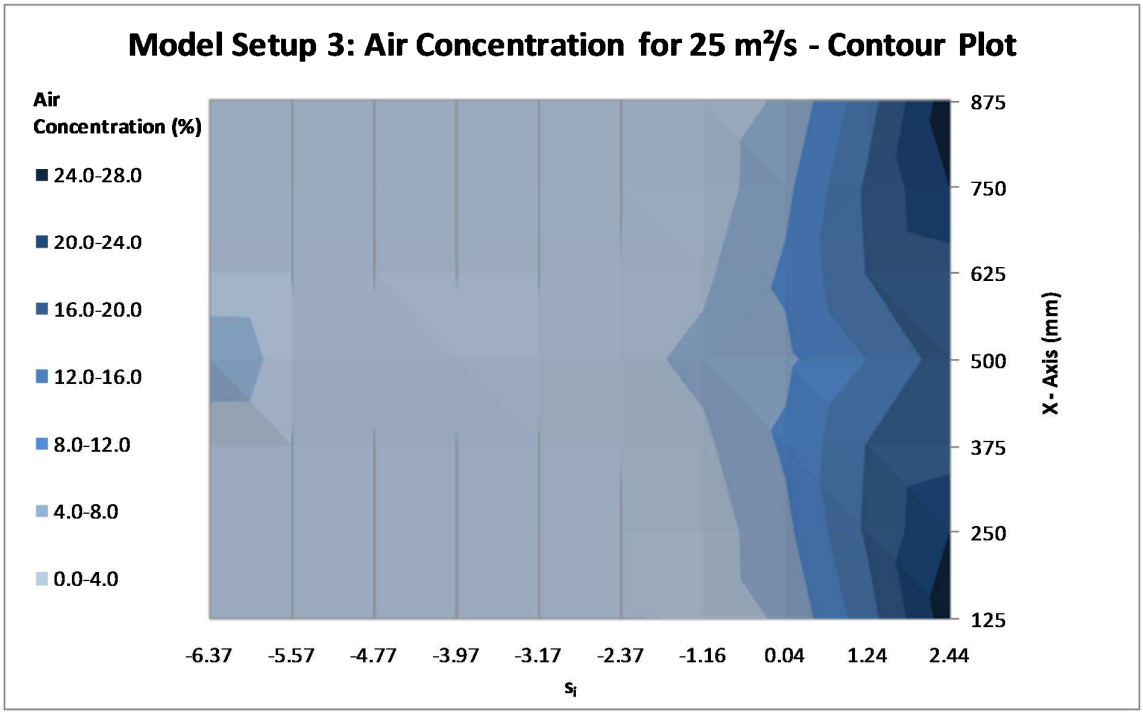

Figure 5-11: Test B results of model setup 3-25 m²/s (contour plot)

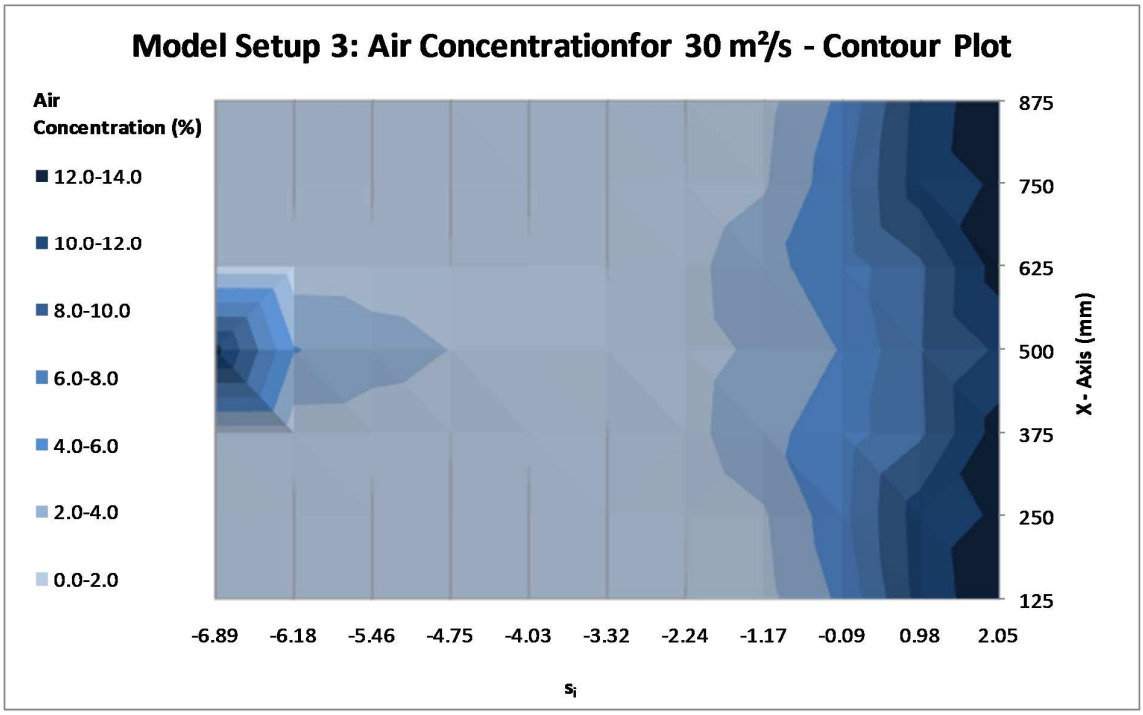

Figure 5-12: Test B results of model setup 3-30 m²/s (contour plot)

5.2.4 Remarks on Test B Results

Comments regarding the results of the investigation into the pseudo-bottom air concentration for the different model setups are summarised below. The inception point (s_i = 0.0) referred to in this section is defined as the pseudo-bottom inception point for a spillway with no pier (as in model setup 1) as determined by Boes and Hager (2003b) (see **Subsection 3.8.1.2**).

5.2.4.1 Model Setup 1(no pier)

- The concentration of air increases uniformly across the spillway width at an exponential rate from the start of the area studied up to the critical point.
- The development of air concentration along the spillway was similar for both the tested discharges when plotted to the dimensionless variable s_i.
- The air concentration at the inception point for both discharges averaged at about 5%.

Note that the air concentration at the pseudo-bottom inception point is more than 1%, as predicted by Boes and Hager (2003b), which can be attributed to the model scale being larger than what the authors used, including due to the fact that a different air probe, with a greater acquisition time than they observed, was utilised for this study.

5.2.4.2 Model Setup 2 (Type 1 pier)

- The large amount of air that was entrained immediately downstream of the pier spread across the spillway width at a diminishing rate. The concentration of air slowly decreased downstream of the pier, to just upstream of the inception point from where the air concentration then increased relatively uniformly across the spillway width, up to the critical point.
- The pattern of air concentration along the spillway was similar for both tested discharges when plotted to the dimensionless variable s_i. However, a higher percentage of air concentration than the above was recorded upstream of the inception point, as the discharge was increased.
- At the inception point, the air concentration averaged about 7-10% for 25 m²/s, and 8-13% for 30 m²/s.

5.2.4.3 Model Setup 3 (Type 2 pier)

- The results indicated, just downstream of the pier, a localised entrainment of air that did not spread across the spillway width as effectively as in the case of model setup 2. The only substantial increase of air concentration was observed in the centre of the spillway.
- The air that was artificially entrained within the centre of the spillway quickly dissipated prior to the inception point. From this inception point, the air concentration was observed to increase approximately uniformly across the spillway width, up to the critical point.
- The air concentration at the inception point averaged out at about 5-9% for 25 m²/s and at about 4-6% for 30 m²/s.

The most promising results with regard to artificial air entrainment into the flow at the pseudo-bottom was achieved with the Type 1 pier design of model setup 2. The design in question not only attained the highest percentage air concentration upstream of the inception point for all the model setups, but also effectively transported air across the spillway width.

It should be noted that the air concentration increased relatively uniformly across the spillway width downstream of the inception point for all model setups. The detrainment of air concentration for model setups 2 and 3 upstream of the inception point corresponds with the detrainment in the findings of the model studies done by Pfister, et al. (2006) (refer to **Subsection 3.3.3**), including in terms of the results that were observed during the preliminary experimental work.

5.3 TEST C: Pressure

The recorded minimum pressure results are presented in a table format, as well as graphically, for each model setup within this section. As with the presented results of Test B, the results are shown for the entire spillway width (x = 125 mm to x = 875 mm), except for the scatter plots, which only illustrate the study area measured. In addition, the scatter plots also include the mean pressure that was observed for the spillway width, including the pressure at which the cavitation inception would occur. The pressure for cavitation inception is based on a prototype pressure of -7 m.

5.3.1 Model Setup 1 (no pier)

The minimum pressure results of model setup 1 for the two unit discharges tested are tabulated in **Table 5-8** and **Table 5-9**, and they are illustrated graphically in **Figure 5-13** to **Figure 5-16**. The results are plotted against the dimensionless distance s_i.

Table 5-8: Test C results of model setup 1-25 m²/s

S_i (normalized distance)	Minimum pressure (p/γ/h)						
	x = 125	x = 250	x = 375	x = 500	x = 625	x = 750	x = 875
-6.31	-0.94	-1.22	-1.04	-0.95	-1.04	-1.22	-0.94
-4.72	-2.27	-2.19	-1.84	-2.09	-1.84	-2.19	-2.27
-3.14	-2.75	-3.14	-2.82	-3.02	-2.82	-3.14	-2.75
-1.55	-3.61	-3.89	-4.03	-3.96	-4.03	-3.89	-3.61
-0.76	-3.72	-3.44	-3.18	-3.59	-3.18	-3.44	-3.72
0.04	-3.77	-3.56	-3.70	-4.30	-3.70	-3.56	-3.77
0.83	-4.52	-4.05	-4.06	-4.78	-4.06	-4.05	-4.52
2.41	-3.48	-3.70	-3.36	-3.58	-3.36	-3.70	-3.48

Table 5-9: Test C results of model setup 1-30 m²/s

S_i (normalized distance)	Minimum pressure (p/γ/h)						
	x = 125	x = 250	x = 375	x = 500	x = 625	x = 750	x = 875
-6.89	-1.09	-0.88	-0.85	-1.12	-0.85	-0.88	-1.09
-5.46	-2.12	-2.41	-1.93	-1.90	-1.93	-2.41	-2.12
-4.03	-3.76	-3.22	-2.81	-3.33	-2.81	-3.22	-3.76
-2.60	-3.91	-3.90	-3.74	-3.97	-3.74	-3.90	-3.91
-1.17	-3.14	-2.63	-3.02	-2.36	-3.02	-2.63	-3.14
-0.45	-4.66	-4.78	-3.01	-3.72	-3.01	-4.78	-4.66
0.26	-5.33	-4.76	-4.94	-5.66	-4.94	-4.76	-5.33
0.98	-5.70	-5.35	-4.49	-5.18	-4.49	-5.35	-5.70
2.05	-3.83	-3.06	-3.55	-3.98	-3.55	-3.06	-3.83

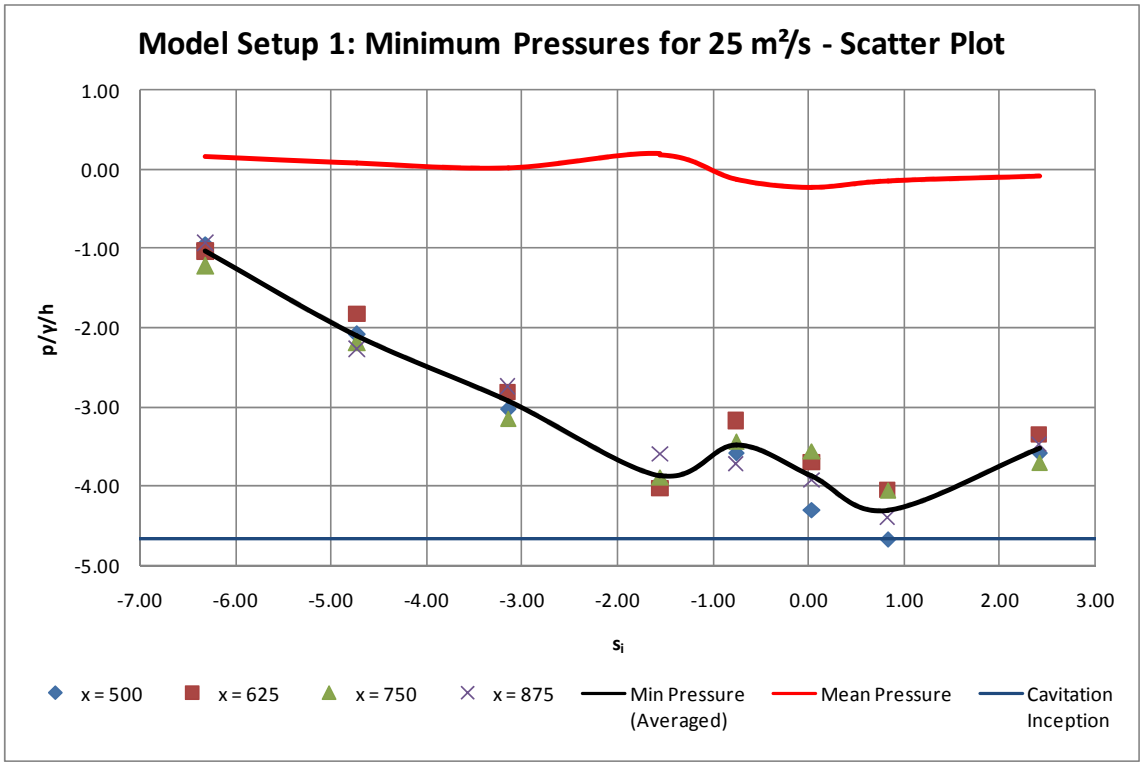

Figure 5-13: Test C results of model setup 1-25 m²/s (scatter plot)

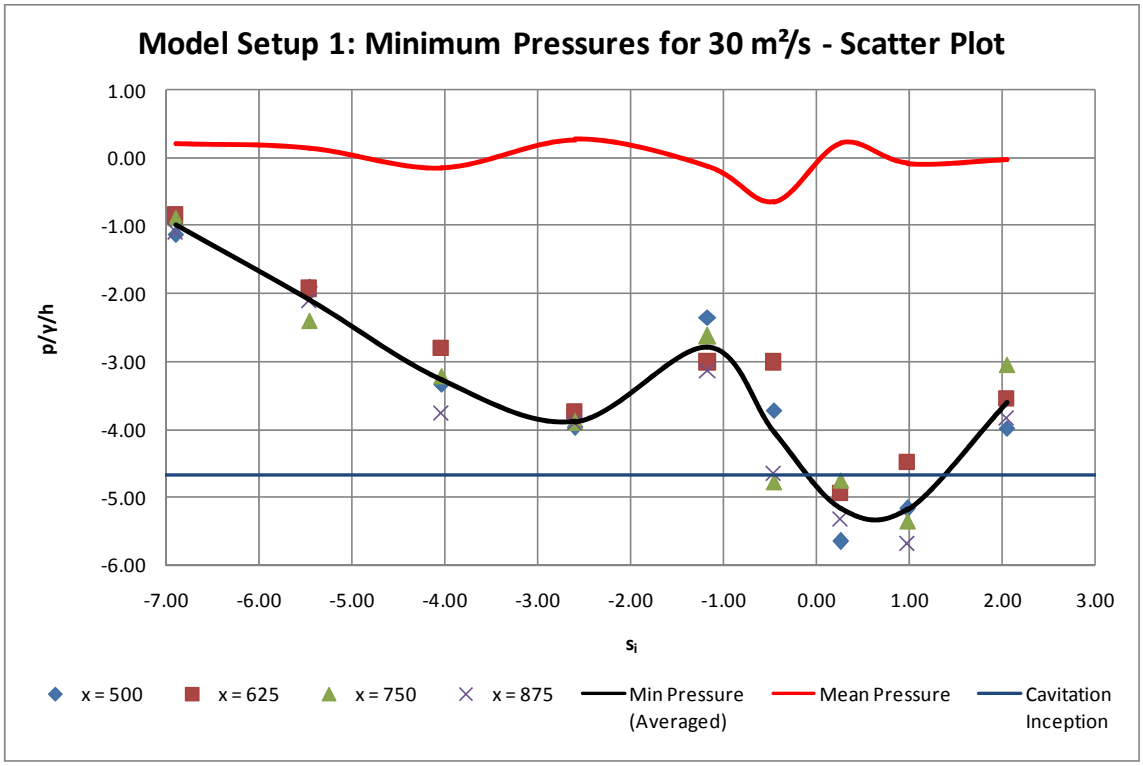

Figure 5-14: Test C results of model setup 1-30 m²/s (scatter plot)

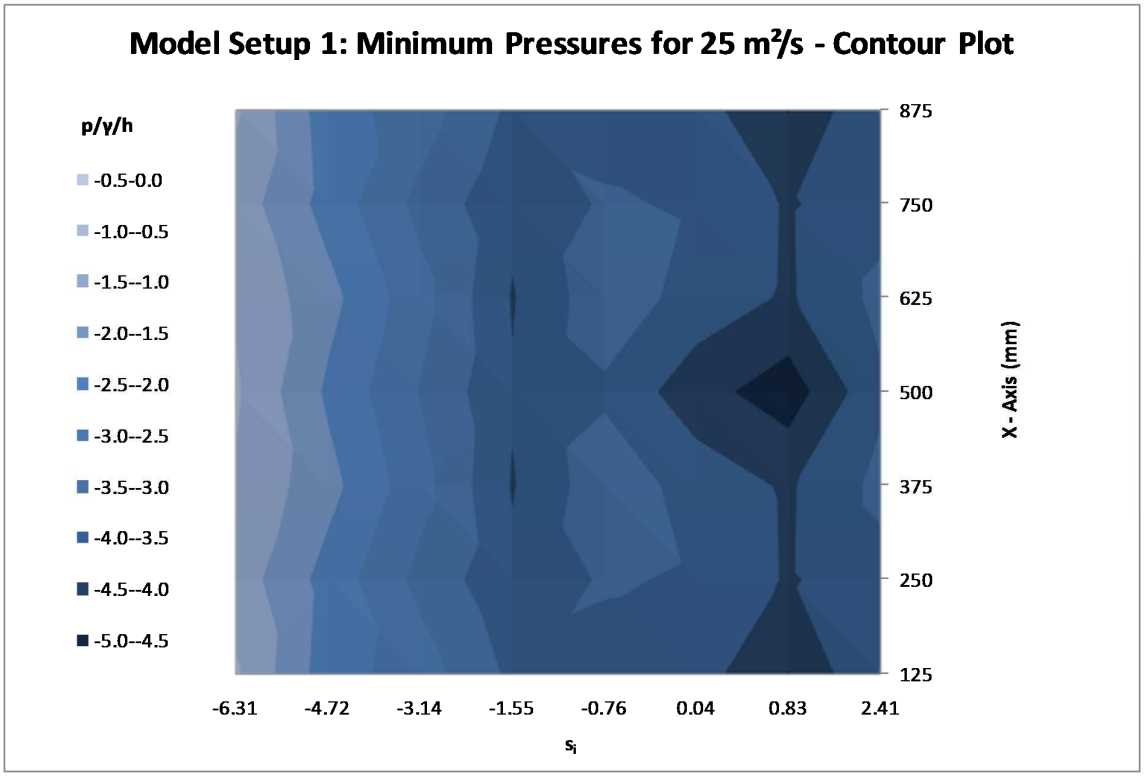

Figure 5-15: Test C results of model setup 1-25 m²/s (contour plot)

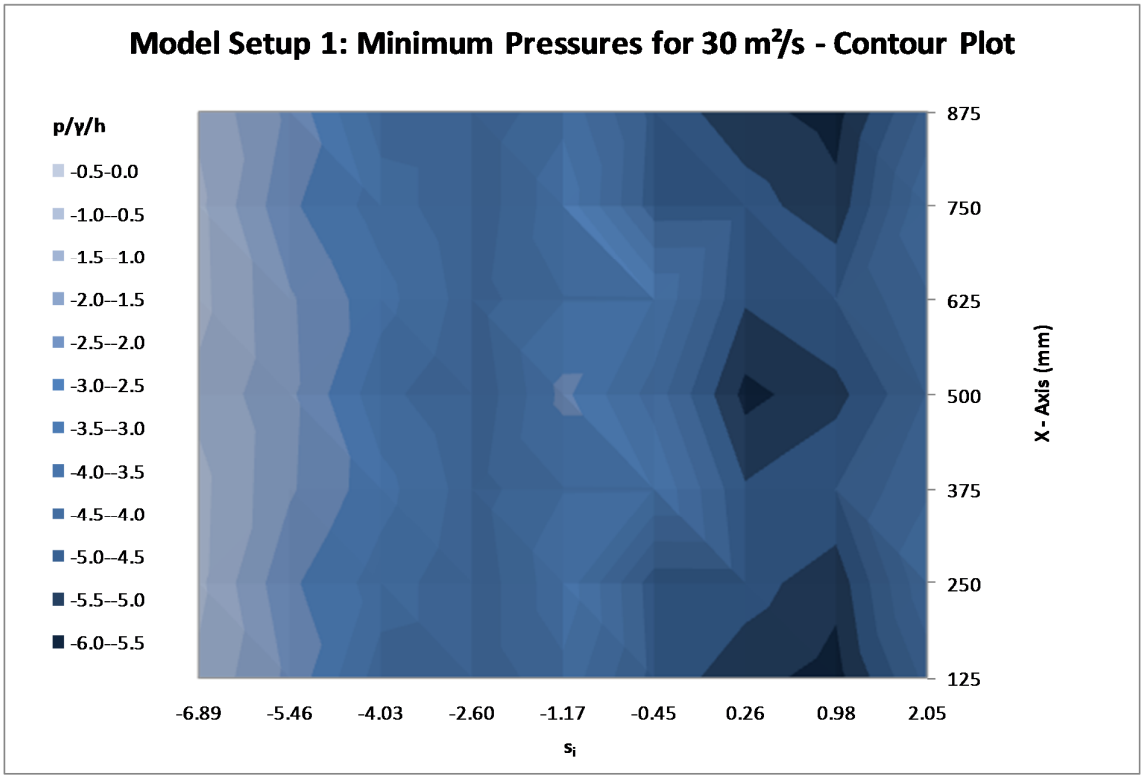

Figure 5-16: Test C results of model setup 1-30 m²/s (contour plot)

5.3.2 Model Setup 2 (Type 1 pier)

The minimum pressure results of model setup 2 for the two unit discharges tested are tabulated in **Table 5-10** and **Table** 5-11, and they are illustrated graphically in **Figure 5-17** to **Figure 5-20**. The results are plotted against the dimensionless distance s_i.

Table 5-10: Test C results of model setup 2-25 m²/s

S_i (normalized distance)	Minimum pressure (p/γ/h)						
	x = 125	x = 250	x = 375	x = 500	x = 625	x = 750	x = 875
-6.31	-0.80	-0.54	-1.10	-0.84	-1.10	-0.54	-0.80
-4.72	-2.33	-2.05	-1.87	-1.65	-1.87	-2.05	-2.33
-3.14	-2.52	-2.94	-2.42	-2.43	-2.42	-2.94	-2.52
-1.55	-3.65	-3.69	-3.17	-3.34	-3.17	-3.69	-3.65
0.04	-3.46	-4.16	-3.95	-4.13	-3.95	-4.16	-3.46
0.83	-4.24	-3.38	-3.12	-3.28	-3.12	-3.38	-4.24
1.62	-4.24	-3.46	-3.06	-3.50	-3.06	-3.46	-4.24
2.41	-3.51	-3.35	-3.64	-3.31	-3.64	-3.35	-3.51

Table 5-11: Test C results of model setup 2-30 m²/s

S_i (normalized distance)	Minimum pressure (p/γ/h)						
	x = 125	x = 250	x = 375	x = 500	x = 625	x = 750	x = 875
-6.89	-0.39	-1.34	-0.91	-1.21	-0.91	-1.34	-0.39
-5.46	-2.08	-2.18	-1.71	-1.44	-1.71	-2.18	-2.08
-4.03	-2.75	-2.81	-2.60	-2.45	-2.60	-2.81	-2.75
-2.60	-3.79	-3.44	-3.09	-3.03	-3.09	-3.44	-3.79
-1.17	-3.16	-4.43	-4.02	-4.29	-4.02	-4.43	-3.16
-0.45	-4.79	-3.62	-3.42	-3.48	-3.42	-3.62	-4.79
0.26	-4.91	-4.10	-3.42	-3.82	-3.42	-4.10	-4.91
0.98	-4.70	-4.49	-3.78	-4.01	-3.78	-4.49	-4.70
2.05	-4.17	-3.71	-3.87	-3.41	-3.87	-3.71	-4.17

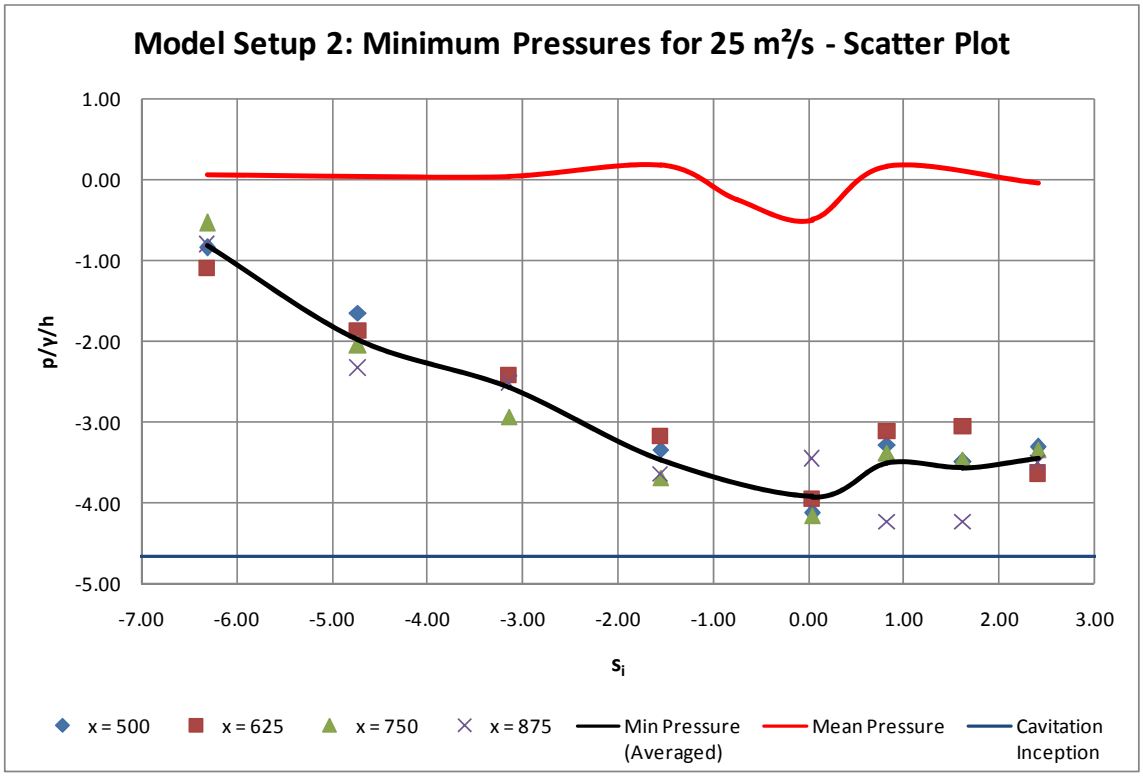

Figure 5-17: Test C results of model setup 2-25 m²/s (scatter plot)

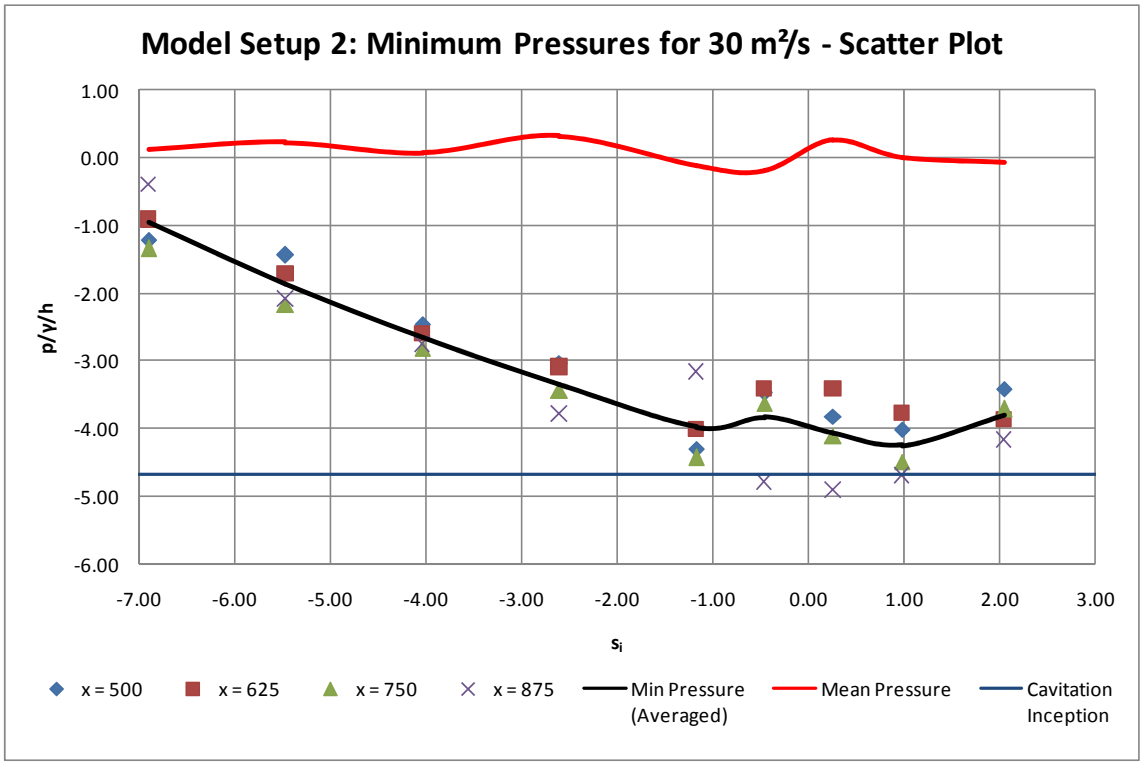

Figure 5-18: Test C results of model setup 2-30 m²/s (scatter plot)

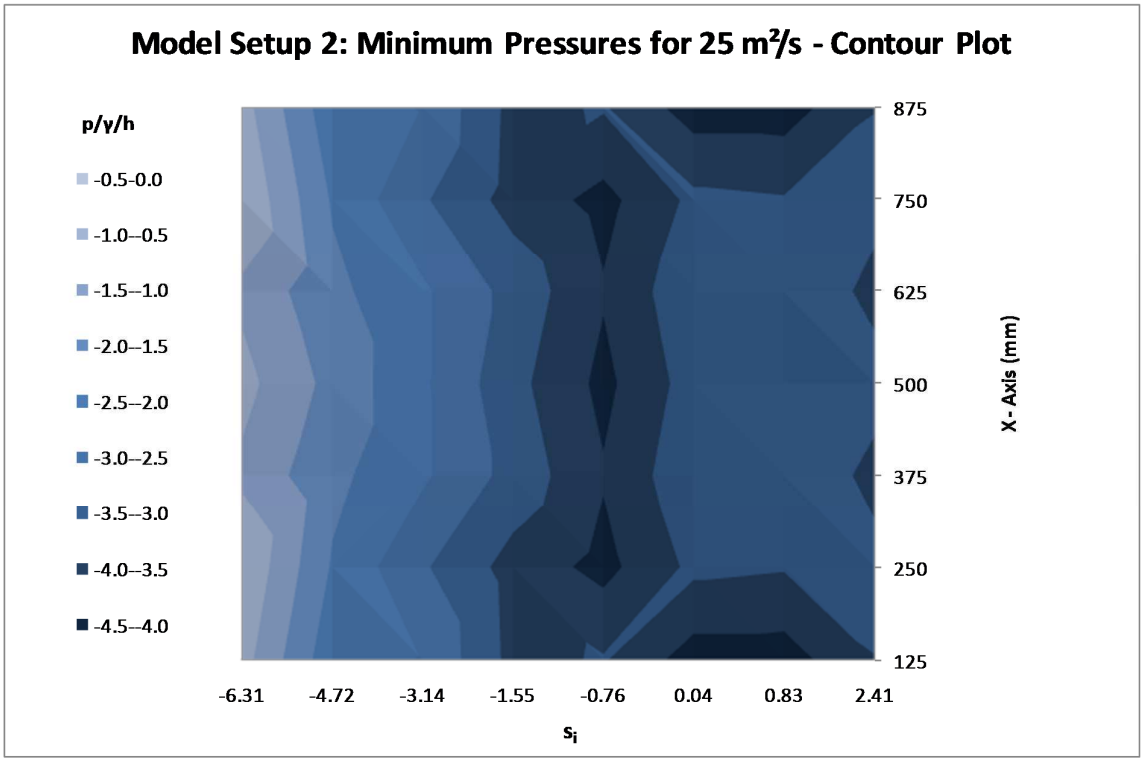

Figure 5-19: Test C results of model setup 2-25 m²/s (contour plot)

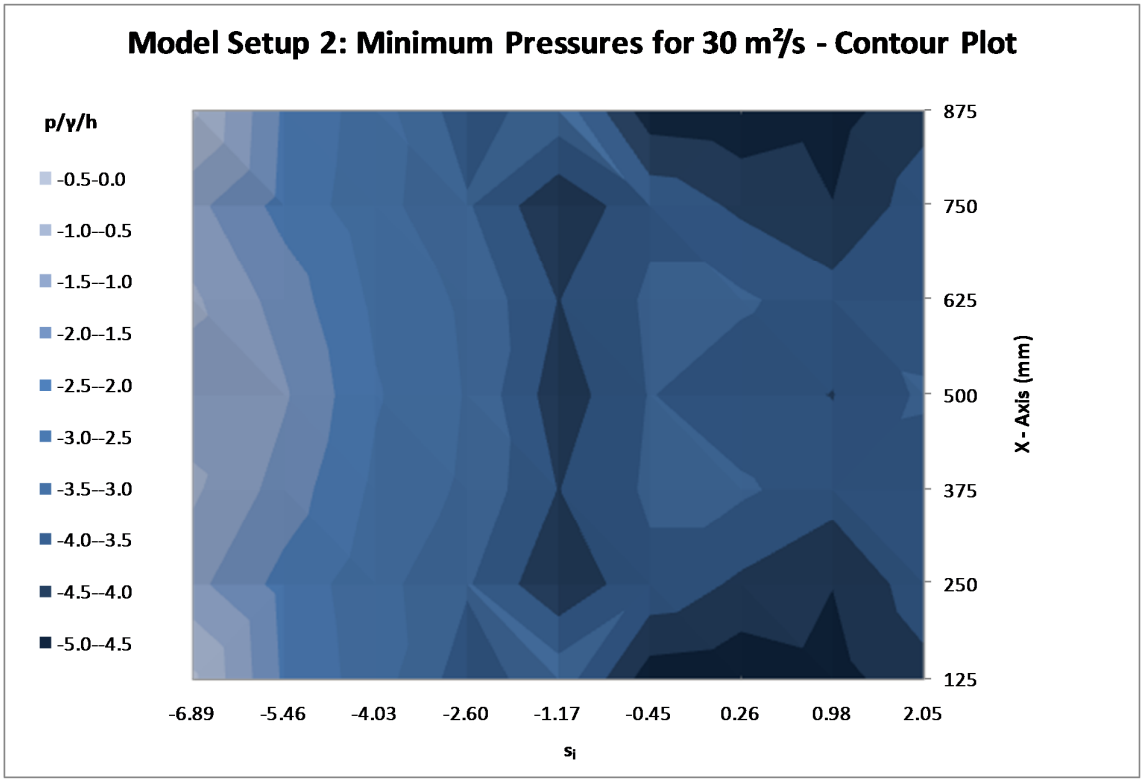

Figure 5-20: Test C results of model setup 2-30 m²/s (contour plot)

5.3.3 Model Setup 3 (Type 2 pier)

The minimum pressure results of model setup 3 for the two unit discharges tested are tabulated in **Table 5-10** and **Table** 5-11, and they are illustrated graphically in **Figure 5-17** to **Figure 5-20**. The results are plotted against the dimensionless distance s_i.

Table 5-12: Test C results of model setup 3-25 m²/s

S_i (normalized distance)	Minimum pressure (p/γ/h)						
	x = 125	x = 250	x = 375	x = 500	x = 625	x = 750	x = 875
-6.31	-1.11	-1.35	-1.41	-1.36	-1.41	-1.35	-1.11
-4.72	-2.07	-2.58	-1.92	-2.06	-1.92	-2.58	-2.07
-3.14	-3.22	-3.34	-3.32	-3.23	-3.32	-3.34	-3.22
-1.55	-3.81	-3.83	-3.39	-3.66	-3.39	-3.83	-3.81
0.04	-2.81	-3.93	-3.50	-3.50	-3.50	-3.93	-2.81
0.83	-2.79	-2.52	-2.63	-3.31	-2.63	-2.52	-2.79
1.62	-4.17	-3.02	-3.25	-3.75	-3.25	-3.02	-4.17
2.41	-0.27	-1.40	-0.96	-0.95	-0.96	-1.40	-0.27

Table 5-13: Test C results of model setup 3-30 m²/s

S_i (normalized distance)	Minimum pressure (p/γ/h)						
	x = 125	x = 250	x = 375	x = 500	x = 625	x = 750	x = 875
-6.89	-0.93	-1.64	-1.26	-1.55	-1.26	-1.64	-0.93
-5.46	-2.20	-2.65	-1.86	-1.98	-1.86	-2.65	-2.20
-4.03	-3.21	-3.40	-3.04	-2.53	-3.04	-3.40	-3.21
-2.60	-3.96	-3.99	-3.82	-3.94	-3.82	-3.99	-3.96
-1.17	-5.05	-4.27	-4.41	-4.83	-4.41	-4.27	-5.05
-0.45	-4.77	-3.47	-4.49	-4.19	-4.49	-3.47	-4.77
0.26	-5.12	-4.09	-4.49	-5.05	-4.49	-4.09	-5.12
0.98	-5.19	-4.78	-4.76	-4.73	-4.76	-4.78	-5.19
2.05	-4.24	-4.39	-4.42	-5.06	-4.42	-4.39	-4.24

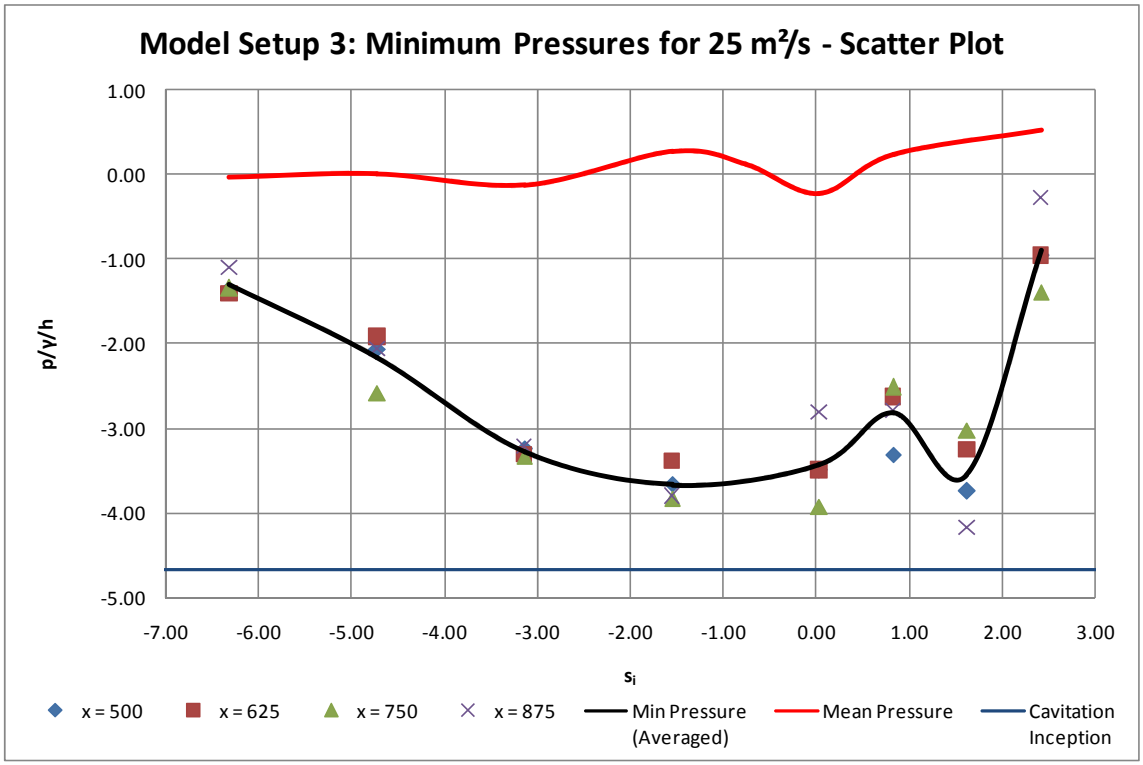

Figure 5-21: Test C results of model setup 3-25 m²/s (scatter plot)

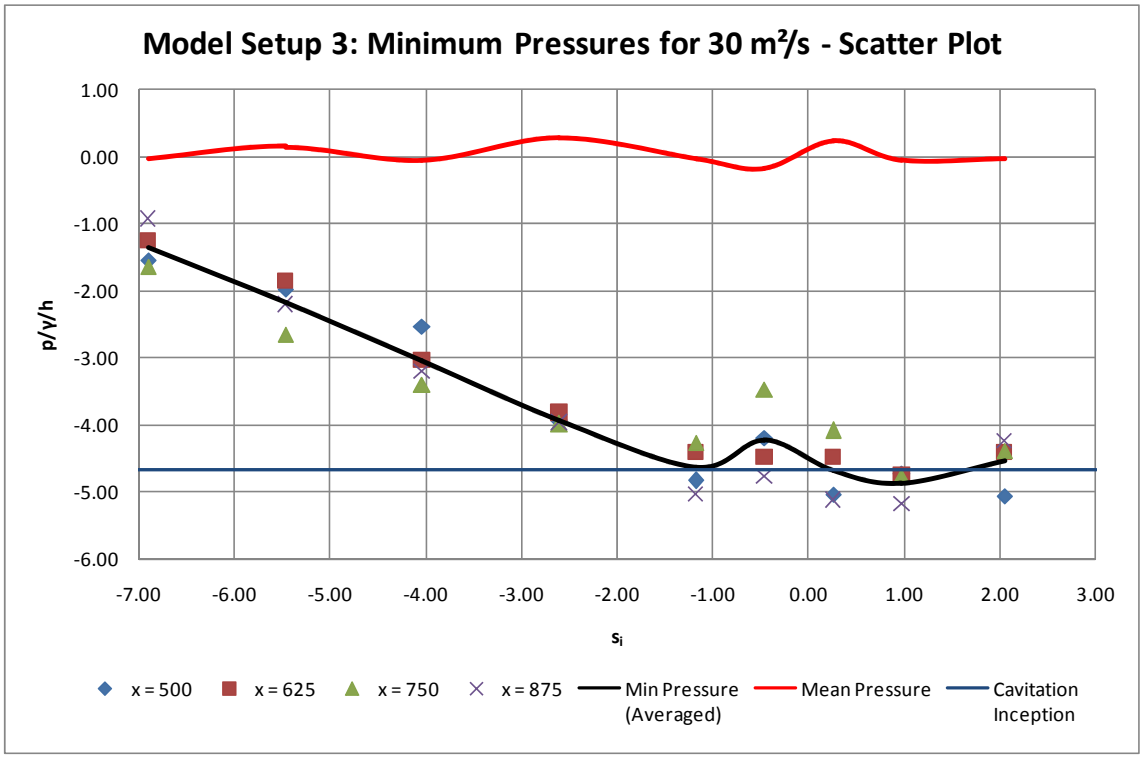

Figure 5-22: Test C results of model setup 3-30 m²/s (scatter plot)

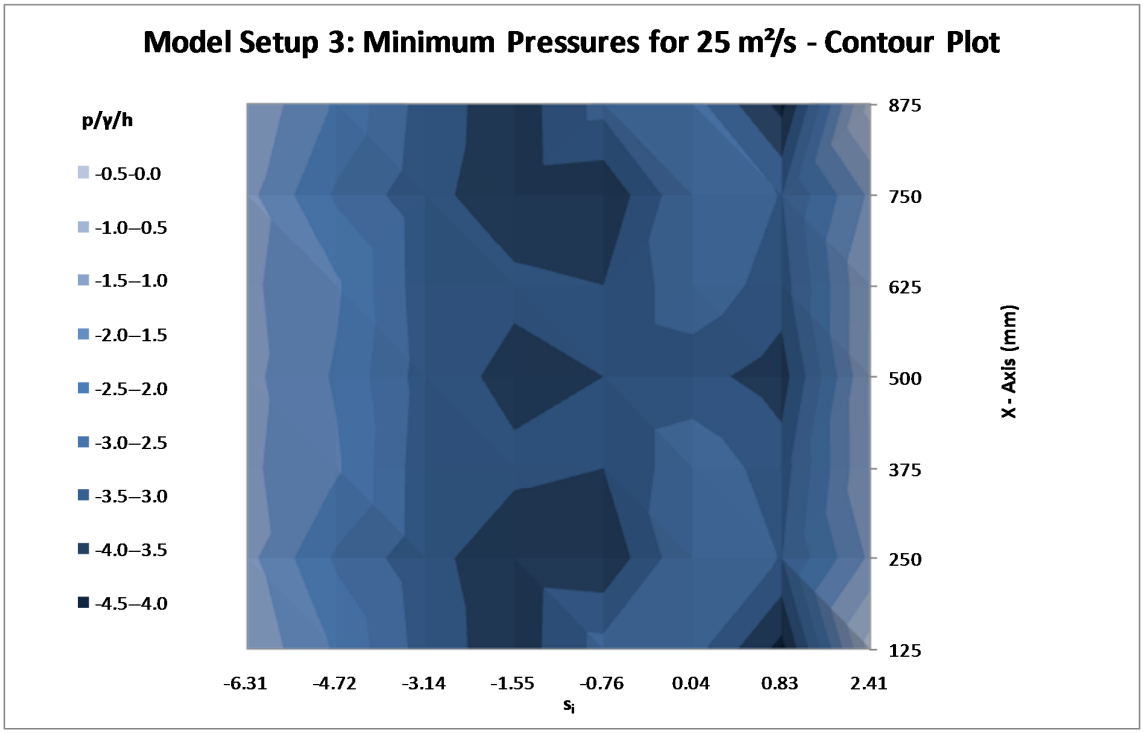

Figure 5-23: Test C results of model setup 2-25 m²/s (contour plot)

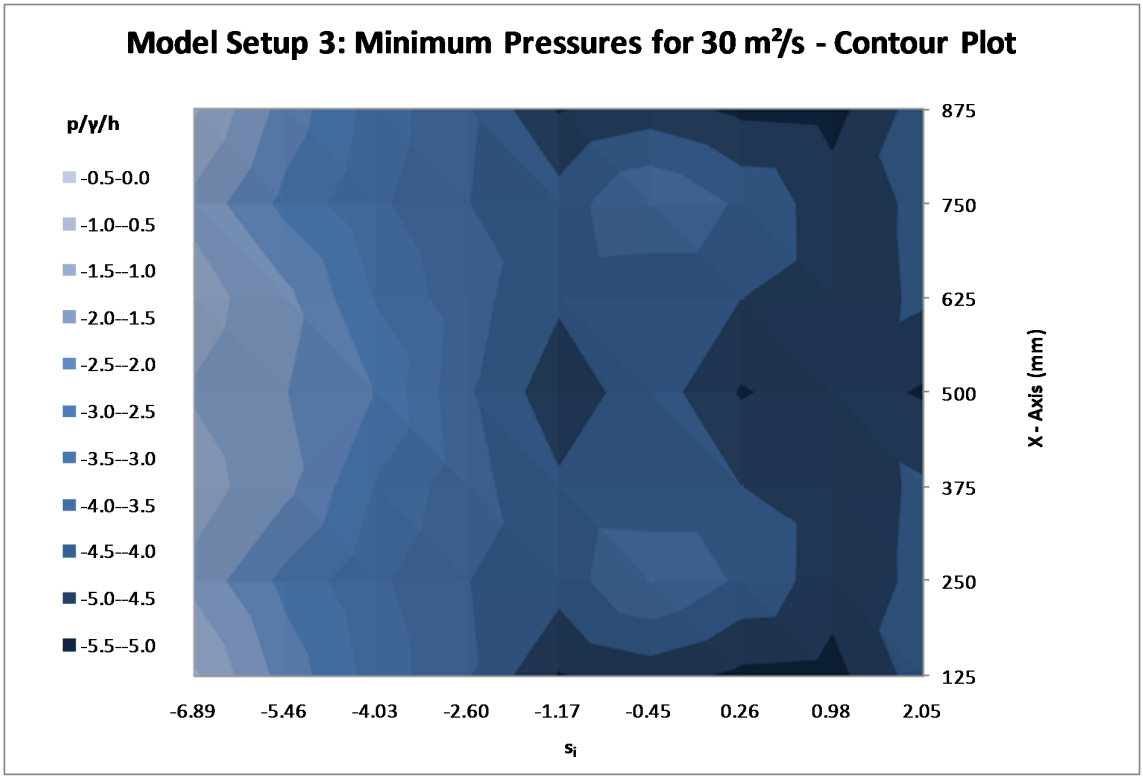

Figure 5-24: Test C results of model setup 3-30 m²/s (contour plot)

5.3.4 Remarks on Test C Results

Comments regarding the results of the investigation into the pressures found at the upper vertical step face for the different model setups are summarised below. The inception point (s_i = 0.0) referred to in this section is defined as the pseudo-bottom inception point for a spillway with no pier (as in model setup 1), as determined by Boes and Hager (2003b) (see **Subsection 3.8.1.2**).

Cognisance should be taken of the fact that the minimum pressures shown in the results are a function of the calculated standard deviation, as was discussed in **Subsection 4.3.2.2**. As a result, the larger the difference between the mean and the minimum pressures shown on the scatter plots, the higher the pressure fluctuation would be for that specific location, meaning that the lower minimum pressures would also mean higher maximum pressure.

5.3.4.1 Model Setup 1 (no pier)

- The lowest mean pressures occurred upstream of the inception point for both tested discharges, in as accordance with the findings in the literature.
- The lowest minimum pressures were found to be downstream of the inception point. The occurrence of an increase in minimum pressures just before the inception point was also noted.
- The unit discharge of 30 m²/s subjected the spillway to minimum prototype pressures that exceeded the pressure at which cavitation can occur. However, for a unit discharge equal to 25 m²/s, the minimum pressures did not exceed the cavitation limit.
- The contour plots show that the minimum pressures across the spillway width were not uniform, especially within the proximity of the inception point.

5.3.4.2 Model Setup 2 (Type 1 pier)

- For both tested discharges, the lowest mean pressures either occurred upstream, or at the inception point.
- The lowest minimum pressures were found to be either at, or downstream of, the inception point, and the lowest minimum pressure occurred at the sides of the spillway around the inception point for both discharges tested.
- Only the minimum prototype pressures at the sides of the spillway for a unit discharge of 30 m²/s exceeded the pressure at which cavitation can take place.
- A more uniform distribution of the minimum pressure is illustrated by the contour plots when compared to model setup 1, except for the pressure at the spillway sides.

5.3.4.4 Model Setup 3 (Type 2 pier)

- The lowest mean pressures either occurred upstream, or at the inception point, for both tested discharges.
- The lowest minimum pressures were found to be downstream of the inception point. Similar to model setup 1, an increase in minimum pressures was observed just before the area where the lowest minimum pressures occurred.
- The unit discharge of 30 m²/s subjected the spillway to minimum prototype pressures that exceeded the pressure at which cavitation could occur. For a unit discharge equal to 25 m²/s, the minimum pressures did not exceed the cavitation limit.
- Non-uniformity of minimum pressures across the spillway width, especially around the inception point, was also observed for this model setup.

The Type 1 pier of model setup 2 proved to be the best performing pier design to increase minimum pressures, and to reduce pressure fluctuations, when compared to the design of a spillway with no piers, suggesting that a discharge higher than the current recommended values can be applied for a spillway that is equipped with a Type 1 pier. Nevertheless, the minimum pressure that was recorded at the spillway sides within the proximity of the inception point raises the concern that cavitation damage might occur at these locations. More detail is provided on this subject in **Subsection 6.4.2**.

For a spillway with no piers, the literature showed that the lowest mean pressure occurs just upstream of the inception point. This was also observed with the results of model setup 1. However, the studies of model setup 1 indicated that the lowest minimum pressures are actually to be found downstream of the inception point, within the rapid and gradually varying flow region, and not in the developing flow region, as one might have expected. As this finding has not previously been documented, it has led to new methods being proposed to evaluate cavitation on stepped spillway, which are further discussed in detail in **Section 6.5**.

In addition, it would be expected that the pattern of the mean pressure would be similar to that of the averaged minimum pressure, but, in actual fact, it is not. This is in agreement with the conclusion drawn when the pressure data were statistically analysed, namely that the pressure data are skewed.

6. COMPARISON AND DISCUSSION OF TEST RESULTS

The results that were presented in the preceding chapter are discussed in detail within this chapter with regard to the stated objective of the study, which was to investigate the maximum discharge possible when creating an earlier onset of air entrainment by means of introducing a pier at the spillway crest.

6.1 ACHIEVING THE STUDY OBJECTIVE

The stated objective of the current study was to investigate whether the introduction of piers at the spillway crest can facilitate an earlier onset of air entrainment at the pseudo-bottom, so as to pass discharges greater than the current recommended values without there being risk of causing cavitation damage.

The first step in achieving the objective was to pre-aerate the pseudo-bottom flow with the crest piers. The experiment was successful for the two pier designs tested, with the Type 1 pier of model setup 2 showing the most promising results.

The next step is to evaluate, with the results of Test B and Test C, whether flows higher than the current recommended values can be safely discharged, without risking cavitation damage. The following sections discuss the possibility of exceeding the current recommended discharge values (18 m^2/s) examined in the literature review.

6.2 NON-UNIFORMITY OF MINIMUM PRESSURES FOR A SPILLWAY WITH NO PIER

As was found to have been discussed in the literature, the negative pressures at the upper vertical step face are generated due to flow separation at the step edge. When the discharge is constant, it can be accepted that the flow depth across the spillway width at any specific location along the chute will not vary for a spillway with no pier; therefore, the velocity will also not vary across the spillway concerned. If the velocity and flow depth are constant, thereby not influencing the shear stress created by the flow separation of the step edge, then the reason for a non-uniform distribution of minimum pressures being observed, especially around the inception point (s_i = 0.0), is debateable. This phenomenon is what this section is aimed at exploring.

Excluding the possibility that the variation of pressure is caused by unstable zones of flow separation over the step edge, it is believed that the non-uniformity pattern is either created by the aeration of the pseudo-bottom, by turbulence within the step cavity, or by a combination of both.

The turbulent zone consists of streamwise vortex structures, and of a shear layer acting above the vortex. Once the shear layer is aerated, it is referred to as the mixed layer. **Figure 6-1** depicts the turbulent zone that is bordered on by the step edges.

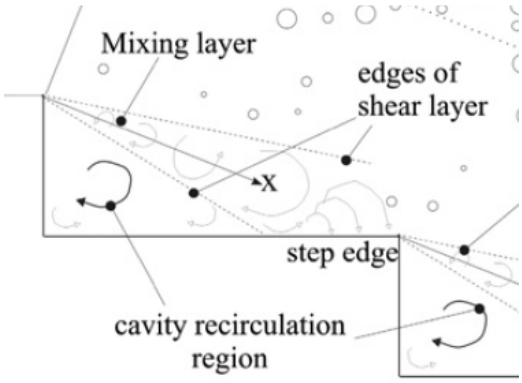

Figure 6-1: Turbulent zone within step cavity (Felder & Chanson, 2011)

The idea that aeration is the sole reason for the uneven distribution of pressure is based on the premise that the air concentration also varies across the spillway width. However, this argument is not conclusive when evaluating the air concentration results obtained when using model setup 1 (refer to **Figure 5-3** and **Figure 5-4**), which shows uniform distribution of air across the spillway width.

In contrast, the theory of the turbulent zone being the sole reason for this phenomenon also does not hold, due to the relatively uniform distribution of pressure that was observed upstream of the inception point (refer to **Figure 5-15** and **Figure 5-16**). Therefore, it is believed that the reason for the non-uniformity of minimum pressures is the combination of aeration and the turbulent effects within the step cavity.

The concentration of air starts to increase upstream of the inception point, which is also the point at which the uneven distribution of pressure across the spillway width commences. As the air concentration increased, a greater difference between adjacent pressure locations was observed, in particular just downstream of the inception point. Further downstream of the flow inception, the pressures start to converge to a uniform state again.

The turbulence zone is argued to create the fluctuation of pressure across the spillway width, while undergoing aeration, which occurs during the air entrainment process. Once this zone is aerated to a certain percentage, which occurs downstream of the inception point, the pressures across the spillway width return to a state of even distribution. **Figure 6-2** shows an unaerated step cavity within the developing zone, with **Figure 6-3** showing an aerated step cavity at the inception point. (Note the aerated vortex occupying the whole step cavity in **Figure 6-3**.)

Figure 6-2: Unaerated step cavity for a prototype discharge of 30 m²/s

Figure 6-3: Aerated step cavity for a prototype discharge of 30 m²/s

From the arguments presented above, it is concluded that the non-uniform distribution of minimum pressures across the spillway width is caused by the turbulent zone within the step cavity, while in the process of being aerated. The location of this phenomenon was observed to be centred around the inception point. Once the turbulent zones are sufficiently aerated, uniform pressures over the width of the spillway seem to return. Note that, for this study, the dynamics of the turbulent zone were not evaluated in any further detail. This included the investigation into the percentage of air concentration required for the pressure to return to a uniform distribution, as these factors did not form part of the study objective.

How this finding influenced the outcomes of the study has to be considered now. The aerated turbulent zone is held to be responsible for creating a non-uniform pressure distribution along the width of the spillway, by either increasing or reducing the minimum pressures at the upper vertical step edge. Nonetheless, a conservative approach should be followed when evaluating cavitation. In addition, the absolute minimum pressure across the spillway width should be used as a minimum reference pressure, as it is not known how the turbulent zone might affect the pressures for different chute widths and discharges other than those that have been tested.

Following the verdict discussed above, the lowest minimum pressure recorded on the chute for a discharge of 30 m²/s in model setup 1 is shown as an illustrative example in **Figure 6-4**. The exercise was repeated for each discharge and model setup, so as to showcase the lowest minimum pressures found on the spillway, which are shown in **Figure 6-5** and **Figure 6-6** in the form of the pressure at which cavitation inception (-7 m) can occur.

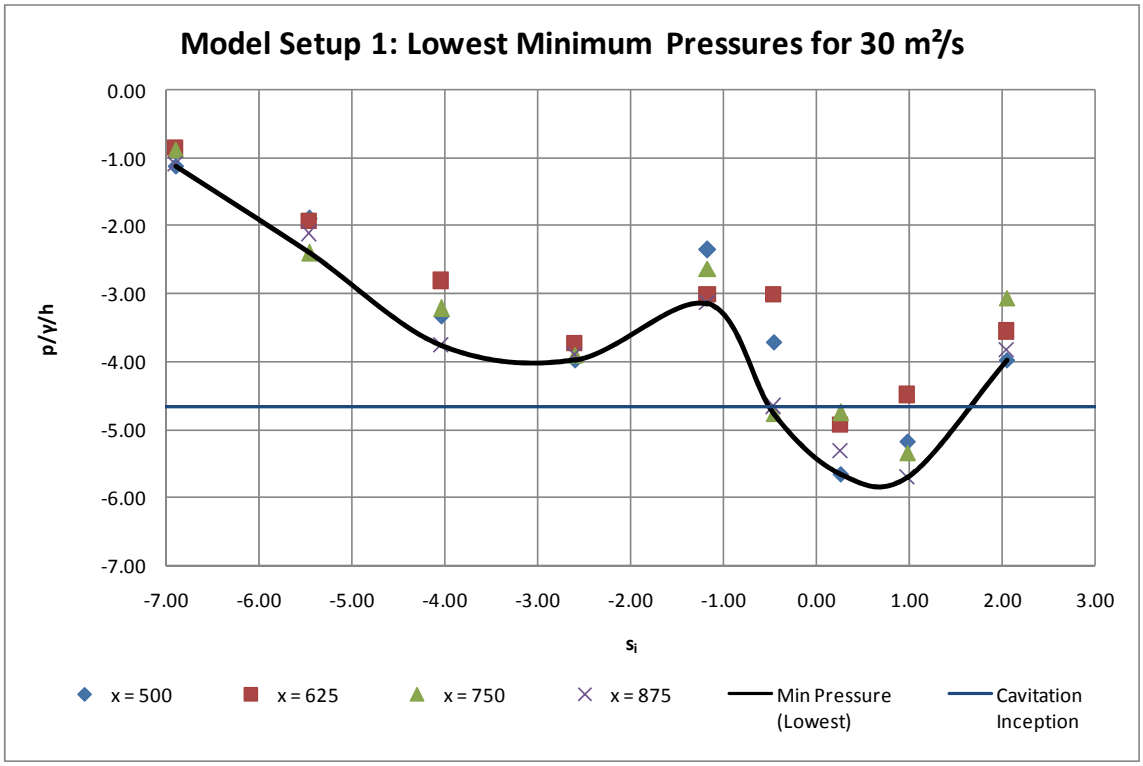

Figure 6-4: Lowest minimum pressures of model setup 1-30 m²/s

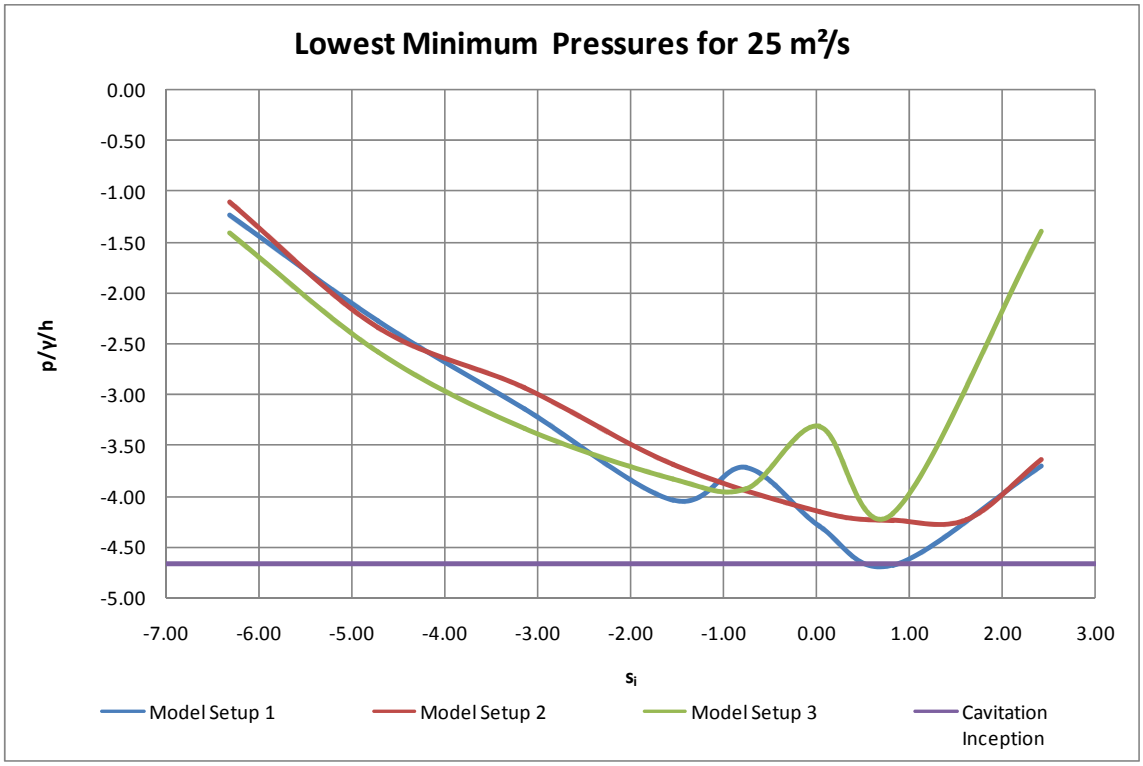

Figure 6-5: Lowest minimum pressures – 25 m²/s

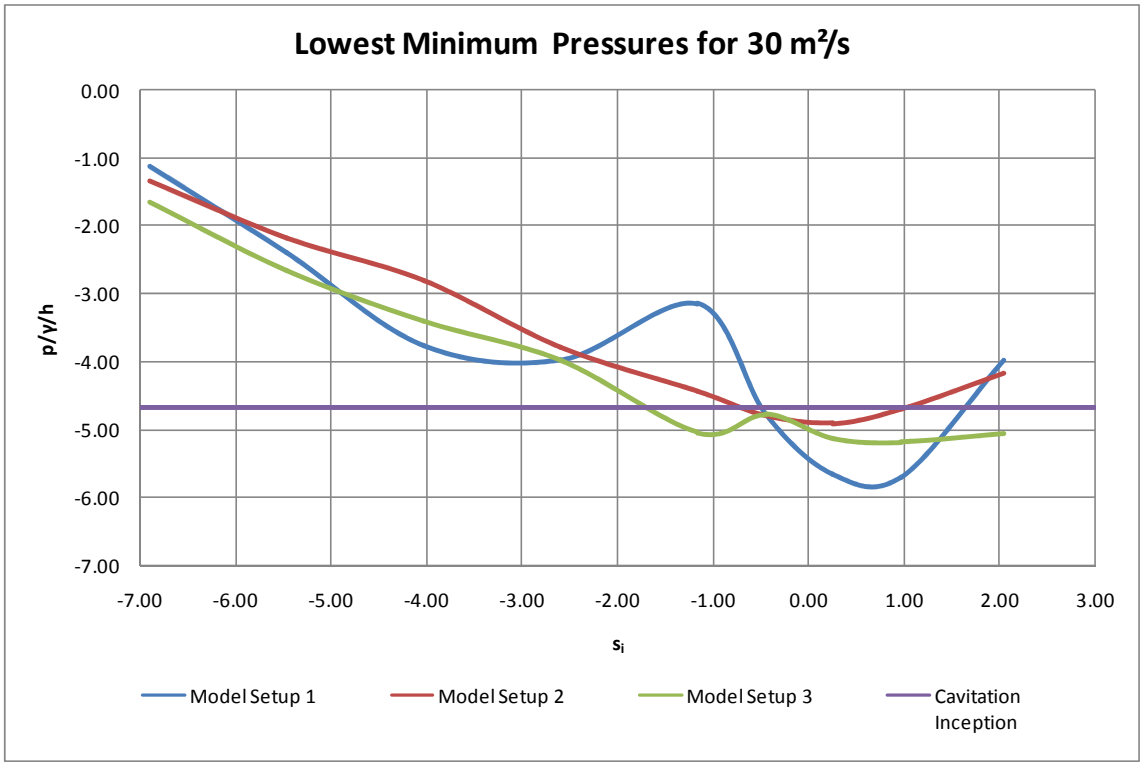

Figure 6-6: Lowest minimum pressures – 30 m²/s

6.3 FLOW EFFECT OF PIER DESIGN

The preliminary experimental work found that the main difference between the air entrainment properties of the Type 1 and 2 piers is due to the effect of flow impinging, or not impinging, on the horizontal step.

To reiterate these findings, the downstream end of the Type 1 pier terminates within the ogee profile zone, where flow does not yet impinge on the horizontal step. The flow separation that is created directly downstream of the pier, and which extends all the way to the steps, allows high volumes of air to be entrained within the step cavity. (Refer to **Figure 6-7** for an illustration of flow separation.) It is believed that either the negative envelope at the bottom of the nappe, coupled with the additional wake turbulence, or the turbulence within the shear layer, transports the air across the spillway width.

Downstream of a Type 2 pier, the flow impinges on the horizontal step, which prevents the separation of flow from extending all the way to the step cavity. (Refer to **Figure 6-8** for an illustrative example of this phenomenon.) The thinking is that air cannot be effectively entrained into the pseudo-bottom flow, as is the case with a Type 1 pier, due to the impingement directly downstream of the pier, on the horizontal step, obstructing air flow. Although air is introduced into the flow downstream of the pier, a large amount is localised around the pier, and it also does not reach the percentage of air concentration that was recorded with the Type 1 pier.

Figure 6-7: Flow separation downstream of Type 1 pier at prototype flow of 30 m³/s

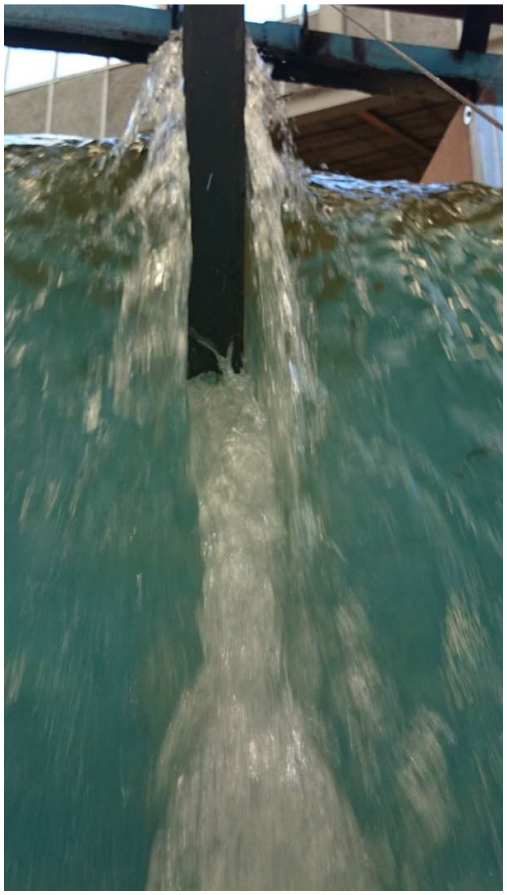

Figure 6-8: Flow separation downstream of Type 2 pier at prototype flow of 30 m³/s

6.4 RECOMMENDED PIER DESIGN

From the results obtained with tests A to C, it can be concluded that the Type 1 pier of model setup 2 would be the recommended pier design when considering the pre-aeration of the pseudo-bottom on a stepped spillway, with the intention of increasing minimum pressures on the upper vertical step face. Note that all references made to 'increased' air concentration and minimum pressures are based on the comparison to the results obtained with model setup 1, being that of a spillway with no pier.

The air concentration and the minimum pressure contour plots of model setup 2 clearly show that the pressure fluctuations were decreased for the areas with increased air concentration, subsequently increasing the minimum pressures. This discovery agrees well with the literature, which argues that minimum pressures can be increased by means of aerating the flow. The statement is further reinforced by the evidence that, in terms of the areas that were not sufficiently aerated, being the sides of the spillway (x = 125; 875 mm), the pressures were observed to be the lowest across the spillway width. The scatter plots of model setup 2 found in Test C (see **Figure 5-17** and **Figure 5-18**) clearly indicate that the lowest minimum pressure was recorded on the spillway side (x = 875 mm).

The results of the model setup 2 experiments also support the finding discussed in **Section 6.2**, which suggests that the uneven distribution of pressures across the spillway width can be reduced if the turbulent zone in the step cavity is sufficiently aerated.

Although the Type 1 pier design can be a major advantage for proposed stepped spillways that are required to pass large discharges, the following items could, nevertheless, be considered as disadvantageous for the use of such a pier:

- The jet flow produced downstream of the pier.
- The unaerated areas at the spillway sides producing high negative pressures.

The above points will be discussed in the following subsections.

6.4.1 Jet flow for a Type 1 Pier

Although the jet flow produced downstream of the Type 1 pier does not, necessarily, give cause for concern, due to the jet flow not being a normal flow condition that is found in the case of large discharges on stepped spillways, the matter should be investigated in more detail which is discussed in this subsection.

The main concern regarding jet flow is that negative pressures can occur within the step cavity. For the jet flow observed for this experiment, the step cavity was either completely, or partially, filled with air. The jet flow condition is made possible by the flow separation gap that is created downstream of the pier, where air moves into the step cavity. Jet flow can only occur if there is no, or minimal, impingement on the horizontal step. When the flow impinges on the step, a recirculating vortex is created, with the known flow properties for skimming flow.

A cross-sectional layout through the pier, depicting the formation of the jet flow condition downstream of a pier, is shown in **Figure 6-9**.

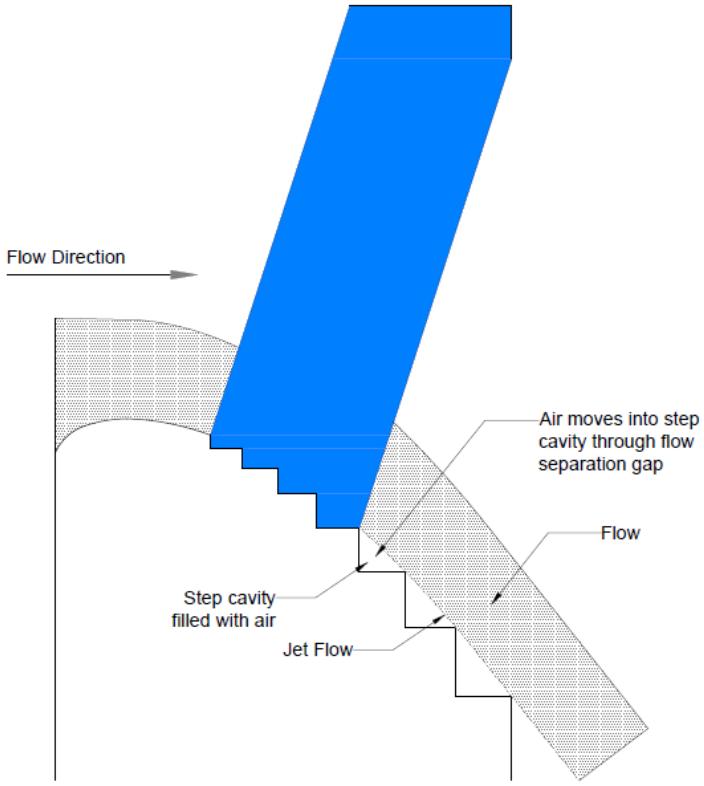

Figure 6-9: Cross-section of Type 1 pier, showcasing the jet flow produced

For air to be introduced through the opening in the step cavity created by the flow separation gap, a pressure differential must exist, so as to allow air to flow into the cavity mentioned. As already previously stated, it is postulated that air is transported across the spillway width, due to the negative pressure envelope at the bottom of the ogee profile, coupled with the aid of the wake turbulence. The negative pressure creates the pressure differential that is required for the air (at atmospheric pressure) to move into the step cavity.

The air within the step cavity is believed to exert positive pressures, and not to create negative pressure spikes, as was originally feared. The following arguments and observations are used to reinforce this belief:

- Air is introduced into the opening in the step cavity via the pressure differential that exists in the ogee profile. The opening in the step cavity is maintained through the existence of the flow separation gap, and, because there is no flow impingement on the horizontal step, continuous air flow into the step cavity is possible.
- Although no pressure measurements were conducted on the crest ogee, the closet pressure sensors showed no signs of potentially concern-raising excessive negative pressures. (Refer to **Figure 5-17** and **Figure 5-18**.
- The velocity of the flow on the spillway where the jet flow was found would not be sufficient to affect a high shear strain rate over the step edges that is likely to cause flow separation and consequent negative pressures.

In conclusion, the jet flow condition produced by a Type 1 pier should be of no concern regarding negative pressures on the upper vertical step.

In addition to the above, it should be stated that, due to the existing pressure differential, one would expect the jet flow to continue from the pier up to the spillway side wall, which, in actual fact, is not the case. The jet flow does not extend to the side wall, due to air being reabsorbed into the pseudo-bottom and the extent of the wake turbulence being limited to a certain distance from the side of the pier. The length of jet flow over the spillway width would be subject to the magnitude of the pressure differential, and to the boundary of the wake turbulence. An increased length of jet flow across the spillway width was observed for relatively large discharges.

6.4.2 Unaerated Areas at the Spillway Sides for a Type 1 Pier

The aeration downstream of the Type 1 pier did not extend over the complete spillway width. The spillway sides were not aerated to the same percentage as was the centre of the spillway, which was expected. Due to the lack of sufficient aeration, high negative pressures were recorded around the inception point at the sides of the spillway.

In practice, the above-mentioned situation can be avoided when using successive piers spaced a certain distance from one another over the length of the crest. The extent of aeration achieved by the one pier for a certain width of the spillway will overlap with the area of aeration created by the adjacent piers, effectively eliminating the unaerated regions. It is estimated that piers should be spaced a distance of approximately $2 \times H_d$ centre-to-centre, so as to achieve sufficient aeration over the width of the spillway.

However, the majority of the spillway will be aerated, due to the successive piers, but the spillway sides might still be left exposed to excessive negative pressures, due to the sides that cannot be aerated with an adjacent pier. For the spillway sides, around the inception point, it is proposed either to:

- Use slotted pipes that daylights beyond the spillway sidewall so as to ingest air into the negative pressure zones, or
- Apply special admixtures to harden the concrete for these areas when cavitation is expected.

6.5 CAVITATION EVALUATION

The final part of this thesis evaluates the potential for cavitation of discharges exceeding the recommended values. This section discussed two separate methods, termed Method A and Method B, for assessing the potential for cavitation of model setups 1 and 2. Model setup 3 is not evaluated, as it has already been determined that the Type 1 pier of model setup is the best alternative, concerning the study objective.

6.5.1 Method A – Cavitation Evaluation with Air Concentration and Minimum Pressures

The premise of this method, which is based on the research done by Peterka (1953), shows that an air concentration of approximately 5-8% at a spillway surface is sufficient to avoid cavitation damage due to the compressibility of the air-water mixture, which absorbs the impact of the imploding vapour-filled bubbles.

In terms of Method A, it can be argued that cavitation would not transpire if the air concentration were sufficient, irrespective of the negative pressures involved that might exceed the limit at which the cavitation inception is prominent. It is accepted that, although vapour-filled bubbles will form and implode on the spillway surface, the air bubbles present will absorb the energy that might otherwise damage the surface.

To apply Method A for purposes of cavitation evaluation, one would need the following information relating to the stepped spillway investigated, as either gathered from physical model studies or from computation fluid dynamics (CFD) analysis:

1. Air concentration data for the entire spillway width from the spillway crest down to the critical point, as defined by Boes and Hager (2003b).
2. Minimum pressures for the same region, as stipulated in (1).

As discussed in **Subsection 5.2.4**, the air concentration across the width of the spillway increases in a relatively uniform fashion from the inception point to the critical point for all model setups. To simplify the application of Method A, the air concentration of all the data points at, and downstream of the inception point was averaged. A conservative approach was followed, by means of specifying the critical percentage of air required to prevent cavitation damage at 8%.

The minimum pressures for the evaluation were based on the lowest minimum pressures found on the spillway width, as was discussed in **Section 6.2**. **Figure 6-10** to **Figure 6-13** show the cavitation evaluation conducted for model setups 1 and 2 for both tested discharges, using Method A. The cavitation inception level was set at -7 m.

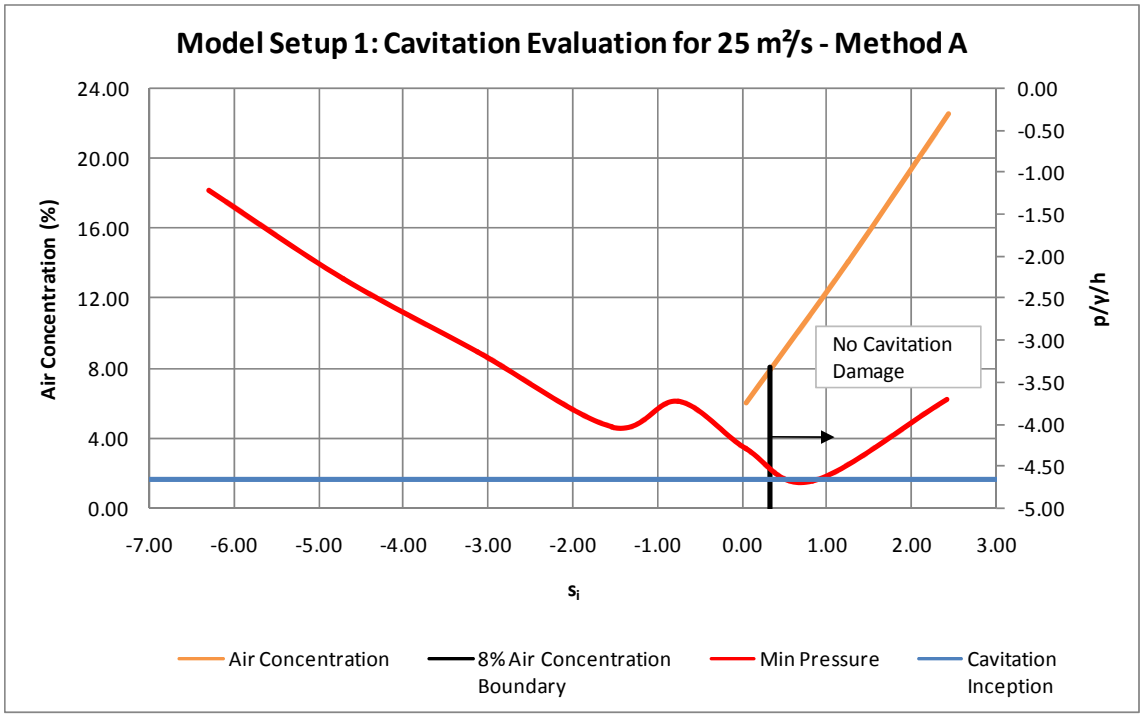

Figure 6-10: Method A cavitation evaluation of model setup 1-25 m²/s

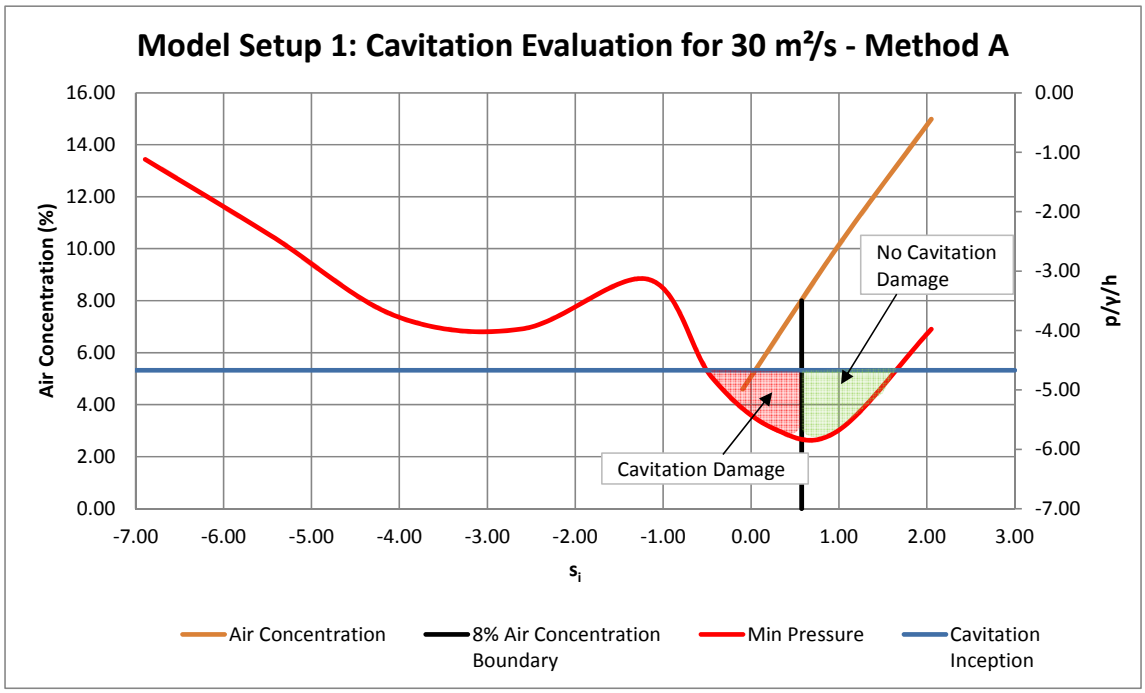

Figure 6-11: Method A cavitation evaluation of model setup 1-30 m²/s

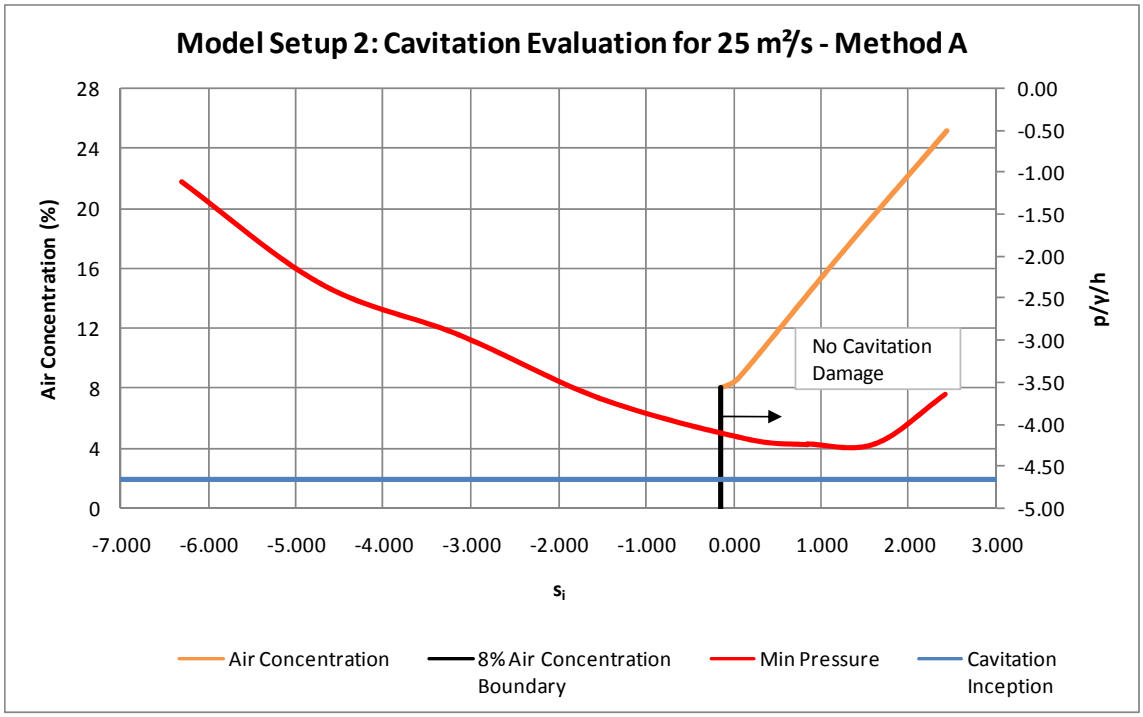

Figure 6-12: Method A cavitation evaluation of model setup 2-25 m²/s

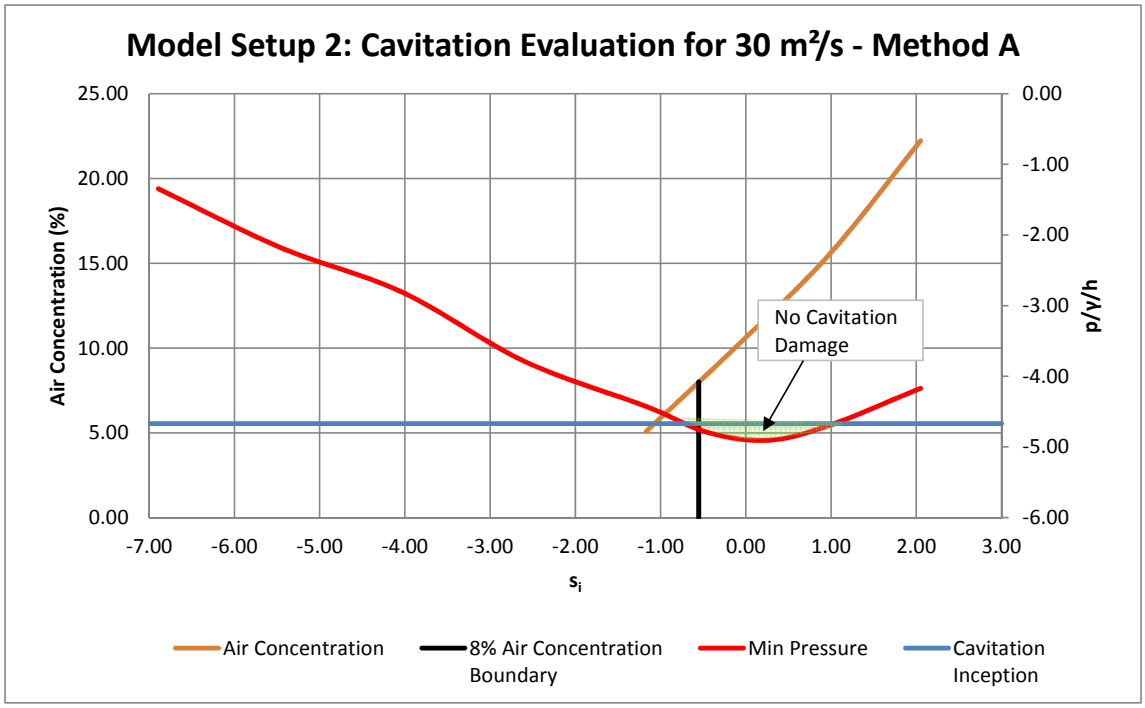

Figure 6-13: Method A cavitation evaluation of model setup 2-30 m²/s

From the above figures, it is evident that the only cavitation damage expected when applying Method A is that for a spillway with no pier (as in model setup 1), when passing a unit discharge greater than 25 m²/s.

6.5.2 Method B – Cavitation Evaluation with Only Minimum Pressures

Method B is a conservative alternate approach to Method A when no air concentration data are available, but data on pressures on the spillway surface are. Method B only evaluates the cavitation potential that is based on the minimum pressures recorded with physical model studies, or by means of CFD analysis.

As with Method A, the pressure that is used for the analysis reflects the absolute minimum pressures across the spillway width, so as to account for the uneven pressure distribution.

Figure 6-14 to **Figure 6-17** show the cavitation evaluation conducted for model setups 1 and 2 for both tested discharges using Method B.

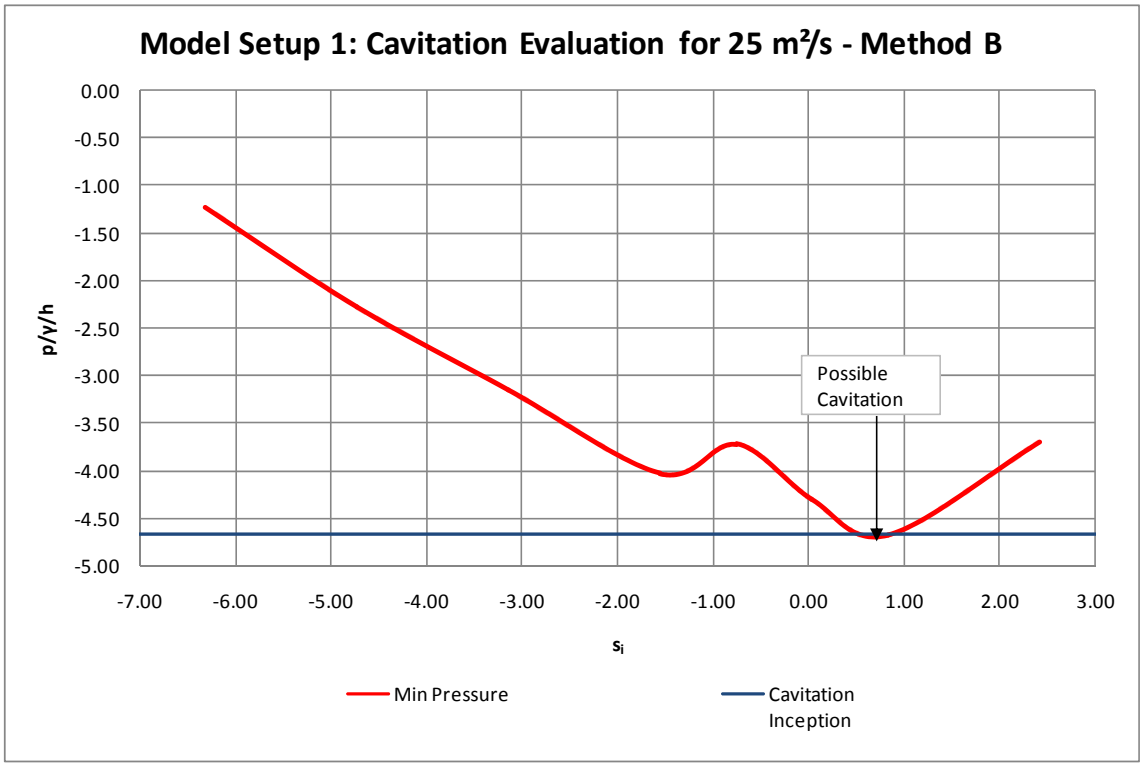

Figure 6-14: Method B cavitation evaluation of model setup 1-25 m²/s

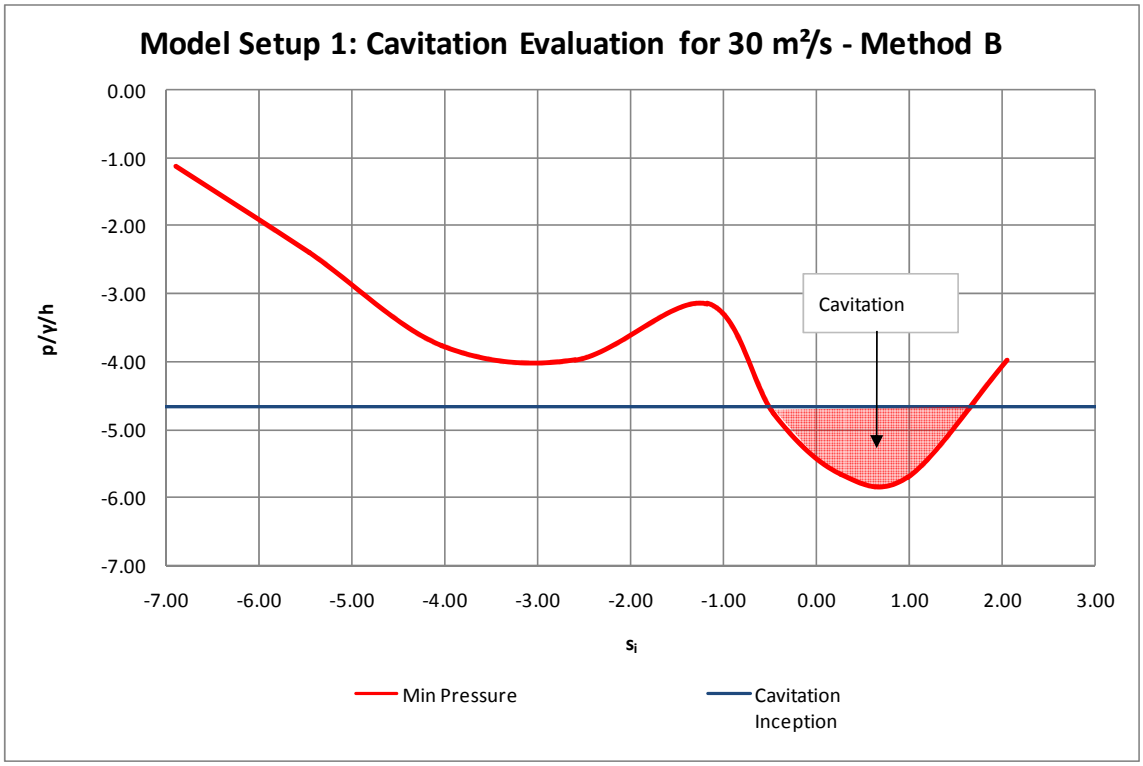

Figure 6-15: Method B cavitation evaluation of model setup 1-30 m²/s

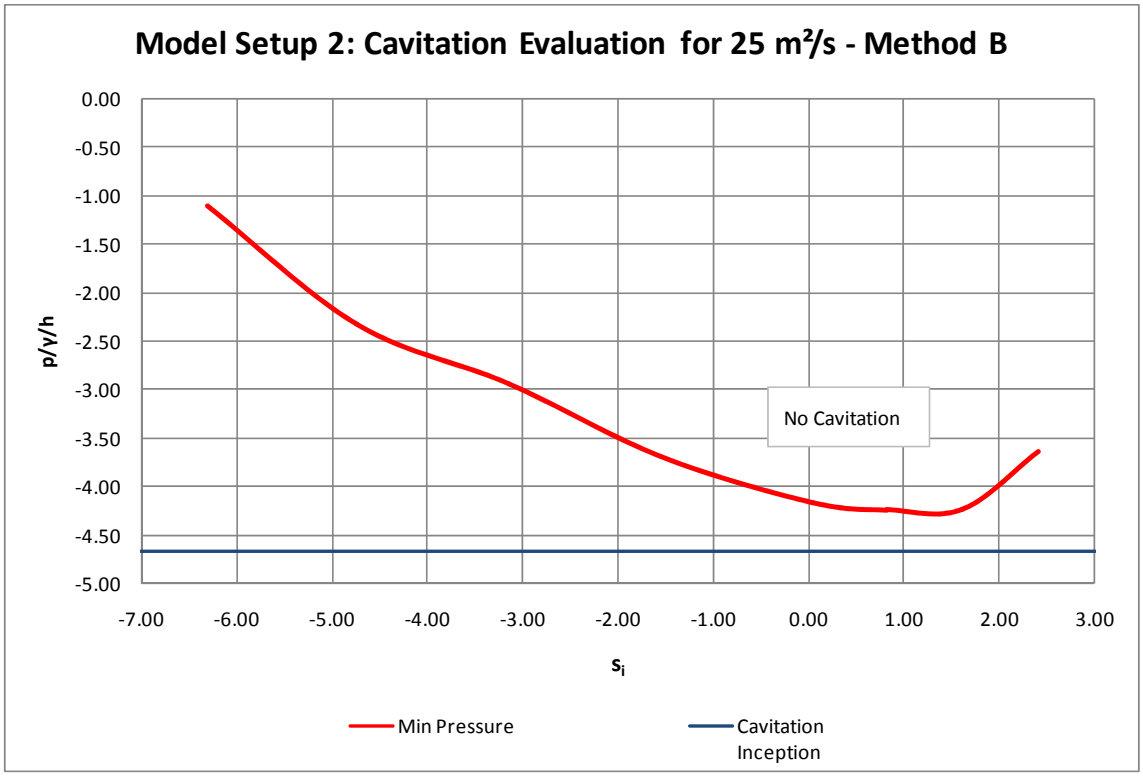

Figure 6-16: Method B cavitation evaluation of model setup 2-25 m²/s

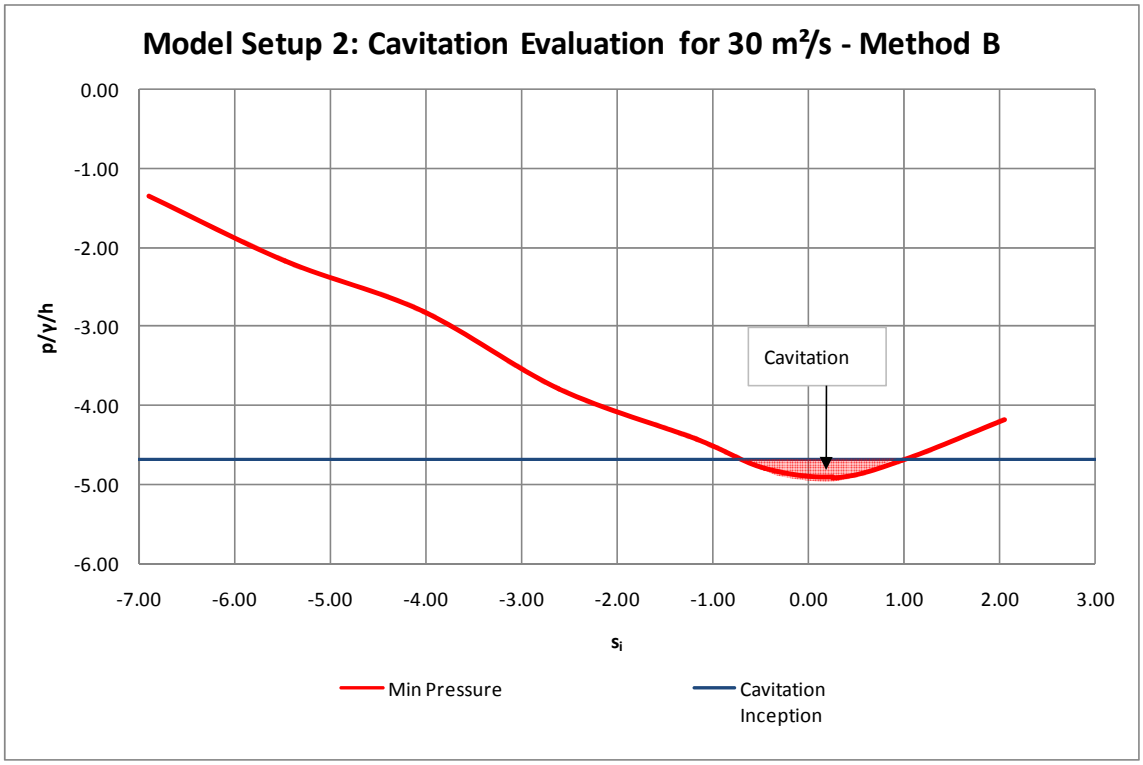

Figure 6-17: Method B cavitation evaluation of model setup 2-30 m²/s

The figures above illustrate that only a unit discharge of 25 m²/s or less could be safely passed for a model setup 2 without the risk of cavitation. All other scenarios would experience (possible) cavitation.

6.5.3 Cavitation Evaluation Summary

6.5.3.1 Summary of Results

A summary of the different methods used to evaluate the possibility of cavitation damage to a spillway is shown in **Table 6-1**.

Table 6-1: Cavitation evaluation summary

Q (m³/s)	Cavitation evaluation for spillway		
	Model setup	Method A	Method B
25	1	No	Small possibility
	2	No	No
30	1	Yes	Yes
	2	No	Yes

The above table shows that Method B yields the most conservative results possible in terms of the scenarios envisaged.

6.5.3.2 Comparison of the Results with the Literature

The cavitation evaluation conducted for a spillway with no piers (as in model setup 1) can be compared to the findings made in the literature surveyed. A comparison of the present evaluation to any to be found in the literature for a spillway with a pier (as in model setup 2) cannot be justified, as no such study has previously been done. Adding a pier to a conventional stepped spillway should be viewed as a modification that is aimed at increasing the discharge capabilities of the spillway concerned.

In the literature, **Figure 3-30** illustrates that a spillway that is configured to the model investigated is able to pass a unit discharge of 18 m²/s safely without being at risk of cavitation. The results of the current study show that a spillway with no piers is able to discharge 25 m²/s when using Method A. According to Method B, cavitation is imminent for 25 m²/s, but, knowing that a conservative approach was followed in evaluating the cavitation, it can be assumed that 25 m²/s would be the upper limit for Method B.

In summary, the literature recommends a maximum discharge of 18 m²/s, but the experimental study has shown that, for a no-pier stepped spillway with chute angled at 51.3° and a prototype step height of 1.5 m, a maximum discharge up to 25 m²/s can be allowed.

6.5.3.3 Proposed Cavitation Evaluation Method

Various methods to assess cavitation have been proposed by various authors, as was discussed in **Subsection 3.5.2**. For a spillway with no piers, these techniques can all be employed, including the two additional methods proposed in this study.

When a pier is added to a stepped spillway crest for the sole purpose of aerating the flow so as to increase minimum pressures, and thereby to allow higher discharges that might otherwise be possible, it is strongly advised to use Method A, as most of the other empirical equations proposed by other authors are based on model studies, or on theoretical relationships, for a non-pier spillway. In addition, using Method B would defeat the purpose of adding a pier so as to optimise the maximum discharge, as it has been proved that the specific method will yield a conservative result.

At this stage, an empirical equation that encapsulates the properties of the pier, discharge and the spillway design cannot yet be established, as more exhaustive tests are required to create and apply such a formula safely for stepped spillways, with a pier added to the crest. It is, therefore, advisable to use Method A as the present method of evaluating cavitation, due to the pier design, the pier position, the crest ogee, the ogee transition steps, the chute angle, and the spillway step height of future stepped spillways most likely being different.

6.5.3.4 Allowable Discharge for a Stepped Spillway with a Type 1 Pier

According to **Table 6-1**, a unit discharge up to 30 m²/s can be endorsed for a spillway that is equipped with a Type 1 pier, a set of transitional steps on the ogee profile, a chute angle at 51.3°, and a prototype step height of 1.5 m. By adding a pier to the crest, the maximum allowable discharge was almost doubled in contrast to the limit of 18 m²/s recommended in the literature.

It should be noted that the unit discharge of 30 m²/s recommended in this study was limited to the maximum flow that could be achieved for the model, but it is envisaged that the higher discharge can be allowed without creating the possibility of cavitation damage. For this study, the absolute lowest pressure found across the spillway width was used to represent the minimum pressures (refer to **Figure 6-4** and **Figure 6-6**), and, for model setup 2, the lowest pressures were found to be at the spillway sides. These specific low pressures can be increased when successive piers that are spaced a certain distance apart and alongside one another are used, thus increasing the minimum representative pressure, and allowing for the passing of a higher discharge.

7. CONCLUSION

A physical hydraulic model study, on a 1:15 scale, was undertaken to investigate whether the introduction of a pier at the crest of a stepped spillway can initiate premature self-aeration, so as to be able to safely pass discharges higher than the recommended value, without the spillway structure being at risk of cavitation damage.

A stepped spillway containing no pier was used as the control test to compare the results of two spillway configurations, each of which was equipped with a different pier type to help determine the optimal pier design for aerating the flow. The following conclusions ensued from the results of the physical model study, and from the associated literature review:

- The literature showed that the point at which air is entrained into the flow at the pseudo-bottom is known as the 'pseudo-bottom inception point' as defined by Boes and Hager (2003b). The literature also revealed that the lowest pressures are to be found at the upper section of the vertical step, just upstream of the pseudo-bottom inception point, which is also the most probable area for cavitation inception. Naturally, these areas of low pressure would limit the discharge capabilities of the spillway, due to the possibility of cavitation damage being caused to the spillway. The literature review demonstrated that the unit discharge possible for a stepped spillway with no pier, and for prototype dimensions scaled to those of the model, would be limited to 18 m^2/s, so as to avoid cavitation.
- Research by others has shown that an air concentration of 5 to 8% at the spillway bottom can prevent cavitation damage to the structure, thereby implying that aeration to the areas of concern can lead to increased discharges being safely passed.
- The experimental tests with the three different model setups were structured to test 1) the length to surface inception, 2) the air concentration at the pseudo-bottom, and 3) the pressures at the upper vertical step upstream of the critical point. The results showed that, when compared to the control test, the spillways fitted with a crest pier performed better for all three parameters tested, with the Type 1 pier producing the best results of the two pier designs considered.
- By means of introducing the Type 1 pier at the spillway crest, the air concentration was increased along the spillway chute, leading to reduced pressure fluctuations, which, in turn, increased the minimum pressures involved.
- Two different approaches to evaluate cavitation for a stepped spillway were established. Method A took into account the air concentration and the minimum pressures found on the spillway chute, whereas Method B only evaluated the possibility of cavitation based on the minimum pressures involved. It was found that Method B recommended a maximum unit discharge of 25 m^2/s for a spillway equipped with a Type 1 pier, whereas Method A suggested that a unit discharge of 30 m^2/s or more could be safely passed.
- Method A is recommended for use in evaluating possible cavitation for a stepped spillway, as it encapsulates the parameters required that affect cavitation damage, namely air concentration and minimum pressures.

- It can be concluded that the addition of a Type 1 pier at the spillway crest will allow a stepped spillway to discharge 30 m²/s safely, without risking cavitation damage to the structure, which is more than the recommended discharge of 18 m²/s for a spillway with no pier.

Apart from the results required to achieve the stated study objective, the experimental studies, in addition to attaining the main objective, also revealed other interesting results that are discussed below:

- The position of the downstream end of the pier on the spillway crest determines, to a large extent, the amount of air that can be entrained directly downstream of a pier. As the downstream end of the pier is moved downstream along the ogee crest, more flow impinges on the subsequent horizontal step that is directly downstream of the pier end. The amount of flow impingement on the horizontal step determines the amount of downstream chute aeration.
- The literature showed that the lowest mean pressures for a stepped spillway with no pier could be found upstream of the inception point, corresponding with the mean pressures recorded for the study. However, it was revealed, by means of the minimum pressure study, that the lowest pressure actually occurs just downstream of the inception point, and not upstream, as had previously been believed. To date, such a phenomenon has not been recorded in any research, so that it is important to incorporate the details of such a finding in any future research regarding cavitation evaluation on a stepped spillway.
- Employing the cavitation evaluation Method A for a stepped spillway with no pier showed that the spillway is able to safely pass a unit discharge of 25 m²/s, which is also greater than the recommended discharge of 18 m²/s.

8. RECOMMENDATIONS

The following items fall outside the scope of this thesis, but they are recommended for pursuit in future research:

- The model study indicated that the optimal pier design should have a pier that terminates within the ogee profile zone, and not downstream of it, although it is not yet known where the optimal position for the downstream end along the ogee crest should be. This subject should be investigated further for a range of different discharges.
- For a discharge greater than the design discharge, a negative pressure envelope develops on a typical ogee crest that leads to better discharge capabilities of the spillway. The introduction of transition steps on the crest, as well as a pier, could influence this phenomenon, as the surface to which the lower nappe adheres has been disturbed. This can lead to a reduction in the crest discharge ability. It is recommended to compare the discharge and the negative pressures of a typical ogee profile to those of a stepped spillway with transitional steps and a possible pier, as a future research topic.
- The argument was expressed that the pressure differential that exists, due to the negative envelope at the lower nappe on the stepped spillway crest, coupled with the energy from the wake turbulence downstream of the pier, was responsible for the transportation of air across the spillway width. This theory could be confirmed with future pressure measurements within this zone.
- It is recommended, as the intent of a future study, to record the air concentration and minimum pressures across the spillway width for a spillway that is equipped with more than one pier, with the pier design being similar to that of Type 1. Such a study would enable the evaluation of the extent of air distribution generated downstream of each pier, which could lead to further increase in the areas of low pressure, which, as a result, could help to determine whether a discharge greater than the current recommend 30 m^2/s could be safely discharged.

REFERENCES

Amador, A., Sànchez-Juny, M. & Dolz, J., 2003. Discussion: Two phase flow characteristics of stepped spillways by R. Boes and W.H. Hager. *Journal of Hydraulic Engineering,* Volume 129, pp. 661-670.

Amador, A., Sànchez-Juny, M. & Dolz, J., 2004. Velocity and pressure field in skimming flow in stepped spillways. In: *Hydraulic of dams and river structures.* London: Taylor and Francis Group, pp. 279-285.

Amador, A., Sànchez-Juny, M. & Dolz, J., 2006. Characterization of the nonaerated flow region in a stepped spillway by PIV. *Journal of Fluids Engineering,* Volume 128, pp. 1266-1273.

Amador, A., Sànchez-Juny, M. & Dolz, J., 2009. Developing flow region and pressure fluctuations on steeply sloping stepped spillways. *Journal of Hydraulic Engineering,* Volume 135, pp. 1092-1100.

Anonymous, 2010. *Magical Southern African Safaris.* [Online] Available at: http://www.magical-southern-african-safaris.com/gariep-dam.html [Accessed 14 December 2014].

ASCE, 1995. *Hydraulic Design of Spillways.* s.l.:American Society of Civil Engineers.

Atencio, B., 2011. *Measurements and Prediction of Laminar-Turbulent Transition at High Free-Stream Turbulence in Boundary Layers with Pressure Gradients,* Sweden: Chalmers University of Technology.

Baylar, A., Emiroglu, M. E. & Bagatur, T., 2006. An experimental investigation of aeration performance in stepped spillways. *Water and Enviromental Journal,* Volume Vol 20, pp. 35-42.

Boes, R. M. & Hager, W. H., 2003a. Hydraulic design of stepped spillways. *Journal of Hydraulic Engineering,* Volume 129, pp. 671-679.

Boes, R. M. & Hager, W. H., 2003b. Two-phase flow charateristics of stepped spillways. *Journal of Hydraulic Engineering,* Volume 129, pp. 661-670.

Boes, R. M. & Minor, H. E., 2000. Guidelines for the Hydraulic Design of Stepped Spillways. In: *Hydraulics of Stepped Spillways.* Switzerland: A.A. Balkema.

Chadwick, A., Morfett, J. & Borthwick, M., 2006. *Hydraulics in Civil and Enviromental Engineering.* s.l.:Taylor & Francis Group.

Chamani, M. R., 2000. Air Inception in Skimming Flow Regime over Stepped Spillways. In: *Hydraulics of Stepped Spillways.* Switzerland: A.A.Balkema.

Chanson, H., 1994. *Hydraulic design of stepped cascades, channels, weirs and spillways.* Brisbane: Pergamon.

Chanson, H. & Carosi, G., 2007. Advanced post processing and correlation analyses in high-velocry air-water flows. *Environ Fluid Mech,* Volume 7, pp. 495-508.

Eccher, L. & Siegenthaler, A., 1987. Spillway aeration of the San Roque project. *Int. Water Power Dam Contr.,* Volume Vol 34, pp. 37-41.

Farooq, R., 2013. *Top 15 worst dam disasters ever.* [Online] Available at: http://chillopedia.com/interesting/top-15-worst-dam-disasters-ever/ [Accessed 16 December 2014].

Felder, S. & Chanson, H., 2011. Air-water flow properties in step cavity down a stepped chute. *Internation Journal of Mutliphase Flow,* Volume 37, pp. 732-745.

Fitzpatrick, R., 2012. *Boundary layer separtion.* [Online] Available at: http://farside.ph.utexas.edu/teaching/336L/Fluidhtml/node90.html [Accessed 19 December 2014].

Frizell, K. W., Renna, F. M. & Matos, J., 2013. Cavitational potential of Flow on Stepped Spillways. *Journal of Hydraulic Engineering,* Volume 139.

Husain, S. M., Muhammed, J. R., Karunarathna, H. U. & Reeve, D. E., 2014. Investigation of pressure variationsover stepped spillway using smooth particle hydrodynamics. Volume 66, pp. 52-69.

Kobus, H., 1984. *Local air entrainment and detrainment.* Germany, s.n., pp. 1-10.

Matos, J., 2000. Hydraulic design of stepped spillways over RCC dams. In: H. E. Minor & W. H. Hager, eds. *Hydraulics of stepped spillways.* Switzerland: A.A. Balkema, pp. 187-194.

Mehta, P. K. & Monteiro, P. J., 2007. *Roller compacting concrete.* [Online] Available at: www.ce.berkeley.edu/~paulmont/165 [Accessed 18 March 2013].

Meireles, I., Matos, J. & Frizell, K., 2007. *Measuring air entrainment and flow bulking in skimming flow over steeply sloping stepped chutes.* s.l., s.n.

Nikseresht, A. H., Talebbeydokhti, N. & Rezaei, M. J., 2013. Numerical simulation of twp-phase flow on step-pool spillways. *Scientia Iranica,* Volume 20, pp. 222-230.

Novak, P., Moffat, A. I., Nalluri, C. & Narayanan, R., 2007. *Hydraulic structures.* Oxon: Taylor & Francis.

Ohtsu, I. & Yasuda, Y., 1997. *Characteristics of flow conditions on stepped channels.* San Franciso, s.n., pp. 583-588.

Pegram, G. G. S., Officer, A. K. & Mottram, S. R., 1999. Hydraulics of skimming flow on modelled stepped spillways. *Journal of Hydraulic Engineering,* Volume 125, pp. 500-510.

Peterka, A. J., 1953. *The effect of entrained air on cavitation pitting.* Minneapolis, s.n., pp. 507-518.

Pfister, M. & Hager, W. H., 2010. Self-entrainment of air on stepped spillways. *International Journal of Multiphase Flow.*

Pfister, M., Hager, W. H. & Minor, H. E., 2005. Stepped Chutes: Pre-aeration and spray reduction. *International Journal of Multiphase Flow.*

Pfister, M., Hager, W. H. & Minor, H. E., 2006. Bottom aeration of stepped spillways. *Journal of Hydraulic Engineering,* Volume 132, pp. 850-853.

Pinto, N. L., 1984. *Model evaluation of aerators in shooting flow.* Germany, s.n., pp. 1-6.

Rutschmann, P., 1988. *Belüftungseinbauten in Schussrinnen,* VAW, Zurich, Switzerland: PhD Thesis.

Sànchez-Juny, M., Pomares, J. & Dolz, J., 2000. Pressure field in skimming flow over a stepped spillway. In: *Hydraulics of stepped spillways.* Switzerland: A.A. Balkema, pp. 137-145.

Speerli, J., 1999. *Strömungsprozesse in Grundablassstollen,* VAW, Zurich, Switzerland: PhD thesis.

Syque, 2014. *Measuring Spread.* [Online] Available at: http://www.syque.com/quality_tools/toolbook/Variation/measuring_spread.htm [Accessed 14 December 2014].

Tozzi, M., 1994. Residual Energy in Stepped Spillways.

Turk, G., 1996. *Image guided streamline placement.* [Online] Available at: http://www.cc.gatech.edu/~turk/streamlines/streamlines.html [Accessed 17 December 2014].

USBR, 1987. *Design of Small Dams.* s.l.:United States Bureau of Reclamation.

Vischer, D., Volkart, P. & Siegenthaler, A., 1982. *Hydraulic modeling of air slots in open chute spillways.* Coventry, United Kingdom, s.n., pp. 239-252.

Wahrheit-Lensing, A., 1996. *Selbstbelüftung und Energieumwandlung beim Abfluss über treppenförmige Entlastungsanlagen,* Univ. of Karlsruhe, Karlsruhe, Germany: PhD thesis.

Webber, N., 1979. *Fluid mechanics for civil engineers.* London: Chapman and Hall.

Wood, I., Ackers, P. & Loveless, J., 1983. *General method for Critical Point on Spillways.* s.l.:Journal of Hydraulic Engineering.

Wu, J., Zhang, B. & Ma, F., 2013. Inception point of air entrainment over stepped spillways. *Journal of Hydrodynamics,* Volume 25, pp. 91-96.

APPENDIX: AS-BUILT MODEL DRAWINGS

AS-BUILT DRAWING

1:15 STEPPED SPILLWAY
SCALE MODEL (SHEET 1 OF 2)

AUTHOR:	JA CALITZ
DATE:	2014-07-14
DRG SCALE:	1:50
PAPER SIZE	A3

STELLENBOSCH UNIVERSITY

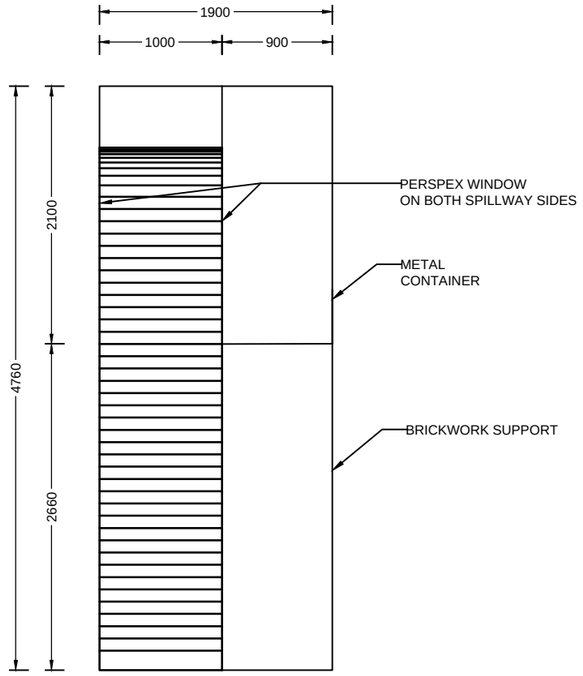

FRONT VIEW
SCALE 1:50

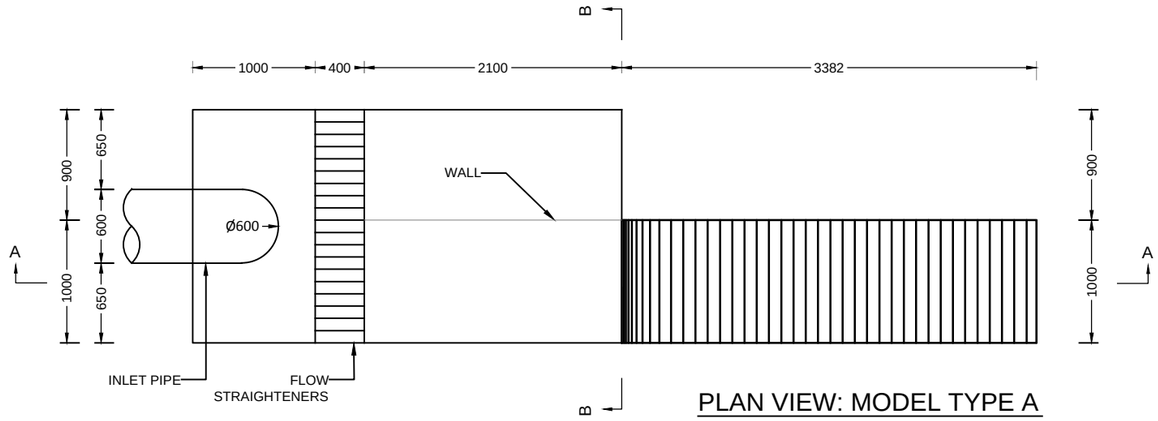

PLAN VIEW: MODEL TYPE A
SCALE 1:50

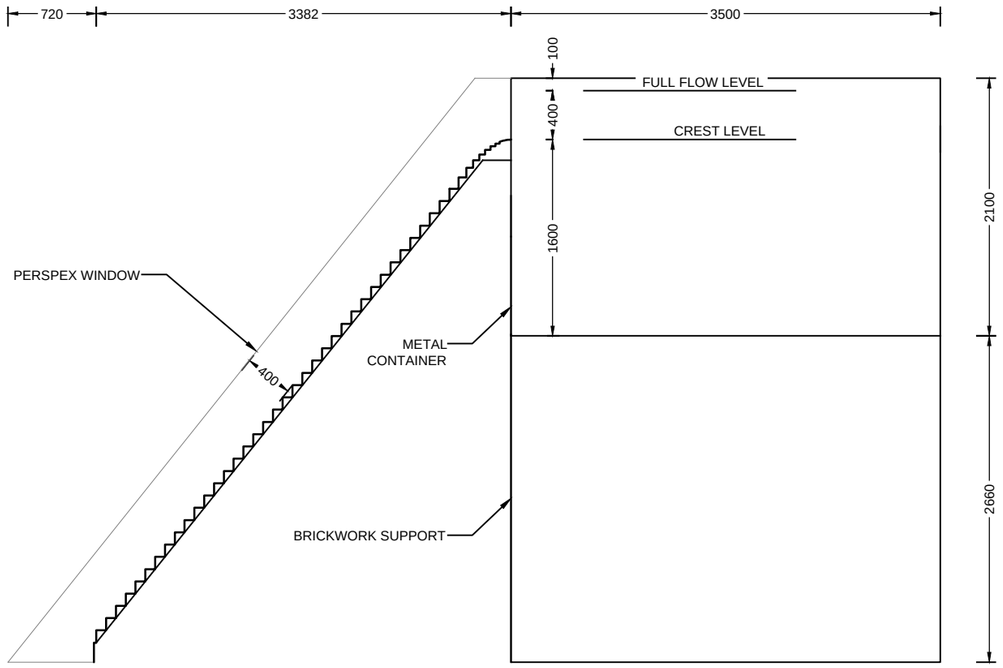

RIGHT VIEW
SCALE 1:50

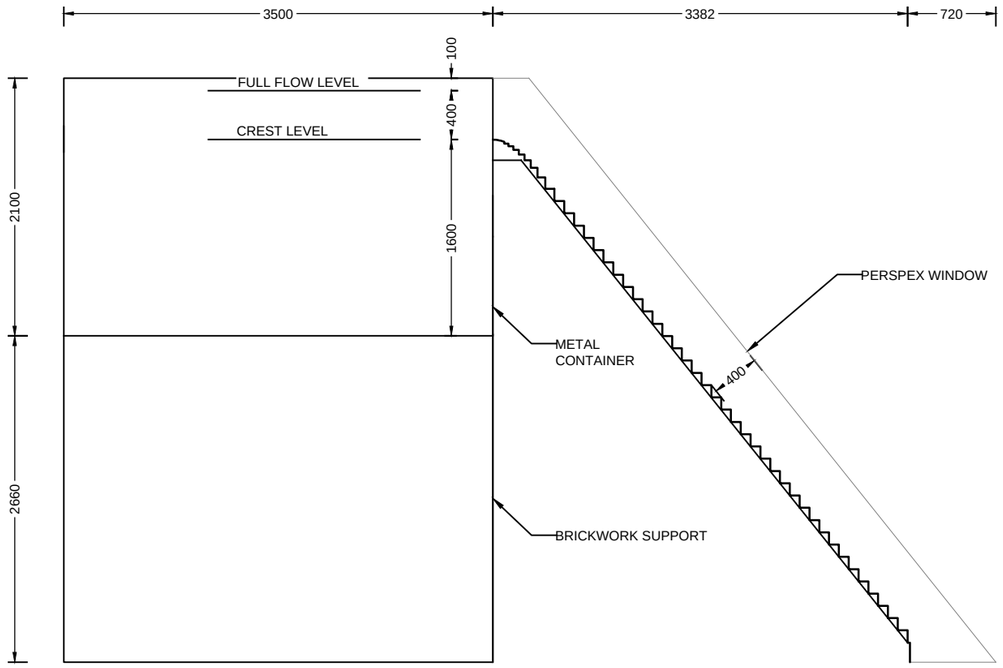

LEFT VIEW
SCALE 1:50

AS-BUILT DRAWING

1:15 STEPPED SPILLWAY
SCALE MODEL (SHEET 2 OF 2)

AUTHOR:	JA CALITZ
DATE:	2014-07-14
DRG SCALE:	AS SHOWN
PAPER SIZE	A3

STELLENBOSCH UNIVERSITY

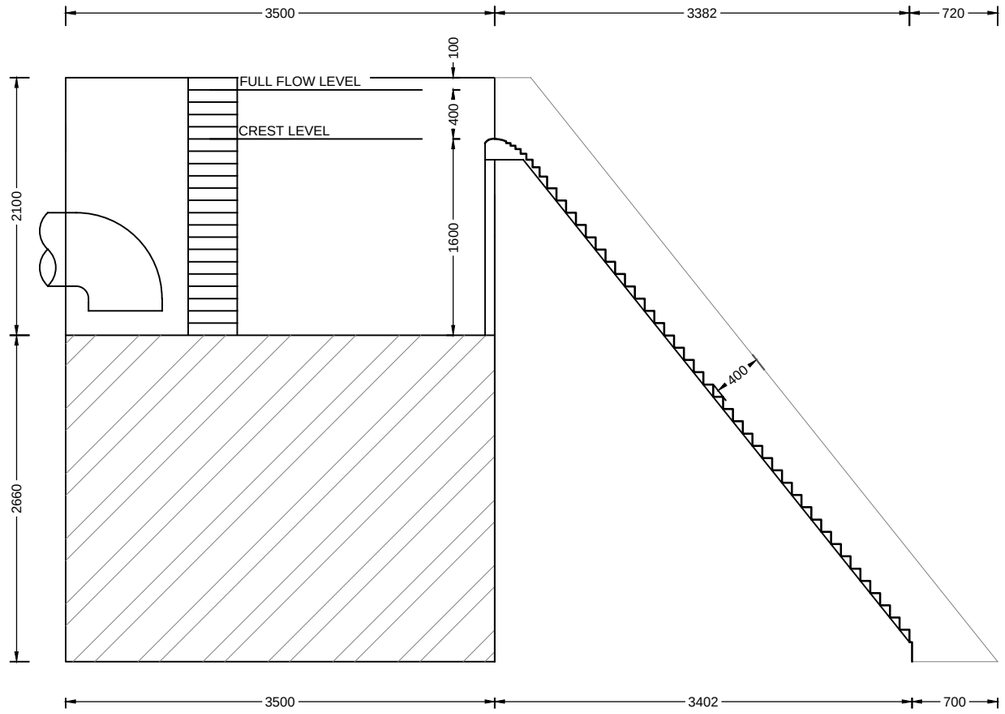

SECTION A-A
SCALE 1:50

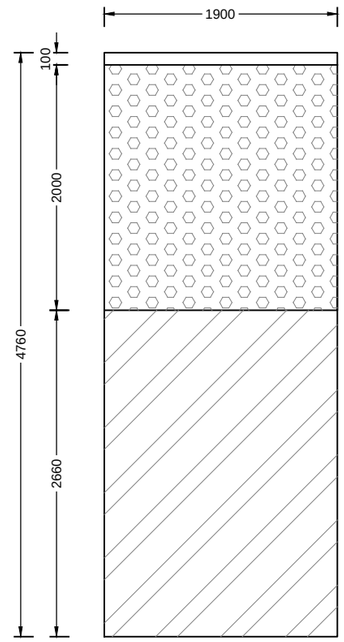

SECTION B-B
SCALE 1:50

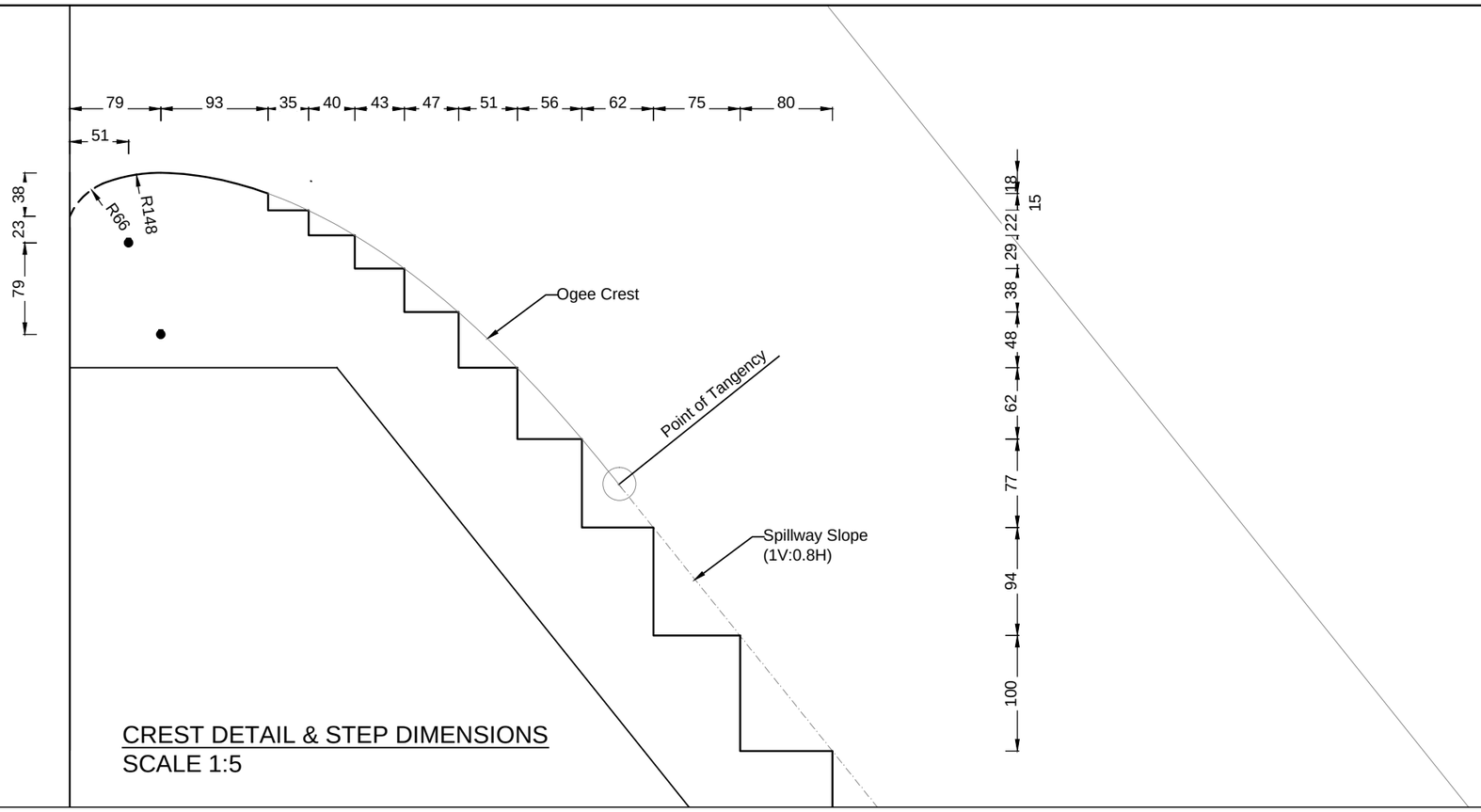

CREST DETAIL & STEP DIMENSIONS
SCALE 1:5